NONLINEAR DISCRETE-TIME CONTROL OF MODERN POWER CONVERTERS WITH ROBUST ADAPTIVE OBSERVER

by

MAURICIO E. HERNANDEZ

A dissertation submitted in partial fulfillment of the
requirements for the degree of

DOCTOR OF PHILOSOPHY IN ELECTRICAL AND COMPUTER ENGINEERING

2023

Oakland University
Rochester, Michigan

Doctoral Advisory Committee:

Mohamed A. Zohdy, Ph.D., Chair
Serge Kruk, Ph.D.
Subra Ganesan, Ph.D.
William Edwards, Ph.D.

To my wife Sanja, whose support and patience made this document possible, to my daughters Ana, and Lucia, and my son Mateo for their encouragement. Thanks to my mother Leticia that established in me at a young age the values of hard work and perseverance.

ACKNOWLEDGMENTS

First of all, I would like to thank and acknowledge Dr. Mohamed Zohdy for his continuous guidance and encouragement over the last ten years; without his constant assistance this dissertation and degree would never have been finished. I would also like to thank my doctoral advisory committee Dr. Serge Kruk, Dr. Subra Ganesan, and Dr. William Edwards for their time and support.

All my gratitude to my family for their unconditional love that allowed me to finish this work.

Mauricio E. Hernandez

ABSTRACT

NONLINEAR DIGITAL CONTROL OF MODERN POWER ELECTRONICS WITH ROBUST ADAPTIVE OBSERVER

by

Mauricio E. Hernandez

Adviser: Mohamed A. Zohdy, Ph.D.

Control systems are an integral part of modern society, crucial to the performance of these systems is the accurate mathematical model representation of the physical systems. However, every physical system is subject to external factors that over time can change its characteristics. Therefore, to adapt the mathematical model representation of the plant over time a State Observer or State Estimator is often used, which would be the main topic of my research. A ZETA Power converter is a type of switch mode power supply that offers high efficiency in addition to various advantages, among some is its low output ripple which is desired for powering modern VLSI electronics. However due to its composition (non-Linear and fourth order), controlling the dynamics could be complex. With the advances in microprocessing and their economical affordability now, implementing the control scheme of a Zeta converter in the discrete time domain makes it an ideal solution for control implementation, given the lack of research regarding discrete-time control for Zeta Power Converters, state space observers, and adaptive state estimation, this dissertation research aims to identify a novel way of controlling Zeta

Converters using adaptive state observers and state feedback in the discrete-time domain that yields robustness in the presence of plant uncertainties that meets certain

The results documented in this dissertation confirm but also outlines the limitations of such Nonlinear discrete-time domain control State-Feedback from a Robust and Adaptive full-state observer/estimator.

TABLE OF CONTENTS

LIST OF TABLES

LIST OF FIGURES

LIST OF FIGURES—Continued

CHAPTER ONE

INTRODUCTION

1.1 Contextual information and research aim

Control systems are an integral part of modern society [1]. Numerous applications are all around us from the temperature control of our homes to the driver assistance systems that keep our vehicles safely between the road lines. Crucial to the performance of these systems is the accurate mathematical model representation of the physical systems often call the Plant. However, every physical system is subject to external factors that over time can change its characteristics of it such as temperature, aging, vibration, humidity, and environmental disturbances, among others. Therefore, to adapt the mathematical model representation of the plant over time a State Observer or State Estimator is often used, which would be the main topic of my research.

A State Observer is a dynamic system that estimates the state of a system based on based on the measurements of the system output y(t) and the system input u(t) as depicted in figure 1.1.

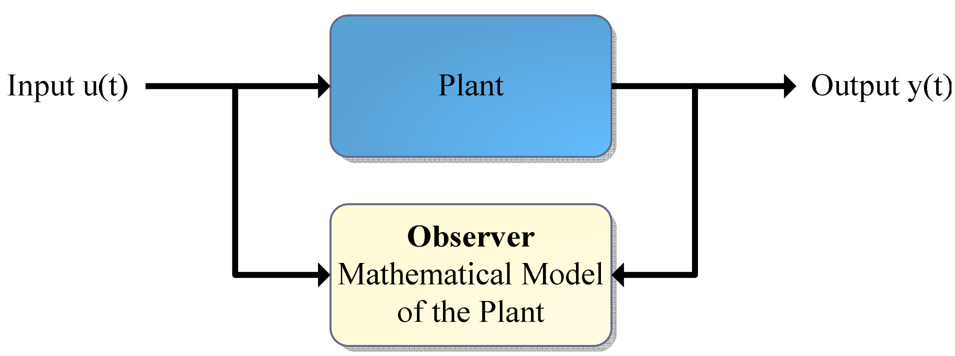

Figure 1.1 Plant and Observer block diagram

The mathematical definition of an observer is in the time domain, also known as state-space representation. The state-space method is characterized by significant algebraization of general system theory, which makes it possible to use Kronecker vector-matrix structures [2] and also makes the observer very suitable for computer-based implementation.

Even though the extraordinary development of digital processing is doubling every two years see figure 1.2, the adoption of State feedback controllers and estimation methods has not been exploited yet, this can be observed by the academic interest of control techniques since David G. Luenberger published the first paper on Observers in 1964 *Observing the State of a Linear System* [3] till 2019.

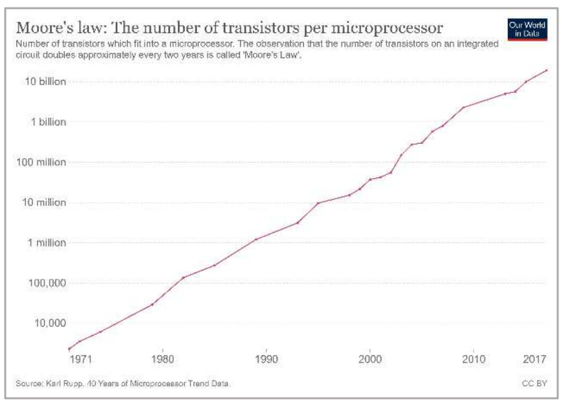

Figure 1.2 Moore’s Law, an observation that the number of transistors in a dense integrated circuit (IC) doubles about every two years

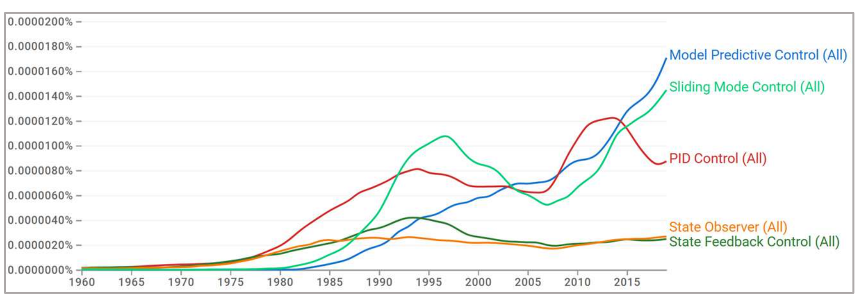

Figure 1.3 Ngram search for Control techniques from 1960 to 2019 Google

In the Industry, the **P**roportional–**I**ntegral–**D**erivative controller PID depicted in figure 1.3 is by far the most common solution to practical control problems. Today, the PID controller is by far the most dominating form of feedback control in use. More than 90% of all control loops are PID.

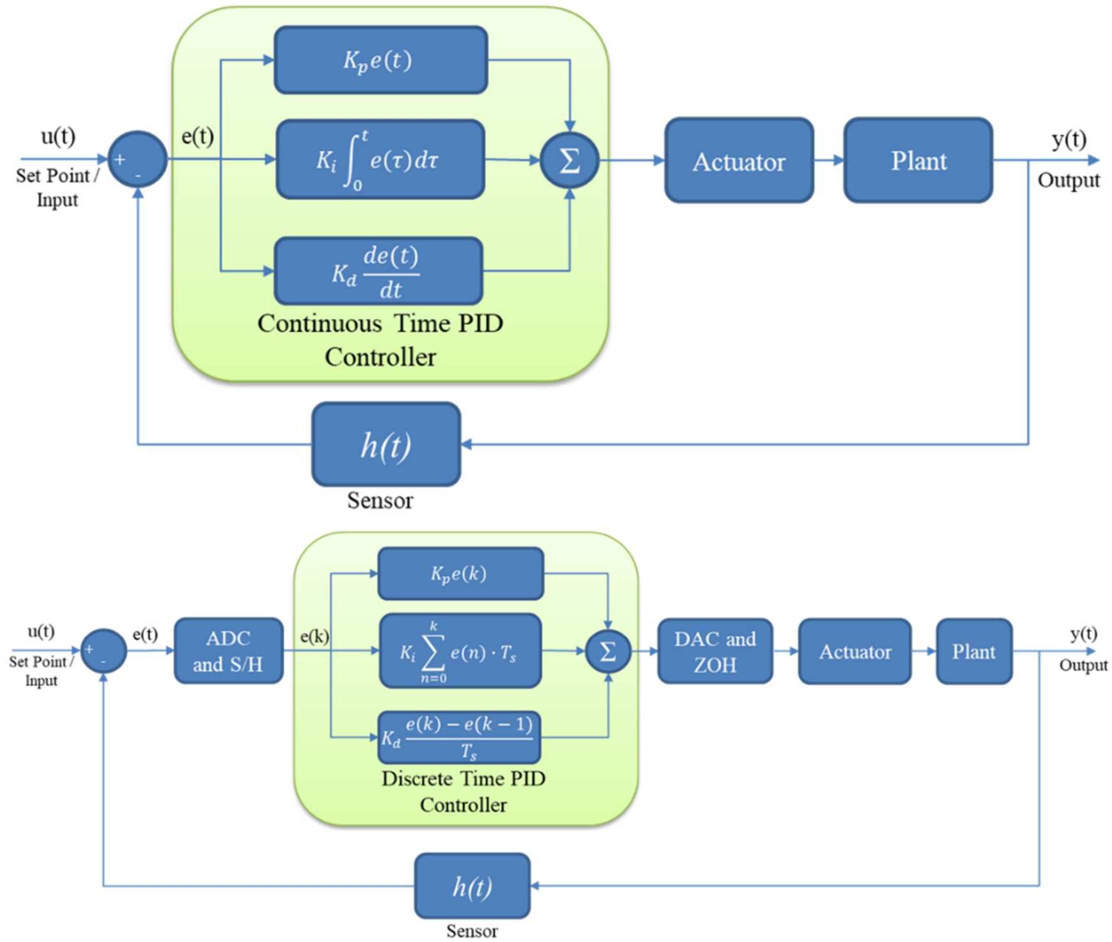

Figure 1.4 PID controller Continuous and Discrete Time

The first form of PID control emerged in the 1930s with pneumatic controllers [4]–[6]. The popularity of the PID controller (eq.1.1 PID Continuous Time and eq.1.2 PID Discrete Time) can be attributed to its functional simplicity of understanding, robustness against system disturbances due to its feedback nature (error manipulation), and its three-step implementation: Step 1: improve the steady state error with a gain (P), and integration of the feedback error (I); Step 2: improve the transient response by differentiating the error (D); Step 3: Trial and error tunning of the PID gains till the satisfactory response is achieved.

$$\text{PID Control Variable}(t)=K_p e(t)+K_i \int_0^t e(\tau)d\tau + K_d \frac{de(t)}{dt} \qquad \text{Eq1.1 [1]}$$

$$\text{PID Control Variable}(k)=K_p e(k)+K_i \sum_{n=0}^{k} e(n) \cdot T_s + K_d \frac{e(k)-e(k-1)}{T_s} \qquad \text{Eq1.2 [7]}$$

However, the PID has limitations, and a different control scheme is more suitable for systems of an order higher than two, multivariable systems (MIMO Systems) and Non-linear systems [4]–[6].

A consequence of Moore's Law is that Power Converters have become an increasingly larger portion of any electronic system [8]. The reasons include:

1) The use of microelectronics, in conjunction with advanced packaging techniques, permits higher load power densities (SoC, SoPC, SiP, Chiplets)
2) As semiconductor process dimensions shrink, lower power supplies voltages are required to prevent voltage breakdown, therefore reducing power supply efficiency, and increasing the required thermal mass of the power supply
3) An increasingly larger portion of the power delivered to these new and more sensitive VLSI devices must be very well regulated/controlled to avoid Electrical breakdown due to voltage overshoots.

High efficiency is essential in any power processing application [9]. The high-efficiency converters are necessary because the construction of low-efficiency converters, producing substantial output power, is impractical. The efficiency of a converter having an output power P_{out} and an input power P_{in} is η defined by Eq.1.3

$$\eta = \frac{P_{out}}{P_{in}} \qquad \text{Eq 1.3}$$

The power loss in a converter $P_{loss} = P_{out} - P_{in}$ is transformed into heat, therefore, minimizing the Power loss P_{loss} and maximizing the output power P_{out} thus having a low ratio of P_{loss} / P_{out} as illustrated in figure 1.5 is desirable.

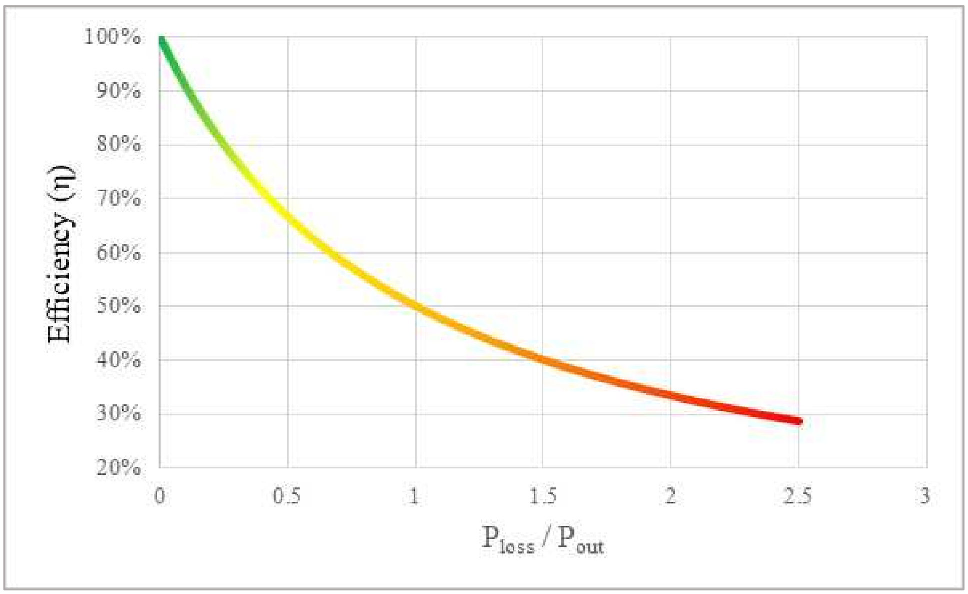

Figure 1.5 Converter power loss vs. efficiency

The goal of power electronics technology in terms of packaging is to construct converters of small size and weight, which can process substantial power at high efficiency see figure 1.6.

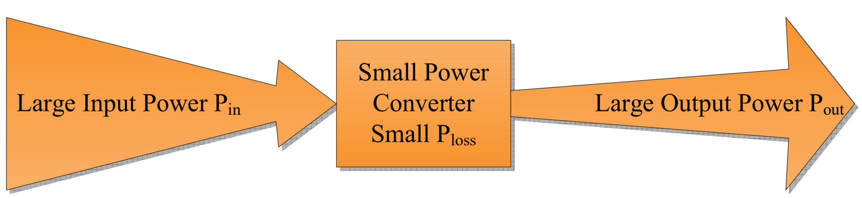

Figure 1.6 Power Converter Goal

Switching regulation is a technique by which unregulated source power is efficiently converted to regulated load power through the use of controlled power switching devices. The emphasis on switching techniques, as opposed to linear techniques, relates to efficiency. An ideal switch has no losses, there is either voltage or current, but not simultaneously [8]. Switching regulation can take different forms as illustrated in Table 1.1.

Converter	Conversion Type	Typical Use
AC-DC	Alternating Current to Direct Current	Typical used Power Rectification from a higher input Voltage to a lower Voltage
AC-AC	Alternating Current to Alternating Current	Converters the AC waveforms with one particular frequency and magnitude to another AC waveform with a different frequency and/or magnitude like the case of speed control of electrical machines.
DC-AC	Direct Current to Alternating Current	These converters are mainly used for driving low-power AC motors
DC-DC	Direct Current to Direct Current	These converters are normally used in battery power electronics, and their purpose is to either Step-Up the Input Voltage $V_{out} > V_{in}$; Step-Down the input Voltage $V_{out} < V_{in,}$ or Step-Down and Step-Up the input Voltage $V_{out} < V_{in}$ or $V_{out} < V_{in}$

Table 1.1 Switching Regulation types of Converters

Step-Down and Step-Up regulators also known as Buck-Boost are a form of switching-mode power converter that can supply a regulated DC output from a source voltage either above or below the desired output voltage. A Buck-Boost can be used in applications in which there is a necessity for the output voltage to be of a fixed value and the input voltage varies, this can be particularly helpful in battery-powered applications in which the battery voltage starts above the desired output but falls below as the battery drains; Automotive Electronics when the battery dips down during cold cranking or a stop-start condition. Or in the opposite condition when there is a need for a variable output voltage, and the input voltage is of a fixed value which is the case for a USB Type- C™ power delivery standard where the output voltage has a variable output voltage that can be higher or lower than the input voltage. USB Type-C has port voltages selectable from 5 V to 20 V. Or a combination of the previous both cases, widely variable output voltage with a variable input voltage like it is the case for Automotive USB Type-C™, all these cases are illustrated in figure 1.7 [10].

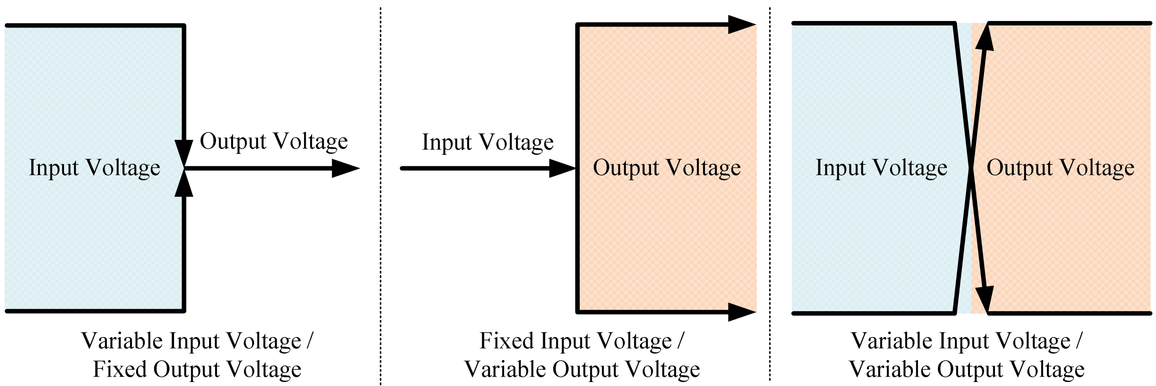

Figure 1.7 Buck-Boost Voltage Configurations

When it comes to designing Buck-Boost converters, there is a huge gap between the simple inverting Buck-Boost converter fully described in textbooks, which produces a negative output voltage, and real-world buck-boost applications that require a positive output [10].

Commonly used solutions for the non-inverting Buck-Boost fall into one of five groups based on the number of inductors, capacitors, switches, and feedback control loops required as well as the system order. A summary is provided in table 1.2. and a circuit diagram for each is shown in figure 1.8.

	Number of Inductors	**Number of Capacitors**	**Number of Switches**	**Number of Control Loops**	**Order of the Control System**	**Output Noise / Ripple** [11]–[14]
Cascaded Boost-Buck	2	2	4	2	Two-second order	Low Input and Output
SEPIC	2	2	2	1	Fourth Order	Low Input
ZETA (Inverse SEPIC)	2	2	2	1	Fourth Order	Low Output
Flyback	2	1	2	1	Third Order	High Input and Output
Merged Buck-Boost	1	1	4	2	Second Order	High Input and Output

Table 1.2 Commonly used solutions for the non-inverting buck-boost

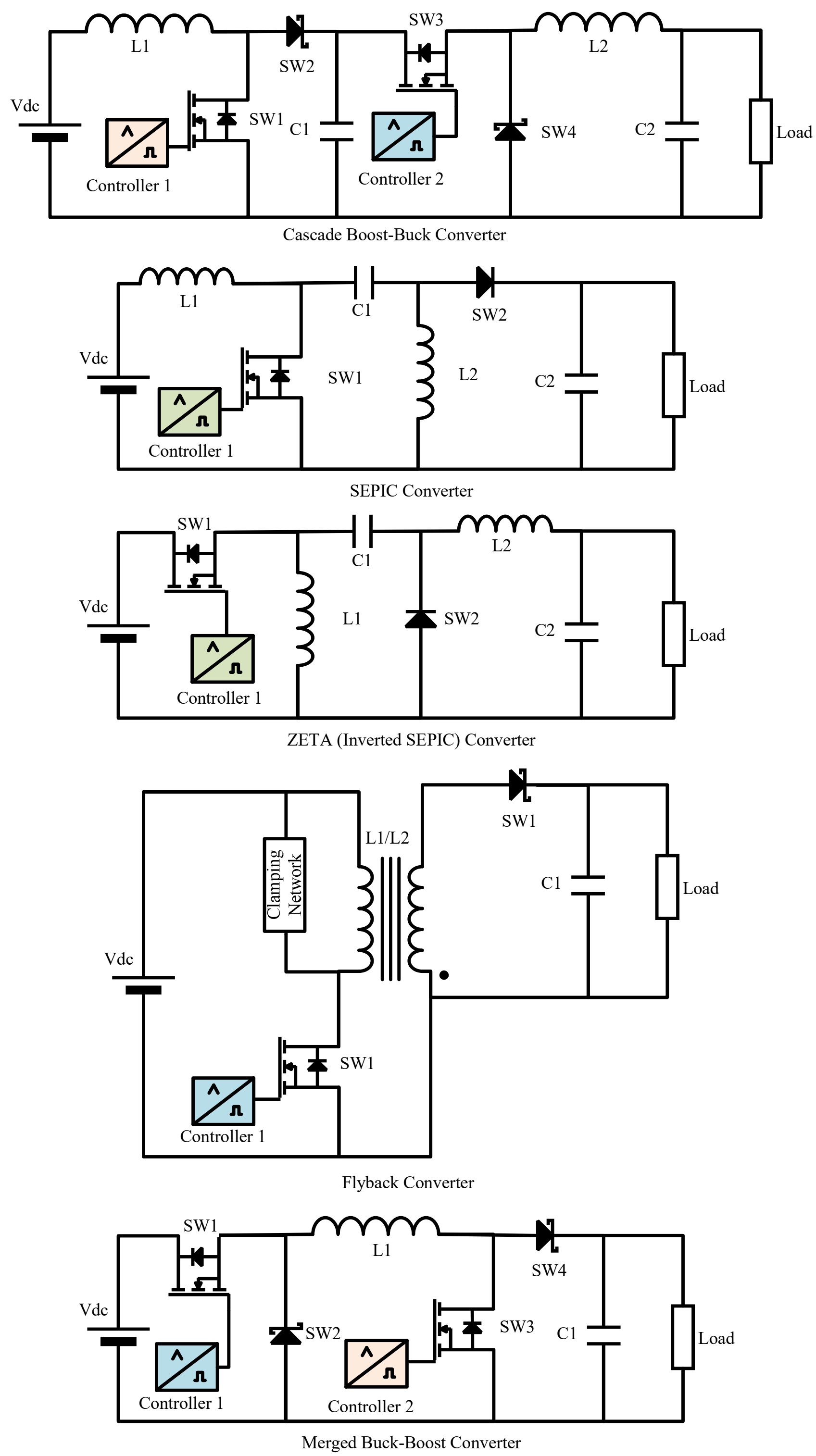

Figure 1.8 Commonly used solutions for the non-inverting Buck-Boost circuit diagrams

From all the five commonly used solutions for the non-inverting Buck-Boost the SEPIC and Zeta converter utilize the least number of switches which is key to achieving high efficiency η and less cost, in addition to only one control loop as well as low input and output voltage noise/ripple which is an important factor while providing power to sensitive VLSI devices.

However, these converters being a fourth-order system, a PID compensator is not suitable as explained in previous pages, therefore requiring a more complex and new method to control the dynamics of these newer power electronics.

There is very little design information available on SEPIC and ZETA converters identified by Raymond A. Mack [15]. In his search of commercially available SEPIC and Zeta Controllers, he found two barely adequate design descriptions, one from Texas Instrument and one from Analog Devices. This makes the SEPIC and Zeta converter an interesting research converter topic, especially the Zeta converter due to his low output ripple which is desired for modern VLSI electronics.

We can conclude from this section that a lot is being written in the academia about PID, MPC, and Sliding Control (figure 1.3) in comparison to State Feedback Control and State Observers / Estimators, suggesting that a contribution in this area could be made. The development of digital processing doubling every year (figure 1.2) makes the state-space methods very suitable for digital-based implementation (Discrete-time vs Continuous time) which has not been exploited. The advances in microelectronics required a new modern type of power electronics suitable for high efficiency and low voltage output ripple to avoid voltage breakdown.

1.2 Literature Review and Gap in the current research

State-space averaging and linearization are analytical approximation techniques that allow switching regulators to be represented as linear systems. More specifically, state-space averaging allows the switched (i.e., discontinuous) system to be approximated as a continuous Non-linear system, and linearization allows the resulting Non-linear system to be approximated as a linear system. The criterion for the continuity approximation is that the circuit's natural frequencies and all modulation frequencies of interest must be sufficiently low with respect to the switching frequency. The criterion for the linearity approximation is that the time variations, or AC excursions, of the pertinent variables about their respective DC operating points, must be sufficiently small [8]. One of many motivations approximating the switching regulator as a linear system is the existence of very well know and efficient control techniques that facilitate the analysis of these power converters.

As previously discussed, the Zeta converter is a fourth-order system, therefore requiring a more complex method to control the dynamics of this DC-DC power converter electronic. Various control schemes have been proposed to address these dynamic difficulties such as transient response, steady-state errors, and guarantee stability. These control techniques range from linear techniques, such as proportional-integral (PI), proportional-integral-derivative (PID), Model Predictive and Adaptive controllers based on average models to fuzzy logic and genetic algorithms and from Non-linear techniques and feedforward control to sliding mode and $H\infty$ methods [16].

Although existing control approaches are effective, several challenges have not been fully addressed yet, such as ease of controller design and tuning, as well as robustness to load parameter variations and plant model uncertainties. Furthermore, the computational power available today has not been fully exploited, most of the available literature (one out of twenty-one publications) is in the continuous time domain and consequently in the frequency Laplace domain (invented in the eighteenth century).

E. Vuthchhay and C. Bunlaksananusorn first published in 2008 an approach to the Dynamic Model of a Zeta Converter with a State-Space Averaging Technique [17] and in 2010 a control method based on a PI compensator in the continuous time domain and frequency domain [18] see figure 1.9 and figure 1.10, respectively.

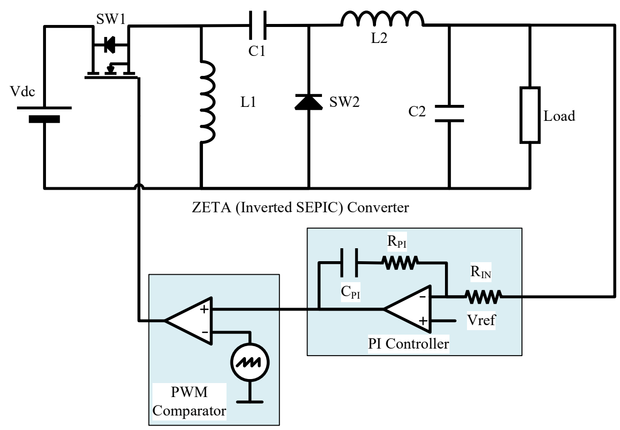

Figure 1.9 Zeta converter with PWM feedback control

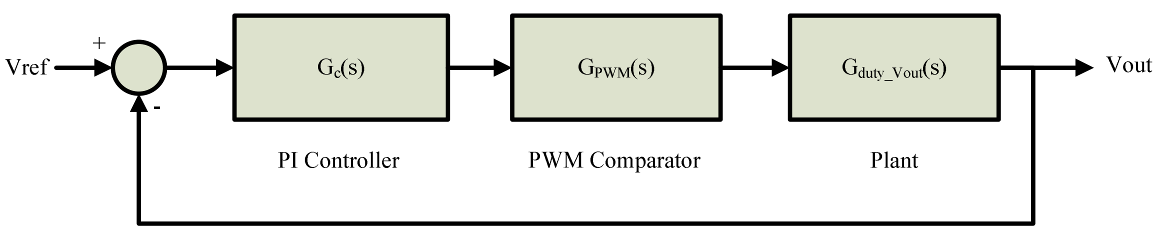

Figure 1.10 Zeta converter with PWM feedback control block diagram in s domain

Although this approach showed satisfactory results for load regulation (Output load variation from one ampere to five amperes) the plant parameters have to be well-known before designing the controller which is not always the case. In addition, plant parameters can change over time thus degrading the performance of such controller implementation.

Similarly, Renan C. Viero and Fernando S. dos Reis proposed an analogous approach in Designing Closed-Loop Controllers Using a Matlab® Dynamic Model of the Zeta Converter in DCM [19] adding a derivative term (PID) and comparing this controller to a Lead Compensator.

P. Ramesh Babu and S. Ram Prasath in Simulation and Performance Analysis of CCM Zeta Converter with PID Controller [20] as well as Zia Ul Ha and Aashir Ali in Comparative study of Zeta converter and Boost converter Using PI controller [21] utilized Ziegler-Nichols method for tunning the gain PID gains [6], method first published in 1945. The Ziegler–Nichols rules for tuning PID controllers have been very influential. The rules do, however, have severe drawbacks, they use insufficient process information and the design criterion gives closed-loop systems with poor robustness. Ziegler and Nichols developed their tuning rules by simulating a large number of different processes and correlating the controller parameters with features of the step response [22]. Man Mohan Garg, Yogesh V. Hote, and Mukesh K. Pathak [23]suggested an approach in their publication "PI Controller Design of a dc-dc Zeta Converter for Specific Phase Margin and Cross-over Frequency" where the gains K_i and K_p are calculated by adding a phase margin tester $e^{-j\Phi}$ in the feed-forward path and solve it for a very specific phase margin. Dual-loop PI control is proposed by Y. T. Yau, K. I. Hwu, C. W. Wang, and J.-J. Shieh in [24]. The outer loop stabilizes the output voltage while the inner loop controls the voltage across the bypass capacitor. A performance test is performed for load variation with satisfactory results; however, this approach only considers well know plant parameters and no uncertainties.

Various intelligent algorithms such as the Genetic Algorithm, Simulating Annealing Algorithm, Artificial Bee Colony Algorithm, and Firefly Algorithm, are implemented in different power converters to study the compatibility of the algorithms as well as improvement of the performances of power converters[25]. K. Durgadevi and R. Karthik in their publication “Performance Analysis of Zeta Converter Using Classical PID and Fractional Order PID Controller (FOPID) ” [26] through simulation it is confirmed that the FOPID controller gives better the transient response of the feedback system by using a significantly smaller control effort, the Internal Absolute Error (Cost Optimization function *J* using Artificial Bee Colony algorithm based on the intelligent foraging behavior of honey bee swarm, proposed by Derviş Karaboğa) of the variations of the output voltage is minimized to variations in the input voltage. Still, this method requires knowledge of the plant and only demonstrates performance to variations of input voltage. S. Suwannaprom [27] proposed Genetics Algorithms for PI controller gain tunning K_p and K_i for transient performance optimization requiring an off-line learning procedure. M. M. Nishat, M. R. K. Shagor, H. Akter, S. A. Mim, and F. Faisal, in their heuristic optimization approach to PID using Particle Swarm for gain tunning, contrast their optimization tunning for three different objective functions and conventional PID, they do not evaluate transient performance for plant variations.

A.Mehta, B. Naik [28] and S. K. Pandey, S. L. Patil, S. B. Phadke and A. S. Deshpande [29] introduced an approach to control a Zeta converter using the Non-linear technique Slide Mode Control (SMC). In their approach a control input $u=u_{eq}+u_n$ where

u_{eq} is designed to take care of the known parameters and u_n about the disturbances to the system. If the disturbances are bounded, then they can be included in u_{eq}. They deal with two uncertainties the load resistor and the input voltage and yield to a simplified control law $u = V_{ref} (V_{c1} + V_{in})^{-1}$, where V_{c1} is the bypass capacitor voltage, V_{ref} the reference/set point voltage, and V_{in} the input voltage. This approach requires that we have an accurate estimation of the V_{c1} which is not always the case (An observer will take care of this).

Another Non-linear approach was presented in [30], a Fuzzy Logic Controller (FLC) for a Zeta Converter. This approach does not rely on any mathematical model of the plant but requires expert knowledge to determine the Fuzzy Logic Rules and also requires a large amount of computing power, the overshoot to changes in input voltage and output resistance was very significant and not practical to modern requirements of current microelectronics (Breakdown voltage).

D. A. M. Cirino, R. D. Zamora, and E. I. O. Rivera in [31] proposed using a Passivity Based Control (PBC). Passivity-based control is a Non-linear methodology that consists in controlling a system to make the closed-loop system passive. Even though their approach showed stability during variations of input voltage and output load, some of the transient performance might not be adequate to the requirements of new microelectronics similar to [30], in addition, implementation of the control law might be a computational challenge.

H. Sarkawi, M. H. Jali, T. A. Izzuddin, and M. Dahari were the first to introduce the concept of state-feedback control to Zeta Converters in 2013 (see figure 1.11) in their " Dynamic Model of Zeta Converter with full-state feedback controller implementation " [32] publication. Compared to another compensator such as PID, a full-state feedback controller is a time-domain approach which makes the controller design less complicated than the PID approach which is based on a frequency-domain approach. This is due to the modeling process being based on state-space matrices (Eq 1.4).

$$\dot{\mathbf{x}}(t)=\mathbf{A}\cdot\mathbf{x}(t)+\mathbf{B}\cdot\mathbf{u}(t)\ ; \qquad \text{Eq 1.4}$$

$$\mathbf{y}(t)=\mathbf{C}\cdot\mathbf{x}(t)+\mathbf{D}\cdot\mathbf{u}(t)$$

Where **x(t)** is the state vector, **y**(t) is the output vector, **u**(t) is the input/control vector, **A** is the state/system matrix, **B** is the input matrix, **C** is the output matrix and **D** is the feedthrough /feedforward) matrix.

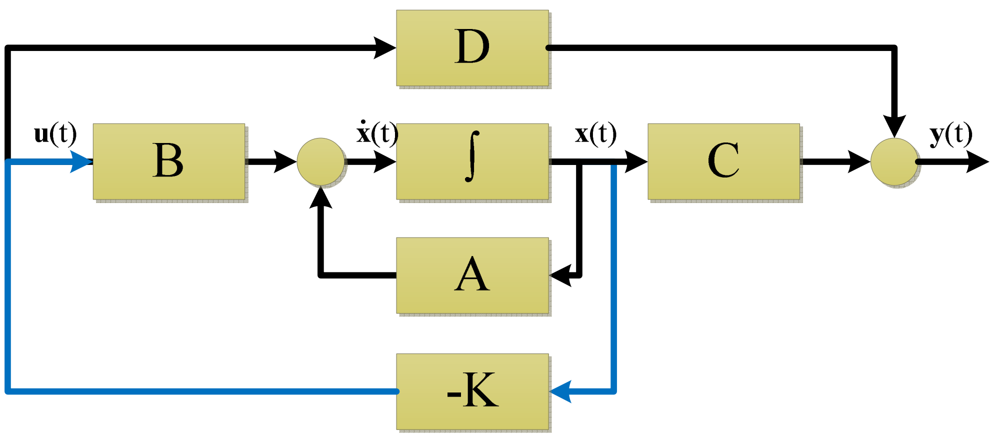

Figure 1.11 Full-state Feedback block diagram [33]

In the Full-state feedback approach a control law for a system that is completely controllable is defined by $\mathbf{u}(t)= -\mathbf{K}\cdot\mathbf{x}(t)$; where **K** is the feedback gain used to position the poles of the plant to their desired value, [32] used the optimization method LQR and a cost function $J=\int_0^\infty (\ \mathbf{x}^T(t)\cdot\mathbf{Q}\cdot\mathbf{x}(t)+\mathbf{u}^T(t)\cdot\mathbf{R}\cdot\mathbf{u}(t)\ )\,dt$ to optimize the K gain. Results meet the regulation specifications however one important element is they assume all states are known and accessible by the controller which is not the case all the time. Also, their approach account for variation in the input voltage and output load but not uncertainties in the plant parameters captured in the system **A** matrix.

H. Sarkawi in [34] added to his previous publication on full state feedback convex polytope model instead of the conventional nominal value model of the dc-dc zeta converter. The convex polytope model of the dc-dc zeta converter considers parameter uncertainty. A linear matrix inequality (LMI) is formulated based on the linear quadratic regulator (LQR) problem to find the state-feedback controller for the convex polytope model.

The difference between classic feedback controllers like PID and adaptive controllers is that the classic controller uses the principle of feedback to compensate for unknown disturbances and states in the process [35]. How the error is processed (Through the controller) is the same in all situations. An adaptive control system on the other hand automatically compensates for variations in system dynamics by adjusting the controller characteristics so that the overall system performance remains the same, or rather maintained at the optimum level, it alters how the error is processed, and it adapts the control law. This control system considers any degradation in plant performance with time [36]–[38]. Even though a unified approach to classifying Adaptive systems has not been agreed [35] suggests an adequate classification for this research see figure 1.12.

An adaptive controller based on a heuristic approach provides adaptability directly either by evaluating the plant output y(t) or its feedback error e(t) = u(t)-y(t) or selected quality criteria for the plant. When synthesizing this kind of controller, the criteria that quantifies the quality of the control plant is optimized. This approach satisfies practical applications while also being robust [35].

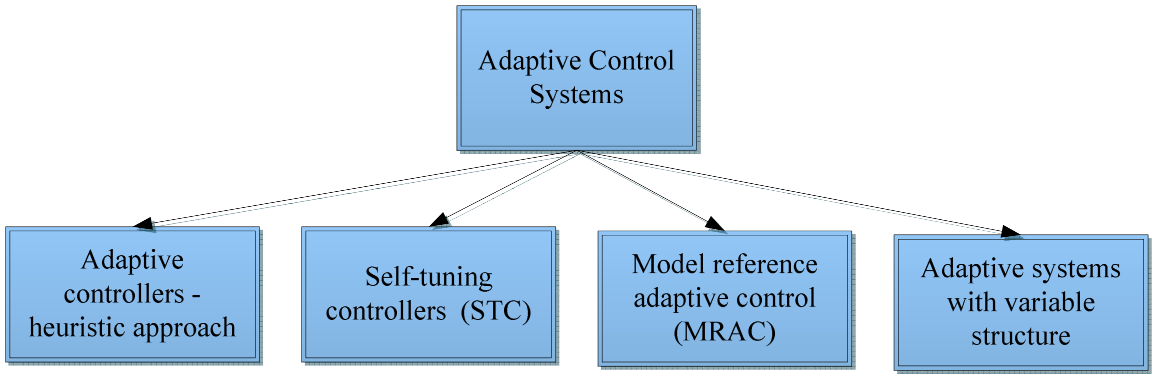

Figure 1.12 Classification of adaptive control systems [35]

Adaptive systems which have a variable structure will purposely alter their structure following the set procedure. Since such a system alters its structure based on experience gained previously in its working life, it may be regarded as a self-organizing system.

Model reference adaptive control (MRAC) system design is theoretically well elaborated and widely discussed in the scientific literature [39], [40], where a reference model is specified with the desired dynamics of the closed loops transient response. The real plant systems response is compared to the reference model and the poles of the system are placed (i.e., gain pole placement) to match each other. The dual character of this adaptive system is important since it can be used both for control and to identify the parameters of the model process or to estimate the state of the system. These systems are, to a certain extent, limited by the fact that they are only suited to deterministic control [35].

A self-tuning controller (STC) is capable of optimizing its internal running parameters to maximize or minimize the fulfillment of an objective function, typically error minimization.

An attempt to implement a Model Reference Adaptive Controller for Zeta Converters is published in [41], [42] in their approach they define an adaptive control law where the gains of the controller are related to the reference input (r), the error between the output of the real plant y_p and the reference model output y_m and the out of the plant, this adaptive control law is expressed as follows $f_y = k_r r + k_e \left(y_p - y_m\right) + k_p y_p$. The gains “k” of the adaptive controller is estimated through a sliding surface. A. Izadian and P. Khayyer focus on [41], [42] on adapting the control law to cope with the uncertainties and variations of the plant parameters.

B. Moaveni1, H. Abdollahzadeh2, and M. Mazoochi in Adjustable Output Voltage Zeta Converter Using Neural Network Adaptive Model Reference Control [43] utilize a Back Propagation of errors neural networks to calculate the gains of the adaptive identifier as well as of the adaptive controller, they successfully identified the plant and control a variable output voltage to static input and output conditions.

1.3 Research objectives and contributions

Out of more than three hundred research papers on Zeta Power Converters published in the IEEE Xplore® digital library, twenty-one of them [17]–[21], [23]–[32], [34], [41]–[45] addressed controllability in the continuous time domain and transient response performance to bounded uncertainties of input and output parameters. Focus has been on coping with uncertainties by making the controller more robust or incentive to disturbances, but no research has been published addressing the uncertainties of the plant and making the plant model more accurate to the initial estimation, posing the question could a discrete time state observer estimate properly the states of the plant. As well research has fallen short to answer the question if state-feedback control law can be properly used with estimated states from the observer. In addition, all adaptability work has been done in the controller field but not explored in the field of state observers, raising the question if an adaptability law can be derived to increase the performance of state-observer estimation.

Given the lack of research regarding discrete-time control for Zeta Power Converters, state space observers, and adaptive state estimation as described in the previous paragraph, this research aims to identify a novel way of controlling Zeta Converters using adaptive state observers and state feedback in the discrete-time domain that yields robustness in the presence of plant uncertainties.

The research objectives of this dissertation are six:

1. Contribute and fill a gap in the academic research field of State Feedback Control and State Observers of Zeta Power Converters Control in the Discrete Time Domain
2. Identify a Discrete-Time Full-State Observer that can properly estimate the plant states in the presence of plant uncertainties in a Zeta Power Converter.
3. Identify, evaluate, and compare a Robust Full-State Observer that could improve the performance of the full-state Observer.
4. Identify, evaluate, and compare an Adaptive and Robust Full-State observer that could improve the performance of the full-state Observer.
5. Prove that the estimated states can be used in combination with the state feedback gain by placing the closed loop poles to achieve a maximum 30% OS of output voltage with load current changes +/- 70%: input voltage changes +/- 50% and other plan uncertainties +/- 20%.

6. Build a MATLAB&SIMULINK® Model that will simulate the dynamics of the Zeta Converter, State Observer, and State Feedback control law to verify objective one through four.

At the end of this research, this study will contribute to the body of knowledge on State-Space Observers, State-Feedback, and Adaptability of Zeta Power Converters in the discrete-time domain. This will help address the current gap of research in this area.

1.4 Dissertation preface and outline

Chapter one has presented an introduction, background, literature overview, aim and objectives of this research as well as the justification. Chapter two will introduce the Zeta converter, and its Non-linear nature and describe in detail the linearization methods for the Power Converter: small-signal canonical models and state-space averaging method. Chapter three will discuss in detail state observers/estimators for control systems, their implications in the discrete-time domain, and the potential instabilities due to sampling time and position of poles. This chapter will also describe the principle of separation of estimation and control which states that under some assumptions the problem of designing an optimal feedback controller for a stochastic system can be solved by designing an optimal observer for the state of the system, which feeds into an optimal deterministic controller for the system. Chapter four will address how to handle plant uncertainties in the state observer/estimator model of the Zeta Power. Chapter five will introduce the concept of adaptability for control and state estimation as well as identification of a suitable adaptive state observer while chapter six will apply it to a zeta converter as well as compare its performance to a full state observer. Chapter seven will summarize the conclusion of the research work and outline potential future research work possibilities.

CHAPTER TWO

LINEARIZATION METHODS FOR NON-LINEAR POWER CONVERTERS

DC-DC Switch Mode Power Converters represent a simple yet efficient way of DC regulation by a discontinuous feedback control action, where packets of energy, store in inductors and capacitors, are transfer from the input source to the output load by switches both transistors and diodes at rate defined by the switching frequency of the converter (see figure 2.1).

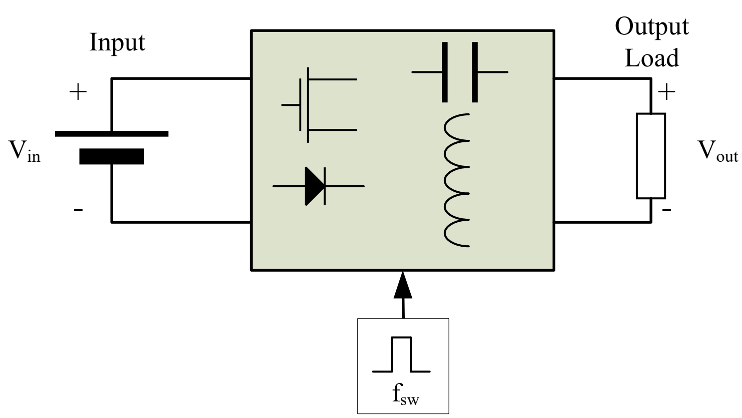

Figure 2.1 DC-DC Power Converter

In DC-DC Power converters, the switches controlling the dynamic transfer of power from input to output are either fully ON or fully OFF, with very short transition times from one of these states to the other. Component voltage waveform shapes take the forms of periodic pulse-width-modulated (PWM) rectangles waves, while the associated current waveform shapes are usually triangular. Due to this Switching behavior the DC-DC power converters are fundamentally Nonlinear.

State Space averaging and linearization are analytical approximations techniques that allow power converters to be represented as linear systems. More specifically, Sate Space Averaging allows the switched DC-DC power converter (discontinuous) system to be approximated as a continuous one but still nonlinear. Linearization allows the resulting nonlinear system to be approximated as a linear one. The condition for the continuity approximation is that the circuit natural frequencies and all modulation, or signal, frequencies of interest must be sufficiently low with respect to the switching frequency. The criterion for the linearity approximation is that the time variations, or ac excursions, of the pertinent variables about their respective DC operating points must be sufficiently small.

Section 2.1 will contemplate the circuit operation and waveforms for an ideal Zeta converter in continuous conduction mode. In Section 2.2, equations for the Zeta Converter large-signal steady-state behavior will be presented in a Nonlinear State-Averaging way. In Section 2.3, a small-signal characterization of the Zeta converter will be derived, and a linear time-invariant model of the Converter will be presented using State-space averaging form for a DC operating point.

2.1 Zeta Power Converter operation

As described in chapter one the Zeta Power Converter topology provides a positive output voltage from an input voltage that varies above and below the output voltage. Figure 2.2 depicts a circuit diagram of the Zeta Power Converter consisting of two inductors L_1 and L_2; a bypass AC coupling capacitor, C_1; a power MOSFET switch SW_1; and a rectified diode, SW_2; and an output Capacitor C_2. The power converter transfers the energy from the input DC voltage source Vin to the output load.

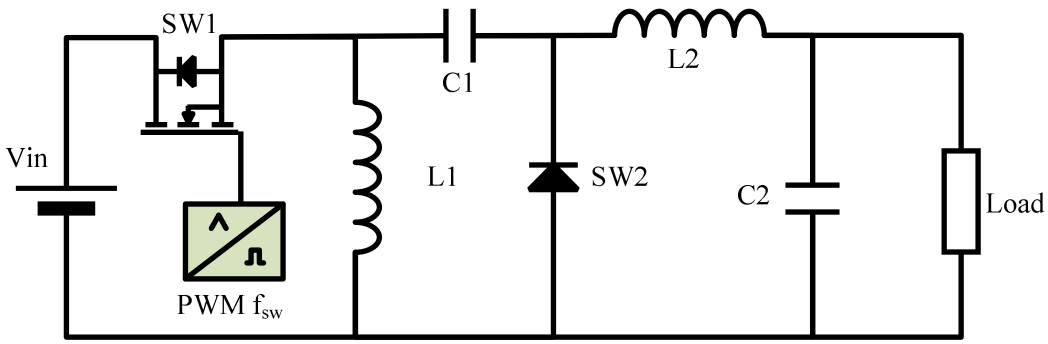

Figure 2.2 Zeta Power Converter

Initially, before starting the circuit operation, it is to be assumed that all the energy-storing components in the circuit, i.e., inductors and capacitors, do not have any energy in them. To easily understand and simplify the working of the zeta converter, the operation of the circuit is divided into four phases.

Phase 1 starts when the SW1 is closed. At this time the voltage source Vin is applied to the inductor and the current starts to flow at a rate $\frac{di}{dt}$. The energy store in the inductor $E_{L1}=\frac{1}{2}L_1 \cdot I_{L1}{}^2$ during in cycle is then discharge in phase 2. During this phase 1, no current is supplied to the load thus the shaded part of the circuit of figure 2.3 is inactive.

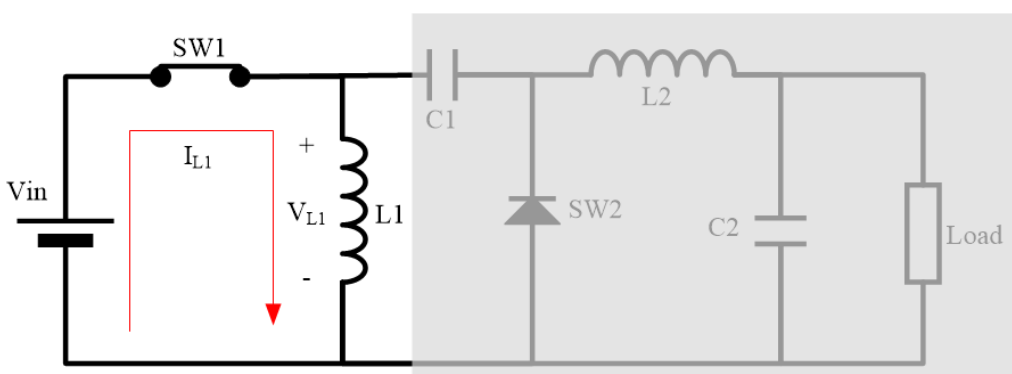

Figure 2.3 Phase 1: Zeta Power Converter Initial charge

Phase 2 starts when SW1 is open, the source current stops flowing through the inductor L1 and since an inductor does not allow a sudden change in current through it, the polarity of the inductor gets reversed according to Lenz law. Now the inductor L1 starts realizing its stored energy with reversed polarity. The diode SW2 will be forward biased thus closed allowing the flow of inductor current through it, therefore the energy from the inductor L1 will flow through the diode and to the capacitor C1. The series capacitor C1 starts charging by the energy supplied by inductor L1. Thus, energy from the inductor L1 gets transferred to capacitor C1. During this phase, current is supplied to the load, nor does the power supply provide any current thus the shaded parts of the circuit of figure 2.4 are inactive.

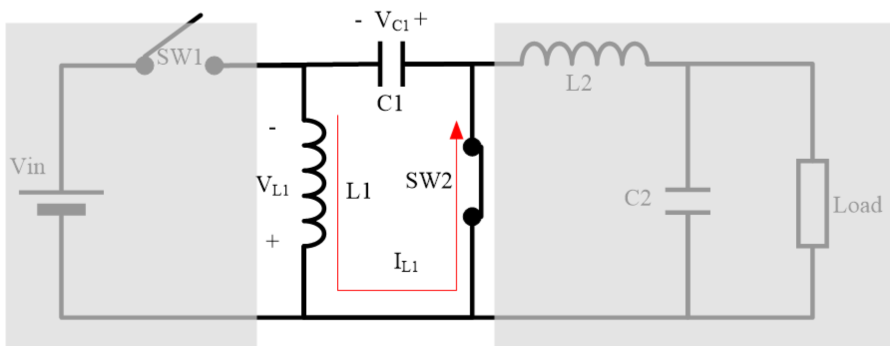

Figure 2.4 Phase 2: Zeta Power Converter Bypass Capacitor charge

Phase 3 starts when the SW1 is switched ON again, the discharged inductor L1 gets charged by the voltage source as in phase 1. Also in this state, the charged capacitor C1 in the previous mode starts discharging through inductor L2, load, source, and back to capacitor C1. The capacitor C1 will supply its energy to the inductor L2, C2 and load. Thus, the load gets power in this mode and inductor L2 gets charged. The SW2 remains OFF as depicted in figure 2.5.

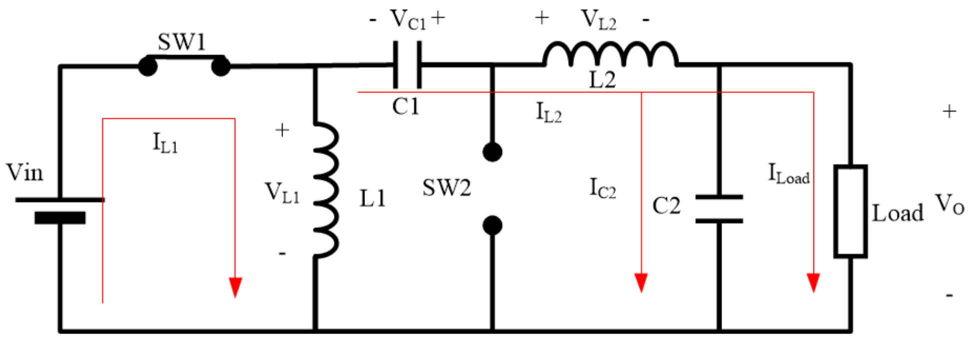

Figure 2.5 Phase 3: Zeta Power Converter

Phase 4 starts when the SW1 is turned OFF again, phase 2 will be repeated, the inductor L1 reverses its polarity and charges the discharged capacitor C1 through SW2. Along with it, the inductor L2 also reverses its polarity due to a sudden change in current and starts providing power to the load through the SW2 as well, C2 discharges and transfers its discharge energy to the load as shown in figure 2.6.

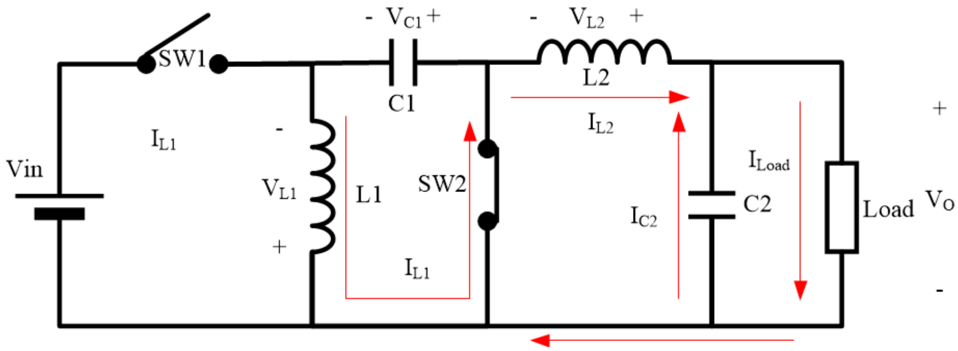

Figure 2.6 Phase 4: Zeta Power Converter

Phases 4 and 5 repeat throughout the operation of the Zeta power converter , when the SW1 is in the ON, inductor L1 gets charged by the voltage source and the inductor L2 by the bypass capacitor C1, when SW1 is OFF, the capacitor C1 gets charged by inductor L1 and inductor L2 and the Capacitor C2 supply energy to the load. Figure 2.8 depicts the waveforms of Phases 3 and 4 over the three periods. The electrical simulation circuit used to generate such waveforms is shown in figure 2.7.

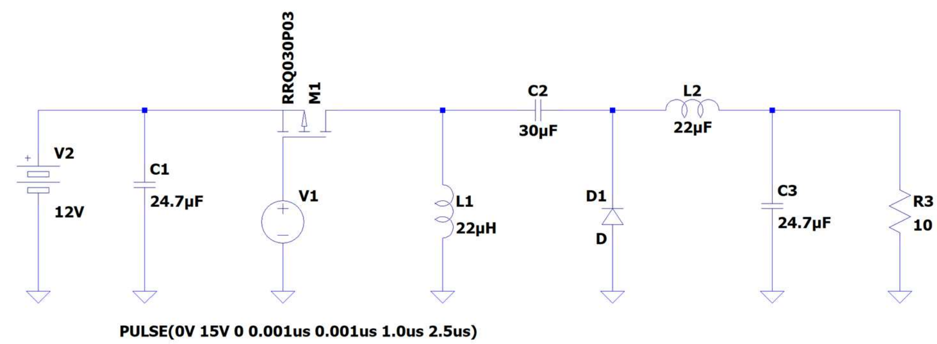

Figure 2.7 Electrical Schematic of Zeta Power Converter

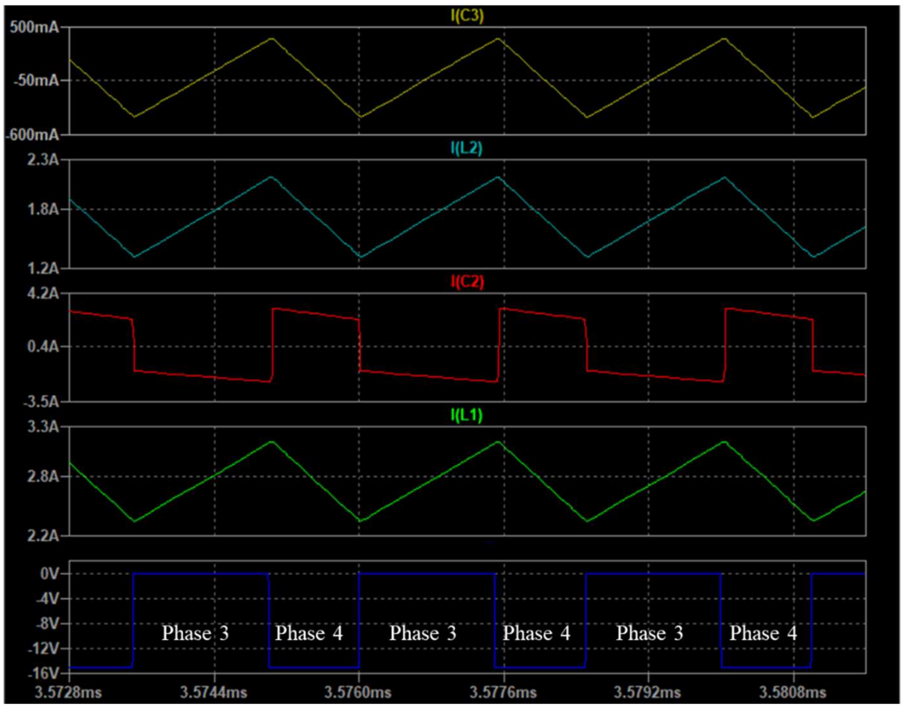

Figure 2.8 Simulation waveforms of Phases 3 and 4

2.2 Zeta Converter Large-Signal Non-Linear model

Modeling is the representation of physical phenomena by mathematical means. In engineering, it is desired to model the important dominant behavior of a system, while neglecting other insignificant phenomena. The resulting simplified model yields physical insight into the system behavior, which aids the engineer in designing the system to operate in a given specified manner [9].

In order to derive the Zeta Converter model, we will analyze the governing equation of the converter when it reaches steady state, phases three and four of section 2.2.

During phase 3 as depicted in figure 2.5 when the SW1 is ON and SW2 off, the voltage across L1 is equal to Vin (Eq 2.1). KVL across the L1, C1, L2 and C2 mesh yields to Eq 2.2. Applying KCL capacitor current I_{C1} is equal to minus I_{L2} (Eq 2.3) , while the current of C2 is equal to the current of L2 minus the Load current (Eq 2.4)

$$L_1 \frac{di_{L1}(t)}{dt} = V_{in}(t) = V_{L1}(t) \qquad \text{Eq 2.1}$$

$$L_2 \frac{di_{L2}(t)}{dt} = v_{in}(t)+v_{C1}(t)-v_{C2}(t)=V_{L2}(t) \qquad \text{Eq 2.2}$$

$$C_1 \frac{dv_{C1}(t)}{dt} = -i_{L2}(t)=i_{C1}(t) \qquad \text{Eq 2.3}$$

$$C_2 \frac{dv_{C2}(t)}{dt} = i_{L2}(t)-\frac{v_{C2}(t)}{R_{Load}} = i_{C2}(t) \qquad \text{Eq 2.4}$$

During phase 4 as illustrated in figure 2.6, and applying KVL and KCL yield to equation 2.2, 2.6, 2.7 and 2.8 .

$$L_1 \frac{di_{L1}(t)}{dt} = -V_{C1}(t) \qquad \text{Eq 2.5}$$

$$L_2 \frac{di_{L2}(t)}{dt} = -V_{C2}(t)=V_{L2}(t) \qquad \text{Eq 2.6}$$

$$C_1 \frac{dv_{C1}(t)}{dt} = i_{L1}(t)=i_{C1}(t) \qquad \text{Eq 2.7}$$

$$C_2 \frac{dv_{C2}(t)}{dt} = i_{L2}(t)-\frac{v_{C2}(t)}{R_{Load}} = i_{C2}(t) \qquad \text{Eq 2.8}$$

In order to model the full power converter a switching function $\delta^{(i)}$ will be defined as following (Table 2.1):

$\delta^{(1)}=1$ when SW1 is Closed and SW2 is Open	$\delta^{(1)}=0$ when SW1 is Open and SW2 is Closed
$\delta^{(2)}=1$ when SW1 is Open and SW2 is Closed	$\delta^{(2)}=1$ when SW1 is Closed and SW2 is Open

Table 2.1 Non-Linear Switching function $\delta^{(i)}$

Therefore, the Zeta power the complete dynamics of the Zeta power converter can be expressed as following :

$$V_{L1}(t)=L_1\frac{di_{L1}(t)}{dt}=V_{in}\delta^{(1)}+-V_{C1}\delta^{(2)} \quad \text{Eq 2.9}$$

$$V_{L2}(t)=L_2\frac{di_{L2}(t)}{dt}=(v_{in}(t)+v_{C1}(t)-v_{C2}(t))\delta^{(1)}-V_{C2}(t)\delta^{(2)} \quad \text{Eq 2.10}$$

$$i_{C1}(t)=C_1\frac{dv_{C1}(t)}{dt}=-i_{L2}(t)\delta^{(1)}+i_{L1}(t)\delta^{(1)} \quad \text{Eq 2.11}$$

$$i_{C2}(t)=C_2\frac{dv_{C2}(t)}{dt}=\left(i_{L2}(t)-\frac{v_{C2}(t)}{R_{Load}}\right)\delta^{(1)}+\left(i_{L2}(t)-\frac{v_{C2}(t)}{R_{Load}}\right)\delta^{(2)} \quad \text{Eq 2.12}$$

Equations 2.9 through 2.12 models the behavior of the Zeta power converter. This model is called Large-signal model as it describes the nonlinearities of the power converter in terms of the underlying nonlinear equations. This model non-linear and discontinuous systems would be very complex to analysis therefore in order to simplify the analysis of the converter, the non-Linear model and discontinuous system will be linearized and convert into a continuous one which will be the topic of next section.

2.3 Zeta Converter Small-Signal Linear model

An all-signal model is a model that is acceptably accurate over a large range on input signals, is a common analysis method used in electronic engineering to describe nonlinear devices in terms of the underlying nonlinear equations as described in section 2.2. A Small-signal modeling is a common analysis technique in power electronics engineering used to approximate the behavior of electronic circuits in which the high frequency AC signals (i.e., the time-varying currents and voltages in the circuit) are small relative to the low frequency bias currents and voltages.

In order to illustrate this method, we run a Fast Fourier transform to the Inductor current I_{L2} and Capacitor voltage V_{C3} simulating the electrical circuit from figure 2.7. The power converter switching frequency is set to f_s=400 kHz, the power spectrum of the V_{C3} and I_{L2} is illustrated in figure 2.9.

The power spectrum of a signal indicates the relative magnitudes of the frequency components that combine to make up the signal. As it can be observed in figure 2.9 the natural frequency of the Power Zeta converter for this particular circuit (figure 2.7) is $f_n = \frac{1}{2\pi\sqrt{LC}} = \frac{1}{2\pi\sqrt{22uH \cdot 24.7uF}} = 6.83kHz$ which is of 58 magnitude smaller that the switching frequency to f_s=400 kHz, also the magnitude of the current at the natural frequency is approx. 4.68dB compared to -36dB at the switching frequency. Also, it is important to observe that switching frequency harmonics appear every 400kHz however their magnitude keeps decreasing which each harmonic. The magnitude and phase of the Zeta converter depends not only on the control signal and duty-cycle variation, but also on the frequency response of the converter, however we can without harm to the dynamic of the converter neglect switching ripple therefore the objective of the modeling efforts is to predict this low frequency component, derive a small-signal model .

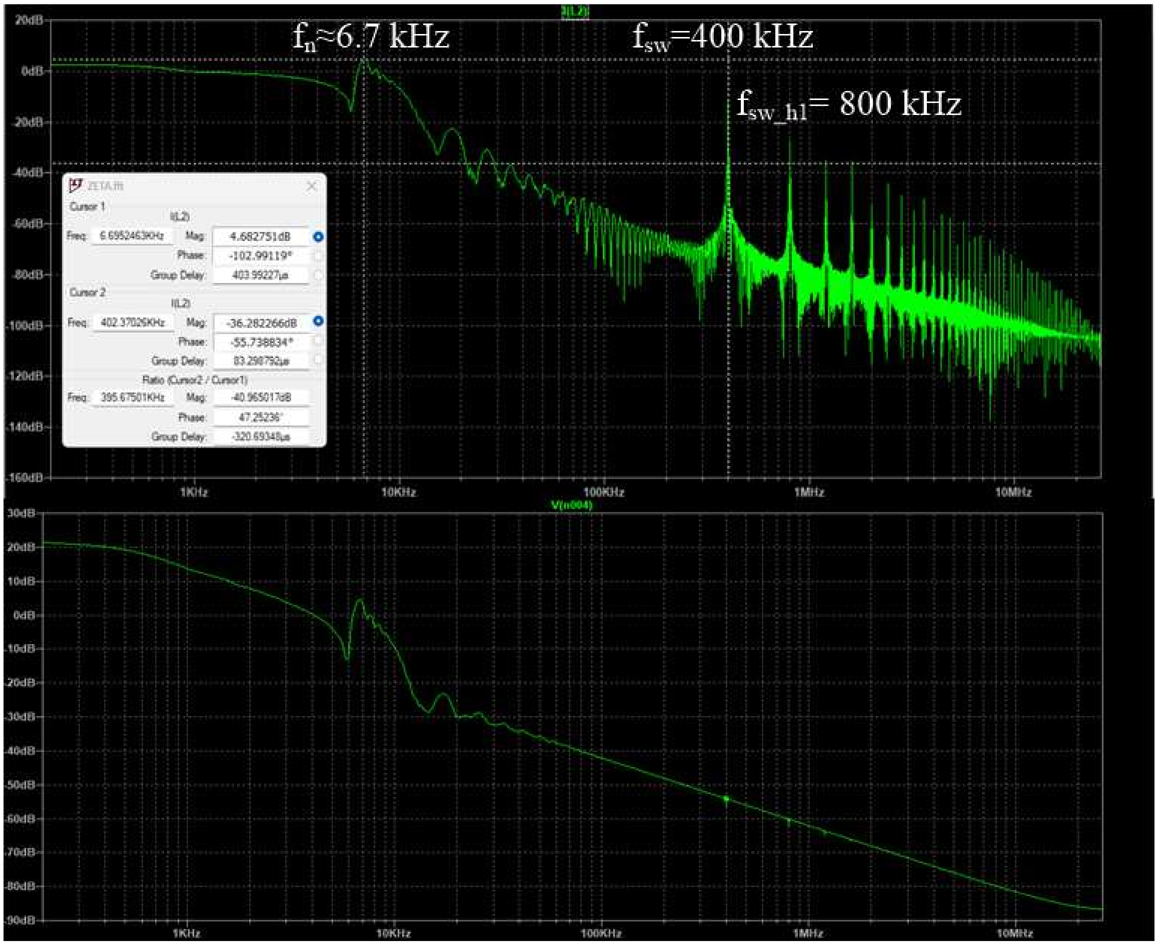

Figure 2.9 Power Spectrum of the V_{C3} and I_{L2}

A simple method for deriving the small-signal model of continuous conduction mode (CCM) converters which are inherently discontinuous is call AC averaging modeling where the switching ripples in the inductor current and capacitor voltage waveforms are removed by averaging over one switching period. Hence, the low-frequency components of the inductor and capacitor waveforms are modeled by equations 2.13 and 2.14 where $[x(t)]_{Ts}$ denotes the average of x(t) over an interval of length T_s, explicitly as following: $[x(t)]_{Ts}= \frac{1}{T_s}\int_{t-T_s}^{t+T_s} x(\tau)d\tau$ called moving average.

$$L\frac{d[i_L(t)]_{T_s}}{dt}=[v_L(t)]_{T_s} \qquad \text{Eq. 2.13}$$

$$C\frac{d[v_C(t)]_{T_s}}{dt}=[i_C(t)]_{T_s} \qquad \text{Eq. 2.14}$$

Through this method the high-frequency switching ripple is removed by averaging over one switching period. Yet the average value is allowed to vary from one switching period to the next, such that low-frequency variations are modeled. In effect, the “moving average” constitutes low-pass filtering of the waveform [9].

In order to illustrate the average and small ripple approximation of the Zeta converter lets looks at the voltage across the inductor L1 (figure 2.10) and the current through the capacitor C1 (figure 2.11) of the Zeta Power converter (figure 2.7) at an arbitrary time t.

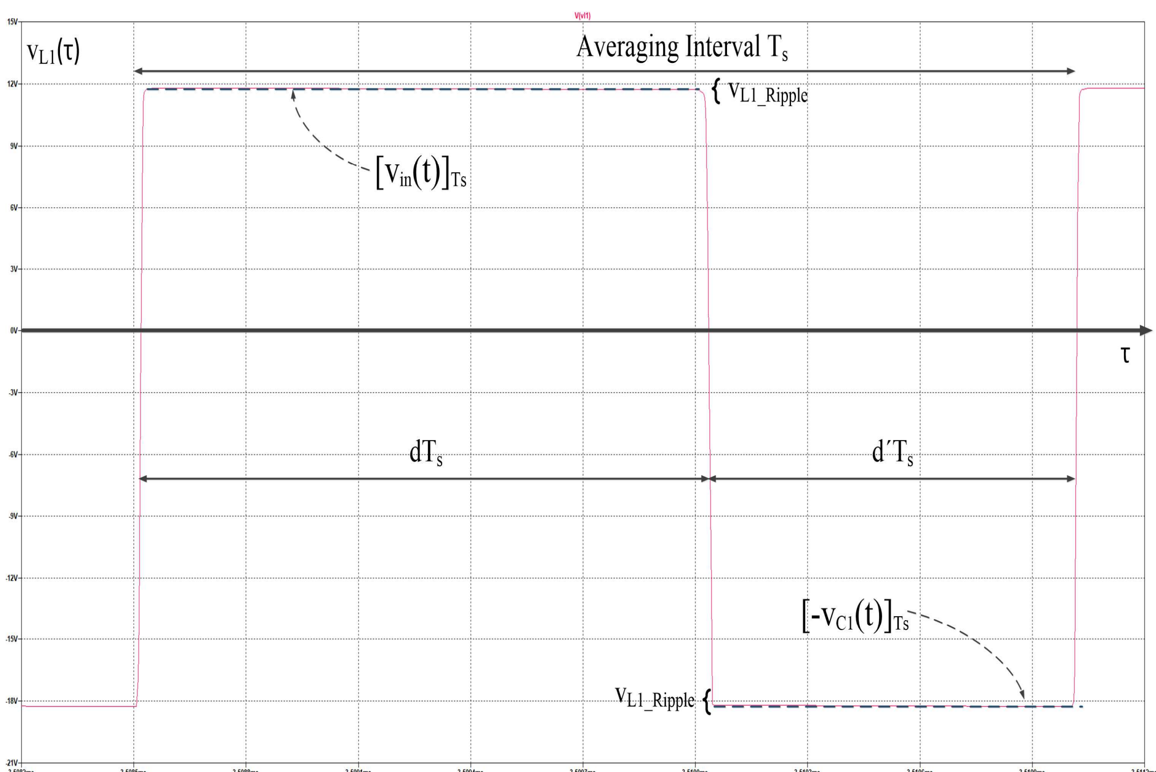

Figure 2.10 Voltage across Inductor L1 of Zeta Converter

The average inductor voltage across L1 can be expressed as $[v_{L1}(t)]_{Ts}=\frac{1}{T_s}\int_{t-T_s}^{t+T_s} v_{L1}(\tau)d\tau$ and the average current through the capacitor C1 is expressed as following $[i_{C1}(t)]_{Ts}=\frac{1}{T_s}\int_{t-T_s}^{t+T_s} i_{C1}(\tau)d\tau$. It can be seen in figures 2.10 and 2.11 that the ripples in the actual inductor current and capacitor voltage waveforms are small compared to their average values. Therefore, the integral can be approximated by calculating the are under the curve multiplying the average values by the respective d or d´ interval cycle of Ts (Eq. 2.15 and Eq. 2.16).

$$[v_{L1}(t)]_{Ts}=\frac{1}{T_s}\int_{t-T_s}^{t+T_s} v_{L1}(\tau)d\tau = d(t)\cdot[v_{in}(t)]_{Ts} + d'(t)\cdot[-v_{C1}(t)]_{Ts} \qquad \text{Eq. 2.15}$$

$$[i_{C1}(t)]_{Ts}=\frac{1}{T_s}\int_{t-T_s}^{t+T_s} i_{C1}(\tau)d\tau = d(t)\cdot[-i_{L2}(t)]_{Ts} + d'(t)\cdot[-i_{L1}(t)]_{Ts} \qquad \text{Eq. 2.16}$$

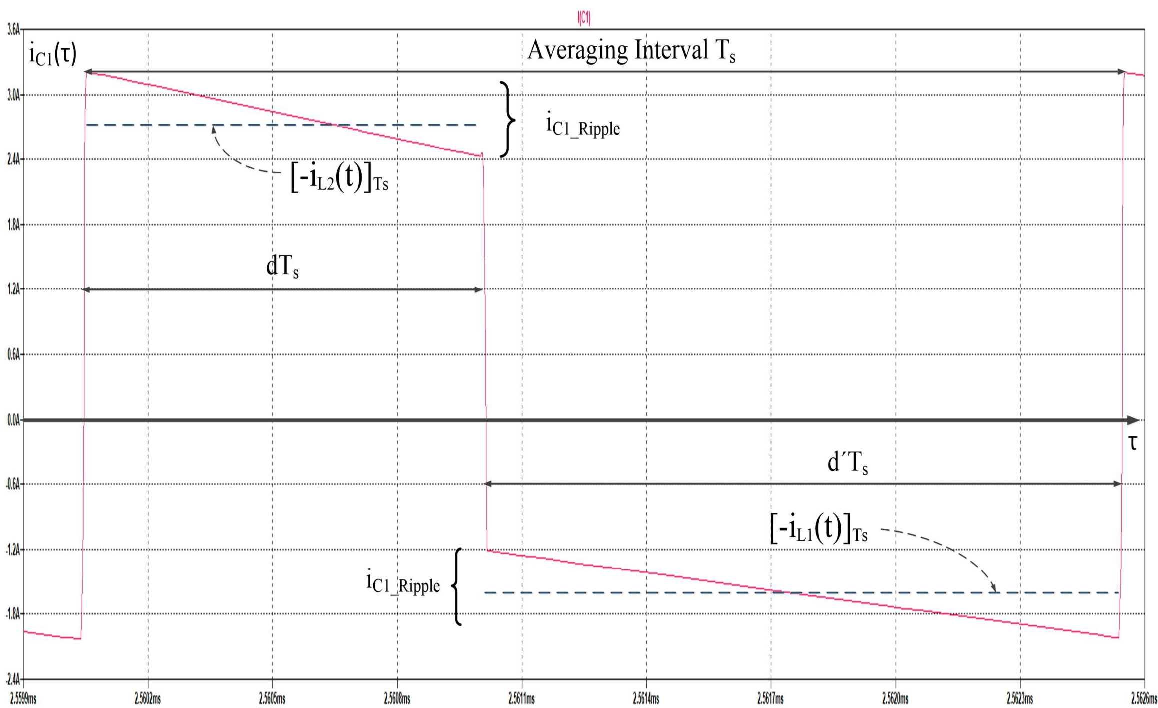

Figure 2.11 Current through Capacitor C1 of Zeta Converter

Insertion of equations 2.13 and 2.14 into 2.15 and 2.16 lead to the following equations (Eq. 2.17 and Eq. 2.18):

$$L1\frac{d[i_{L1}(t)]_{T_s}}{dt} = d(t)\cdot[v_{in}(t)]_{Ts} + d'(t)\cdot[-v_{C1}(t)]_{Ts} \qquad \text{Eq. 2.17}$$

$$C1\frac{d[v_{C1}(t)]_{T_s}}{dt} = d(t)\cdot[-i_{L2}(t)]_{Ts} + d'(t)\cdot[-i_{L1}(t)]_{Ts} \qquad \text{Eq. 2.18}$$

Equations 2.16 and 2.17 describe how the low-frequency components of the inductor current vary with time and it is equal to its average value times the d or d´ interval.

These are very useful derivations which are the basis of the state-space averaging method [46]. The state-space description of dynamical systems is a backbone of modern control theory; the state-space averaging method makes use of this description to derive the small-signal averaged equations of Power Converter. More specifically, Sate Space Averaging allows the switched DC-DC power converter (discontinuous) system to be approximated as a continuous system one but still nonlinear as it will be described hereafter.

Given a Power DC/DC PWM converter operating in continuous conduction mode. The converter circuit contains independent states that form the state vector **x(t)**, the converter is driven by independent sources that form the input vector **u(t)** that produce and output vector **y(t)**, the generalized state space equation is described in Eq 1.4. During the first subinterval, when the switches are in ON position (T_{ON} Figure 2.12), the converter reduces to a linear circuit that can be described by the following state equations 2.19 and 2.20 . During the second subinterval, with the switches in OFF position (T_{OFF} Figure 2.12) , the converter reduces to another linear circuit whose state equations are 2.21 and 2.22.

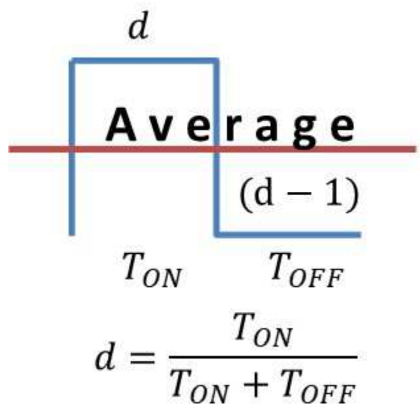

Figure 2.12 Power DC/DC PWM Cycle

$$\dot{\mathbf{x}}(t) = \mathbf{A}_{ON}\, \mathbf{x}(t)+\mathbf{B}_{ON}\, \mathbf{u}(t) \quad \text{Eq. 2.19}$$

$$\mathbf{y}(t)=\mathbf{C}_{ON}\, \mathbf{x}(t)+\mathbf{D}_{ON}\, \mathbf{u}(t) \quad \text{Eq. 2.20}$$

$$\dot{\mathbf{x}}(t) = \mathbf{A}_{OFF}\, \mathbf{x}(t)+\mathbf{B}_{OFF}\, \mathbf{u}(t) \quad \text{Eq. 2.21}$$

$$\mathbf{y}(t)=\mathbf{C}_{OFF}\, \mathbf{x}(t)+\mathbf{D}_{OFF}\, \mathbf{u}(t) \quad \text{Eq. 2.22}$$

During the two subintervals, the circuit elements are connected differently; therefore, the respective state equation matrices A_{ON}, B_{ON}, C_{ON}, D_{ON} and A_{OFF}, B_{OFF}, C_{OFF}, D_{OFF} may also differ. Given these state equations, the result of state-space averaging is the small-signal ac model. Provided that the natural frequencies of the converter, as well as the frequencies of variations of the converter inputs, are much slower than the switching frequency, then the state-space averaged model that describes the converter in equilibrium is embedded in Eq. 2.23 and 2.24.

$$\mathbf{\dot{x}}(t)=(\mathbf{A_{ON}}\ \mathbf{d}(t) + \mathbf{A_{OFF}}[\mathbf{1\text{-}d}(t)])\mathbf{x}(t) + (\mathbf{B_{ON}}\ \mathbf{d}(t) + \mathbf{B_{OFF}}\ [\mathbf{1\text{-}d(}t)]\ )\mathbf{u(}t) \qquad \text{Eq. 2.23}$$

$$\mathbf{y}(t)=(\mathbf{C_{ON}}\ \mathbf{d}(t)+\mathbf{C_{OFF}}\ [\mathbf{1\text{-}d(}t\mathbf{)}])\mathbf{x}(t) + (\ \mathbf{D_{ON}}\ \mathbf{d}(t)+\mathbf{D_{OFF}}\ [\mathbf{1\text{-}d(}t\mathbf{)}]\ )\ \mathbf{u(}t) \qquad \text{Eq. 2.24}$$

Using the previously derived equation that described the dynamics of the Zeta Power converter (Eq 2.9, 2.10, 2.11 and 2.12) and equations 2.17 and 2.18 that described the AC averaging and small-signal approximation equations can form a state-space small-signal averaged model equations of the Zeta Power Converter

$$\begin{bmatrix} \mathbf{\dot{x}_1}(t) \\ \mathbf{\dot{x}_2}(t) \\ \mathbf{\dot{x}_3}(t) \\ \mathbf{\dot{x}_4}(t) \end{bmatrix} = \begin{bmatrix} 0 & 0 & -\frac{(1\text{-}d(t))}{L1} & 0 \\ 0 & 0 & \frac{d(t)}{L2} & -\frac{1}{L2} \\ \frac{(1\text{-}d(t))}{C1} & -\frac{d(t)}{C1} & 0 & 0 \\ 0 & \frac{1}{C2} & 0 & -\frac{1}{R_{LOAD}C2} \end{bmatrix} \begin{bmatrix} \mathbf{x_1}(t) \\ \mathbf{x_2}(t) \\ \mathbf{x_3}(t) \\ \mathbf{x_4}(t) \end{bmatrix} + \begin{bmatrix} \frac{1}{L1}d(t) \\ \frac{1}{L2}d(t) \\ 0 \\ 0 \end{bmatrix} \mathbf{v_{in}}(t) \qquad \text{Eq. 2.22}$$

$$v_{OUT}(t)=[0 \quad 0 \quad 0 \quad 1] \begin{bmatrix} \mathbf{x_1}(t) \\ \mathbf{x_2}(t) \\ \mathbf{x_3}(t) \\ \mathbf{x_4}(t) \end{bmatrix} \qquad \text{Eq. 2.23}$$

Where the state-space variables are $i_{L1}(t)=x_1(t)$; $i_{L2}(t)=x_2(t)$; $v_{C1}(t)=x_3(t)$ and $v_{C2}(t)=x_4(t)$. The State Equation 2.22. is continuous as it has been averaged however as it involves multiplication of time varying quantities, for example $\dot{x_3}(t)$ the multiplication of the inductor's current $i_{L1}(t)$ and $i_{L2}(t)$ equations with the duty cycle d(t) which both variables are time-variant, the end equations are a set of non-linear differential equations that need to be linearized. We will linearize the state equations and construct a linear and small signal model about a quiescent operating point.

Since the state-space system defined in Eq 1.4 is a linear system, superposition holds, and it can be perturbed at the quiescent DC operating point by introduction of line voltage variations from the input voltage supply $\mathbf{v_{in}}(t)=\mathbf{V_{in.DC}}+\tilde{\mathbf{v}}_{\mathbf{in}}(t)$ causing a perturbation in the state vector $\mathbf{x}(t)=\mathbf{X_{DC}}+\tilde{\mathbf{x}}(t)$ where $\mathbf{X_{DC}}$ is the DC value and $\tilde{\mathbf{x}}(t)$ is the superimposed ac perturbation due to $\tilde{\mathbf{v}}_{\mathbf{in}}(t)$. In the same way the output state equation $\mathbf{y}(t)=\mathbf{Y_{DC}}+\tilde{\mathbf{y}}_{\mathbf{in}}(t)$, the new perturbed state space system is expressed in equation 2.24 where $\mathbf{D}= \mathbf{0}$ and $\mathbf{U}(t)= \mathbf{Vin}(t)$ [46].

$$\begin{aligned} &\dot{\mathbf{X}}_{DC} + \dot{\tilde{\mathbf{x}}}(t)=\mathbf{A}\cdot\mathbf{X_{DC}}+\mathbf{B}\cdot\mathbf{V_{in.DC}}+\mathbf{A}\cdot\tilde{\mathbf{x}}(t) +\mathbf{B}\cdot\tilde{\mathbf{v}}_{\mathbf{in}}(t) \\ &\mathbf{Y_{DC}}+\tilde{\mathbf{y}}(t)= \mathbf{C}\cdot\mathbf{X_{DC}}+\mathbf{C}\cdot\tilde{\mathbf{x}}(t) \end{aligned} \qquad \text{Eq. 2.24}$$

Eq 2.24 can be separated into 2 sets of systems, a steady-state DC system and a dynamic-state AC system, due to the fact that $\mathbf{X_{DC}}$ is a constant quantity its derivative $\dot{\mathbf{X}}_{DC}$ is zero. This leads to the following set of DC equations:

$$\mathbf{A}\cdot\mathbf{X_{DC}}+\mathbf{B}\cdot\mathbf{V_{in.DC}} = \mathbf{0} \qquad \text{Eq. 2.25}$$

$$\mathbf{X_{DC}}= -\mathbf{A}^{-1}\mathbf{B}\cdot\mathbf{V_{in.DC}} \qquad \text{Eq. 2.26}$$

$$\mathbf{Y_{DC}}= -\mathbf{C}\cdot\mathbf{A}^{-1}\mathbf{B}\cdot\mathbf{V_{in.DC}} \qquad \text{Eq. 2.27}$$

and a dynamical (ac) model:

$$\dot{\tilde{\mathbf{x}}}(t)=\mathbf{A}\cdot\tilde{\mathbf{x}}(t)\mathbf{B}\cdot\tilde{\mathbf{v}}_{\mathbf{in}}(t) \qquad \text{Eq. 2.28}$$

$$\tilde{\mathbf{y}}(t)= \mathbf{C}\cdot\tilde{\mathbf{x}}(t) \qquad \text{Eq. 2.29}$$

Suppose that the duty ratio changes from cycle to cycle, that is, $d(t)=D_{DC}+\tilde{d}(t)$ is the steady-state (DC) duty ratio as before and $\tilde{d}(t)$ is a superimposed (ac) variation. Applying the corresponding perturbation $\mathbf{x}(t)=\mathbf{X_{DC}}+\tilde{\mathbf{x}}(t)$, $\mathbf{y}(t)=\mathbf{Y_{DC}}+\tilde{\mathbf{y}}_{\mathbf{in}}(t)$ and $\mathbf{v_{in}}(t)=\mathbf{V_{in.DC}}+\tilde{\mathbf{v}}_{\mathbf{in}}(t)$ the basic model becomes equations Eq. 2.30 and 2.31:

$$\dot{X}_{DC} + \dot{\tilde{\mathbf{x}}}(t) = \mathbf{A}\cdot X_{DC}+\mathbf{B}\cdot V_{in.DC} \qquad \text{Eq. 2.30}$$

$$+\mathbf{A}\cdot\tilde{\mathbf{x}}(t)\mathbf{B}\cdot\tilde{\mathbf{v}}_{\mathbf{in}}(t)+\left[(\mathbf{A}_{\mathbf{ON}}-\mathbf{A}_{\mathbf{OFF}})\cdot X_{DC}+(\mathbf{B}_{\mathbf{ON}}-\mathbf{B}_{\mathbf{OFF}})\cdot V_{in.DC}\right]\cdot\tilde{d}(t)$$

$$+\left[(\mathbf{A}_{\mathbf{ON}}-\mathbf{A}_{\mathbf{OFF}})\cdot\tilde{\mathbf{x}}(t)+(\mathbf{B}_{\mathbf{ON}}-\mathbf{B}_{\mathbf{OFF}})\cdot\tilde{\mathbf{v}}_{\mathbf{in}}\right]\cdot\tilde{d}(t)$$

$$\mathbf{Y}_{\mathbf{DC}}+\tilde{\mathbf{y}}(t)=\mathbf{C}\cdot X_{DC}$$

$$+\mathbf{C}\cdot\tilde{\mathbf{x}}(t)+(\mathbf{C}_{\mathbf{ON}}-\mathbf{C}_{\mathbf{OFF}})\cdot X_{DC}\cdot\tilde{d}(t) \qquad \text{Eq 2.31}$$

$$+(\mathbf{C}_{\mathbf{ON}}-\mathbf{C}_{\mathbf{OFF}})\cdot\tilde{\mathbf{x}}(t)\cdot\tilde{d}(t)$$

However, the DC terms in the right side of the equation equal to zero as the derivative $\dot{X}_{DC}$ is zero due X_{DC} being, therefore all the DC terms are zero. The second-order nonlinear terms where there is a multiplication of terms " ˜ " are two small quantities which result into an even smaller amount therefore those terms can be approximate zero. The simplified equations are Eq. 2.32 and 2.33

$$\dot{\tilde{\mathbf{x}}}(t)=\mathbf{A}\cdot\tilde{\mathbf{x}}(t)+\mathbf{B}\cdot\tilde{\mathbf{v}}_{\mathbf{in}}(t)+\left[(\mathbf{A}_{\mathbf{ON}}-\mathbf{A}_{\mathbf{OFF}})\cdot X_{DC}+(\mathbf{B}_{\mathbf{ON}}-\mathbf{B}_{\mathbf{OFF}})\cdot V_{in.DC}\right]\cdot\tilde{d}(t) \qquad \text{Eq. 2.32}$$

$$\tilde{\mathbf{y}}(t)=\mathbf{C}\cdot\tilde{\mathbf{x}}(t)+(\mathbf{C}_{\mathbf{ON}}-\mathbf{C}_{\mathbf{OFF}})\cdot X_{DC}\cdot\tilde{d}(t) \qquad \text{Eq. 2.33}$$

Equations 2.32 and 2.34 represent the linearized AC small-signal low-frequency model of any two-state (ON/OFF) switching dc-to-dc converter working in continuous conduction mode. From equations 2.9, 2.10, 2.11, 2.12, 2.22 and 2.23 we can extract the **A, B, C, A**

$$\mathbf{A}_{\mathbf{ON}}=\begin{bmatrix}0 & 0 & 0 & 0\\ 0 & 0 & \frac{1}{L2} & -\frac{1}{L2}\\ 0 & -\frac{1}{C1} & 0 & 0\\ 0 & \frac{1}{C2} & 0 & -\frac{1}{R_{LOAD}C2}\end{bmatrix} \qquad \text{Eq. 2.34}$$

$$\mathbf{A_{OFF}}=\begin{bmatrix} 0 & 0 & -\frac{1}{L1} & 0 \\ 0 & 0 & 0 & -\frac{1}{L2} \\ \frac{1}{C1} & 0 & 0 & 0 \\ 0 & \frac{1}{C2} & 0 & -\frac{1}{R_{LOAD}C2} \end{bmatrix} \qquad \text{Eq. 2.35}$$

$$\mathbf{A}=\begin{bmatrix} 0 & 0 & -\frac{(1-D_{DC})}{L1} & 0 \\ 0 & 0 & \frac{D_{DC}}{L2} & -\frac{1}{L2} \\ \frac{(1-D_{DC})}{C1} & -\frac{D_{DC}}{C1} & 0 & 0 \\ 0 & \frac{1}{C2} & 0 & -\frac{1}{R_{LOAD}C2} \end{bmatrix} \qquad \text{Eq. 2.36}$$

$$\mathbf{B_{ON}}=\begin{bmatrix} \frac{1}{L1} \\ \frac{1}{L2} \\ 0 \\ 0 \end{bmatrix} \qquad \text{Eq. 2.37}$$

$$\mathbf{B_{OFF}}=\begin{bmatrix} 0 \\ 0 \\ 0 \\ 0 \end{bmatrix} \qquad \text{Eq. 2.38}$$

$$\mathbf{B}=\begin{bmatrix} \frac{1}{L1}D_{DC} \\ \frac{1}{L2}D_{DC} \\ 0 \\ 0 \end{bmatrix} \qquad \text{Eq. 2.39}$$

$$\mathbf{C_{ON}}=[0 \quad 0 \quad 0 \quad 1] \qquad \text{Eq. 2.40}$$

$$\mathbf{C_{OFF}}=[0 \quad 0 \quad 0 \quad 1] \qquad \text{Eq. 2.41}$$

$$\mathbf{C} = [0 \quad 0 \quad 0 \quad 1] \qquad \text{Eq. 2.42}$$

As $\mathbf{C_{ON}} = \mathbf{C_{OFF}}$ and defining $\mathbf{B_d}$ as Eq, 2.43 and using equation Eq. 2.26, equations 2.43, the linearized AC small-signal low-frequency model of the Zeta Power Converter working in continuous conduction mode is represented in Eq. 2.43, Eq. 2.44, and Eq. 2.45.

$$\boldsymbol{B}_d = \left[-(\mathbf{A_{ON}} - \mathbf{A_{OFF}}) \cdot \mathbf{A}^{-1}\mathbf{B} \cdot V_{in.DC} + (\mathrm{B}_{\mathbf{ON}} - \mathbf{B_{OFF}}) \cdot V_{in.DC}\right] \qquad \text{Eq. 2.43}$$

$$\dot{\tilde{\mathbf{x}}}(t) = \mathbf{A} \cdot \tilde{\mathbf{x}}(t) + \mathbf{B} \cdot \tilde{v}_{in}(t) + \mathbf{B}_d \cdot \tilde{d}(t) \qquad \text{Eq. 2.44}$$

$$\tilde{\mathbf{y}}(t) = \mathbf{C} \cdot \tilde{\mathbf{x}}(t) \qquad \text{Eq. 2.45}$$

CHAPTER THREE

STATESPACE OBSERVER/ESTIMATOR FOR CONTROL SYSTEMS

As described in chapter one, control systems are used to regulate a variety of machines, products, processes, and power converters. They control quantities such as motion, temperature, heat flow, fluid flow, fluid pressure, tension, voltage, and current. Most concepts in classical control theory , which is widely used and implemented, are based on having sensors to measure the quantity under control, in fact assuming the availability of near-perfect feedback signals. Unfortunately, such an assumption is often invalid, all physical sensors have shortcomings that can degrade a control system performance [47]. In order for a control system to perform correctly, it is assumed that all signals required for controlling the system are available and accurate.

There are different reasons for such shortcomings, sensors are expensive, and they can reduce the reliability of control systems. A point to note is that some signals are impractical to measure either because they are inaccessible or major modifications would need to be made to the measured them. In addition, sensors usually induce significant errors such as stochastic noise, cyclical errors, and limited responsiveness [47].

Observers can be used to augment or replace sensors in a control system. Observers are algorithms that combine sensed signals with other knowledge of the control system to produce observed signals. These observed signals can be more accurate, less expensive to produce, and more reliable than sensed signals[47].

For instance, in the Zeta Power converter depicted in Figure 2.2, the state variable: Inductor L1 and L2 Current, Capacitor C1 and C2 Voltage as well as the input

Voltage Vin ($i_{L1}(t)=x_1(t)$; $i_{L2}(t)=x_2(t)$; $v_{C1}(t)=x_3(t)$ and $v_{C2}(t)=x_4(t)$) would need to be available to the state space controller in order to implement a suitable and reliable control scheme. This will drastically increase the cost of the design and a major design modification will have to be made. For instance, the loop would have to be open and sense resistor would need to be added in order to measure the inductor currents R_{sense1} and R_{sense2} ; additional differential amplifiers would need to be added in order to amplify the voltage to a suitable range before being process by the Analog to Digital Converters (ADC). Additional ADC channels will need to be allocated. All these additional overheads are depicted in red in figure 3.1.

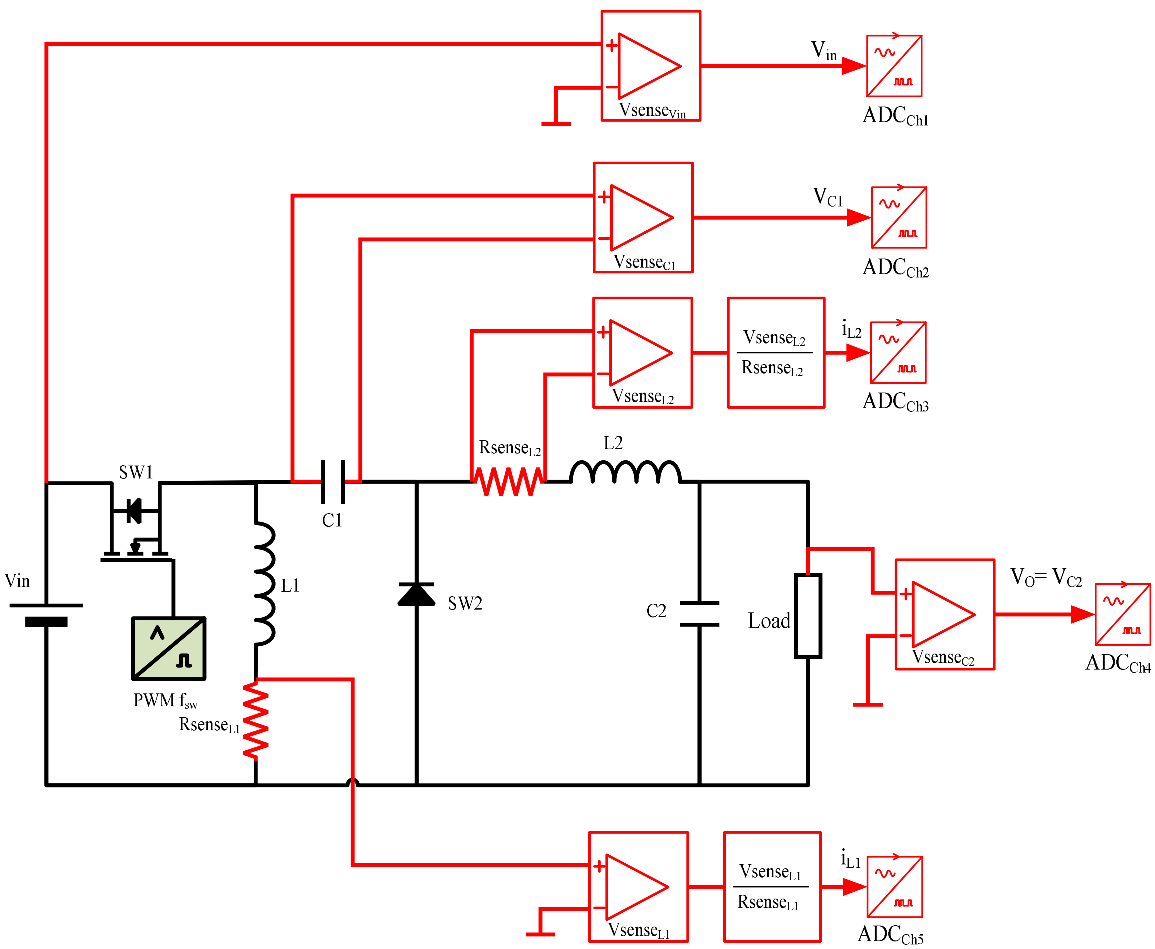

Figure 3.1 Zeta Converter additional components to measure state variables.

3.1 State Observer

Observers work by combining knowledge of the plant, the power converter output, and the feedback device to extract a feedback signal that is superior to that which can be obtained by using a feedback device alone. The principle of an observer is that by combining a measured feedback signal with knowledge of the control-system components (primarily the plant and feedback system), the behavior of the plant can be known with greater precision than by using the feedback signal alone, the observer augments the sensor output and provides a feedback signal to the control laws as depicted in figure 3.2, where **r**(k) is the reference input vector, **y**(k) is the response output vector to **r**(k), **u**(k) is the input vector to the plant, **θp**(k) is a vector of estimated plant parameters, **θc**(k) is a vector of controlled parameters that follow a certain control law with the target of **y**(k)=**r**(k) and **ω**(k) is a vector of disturbances to the plant.

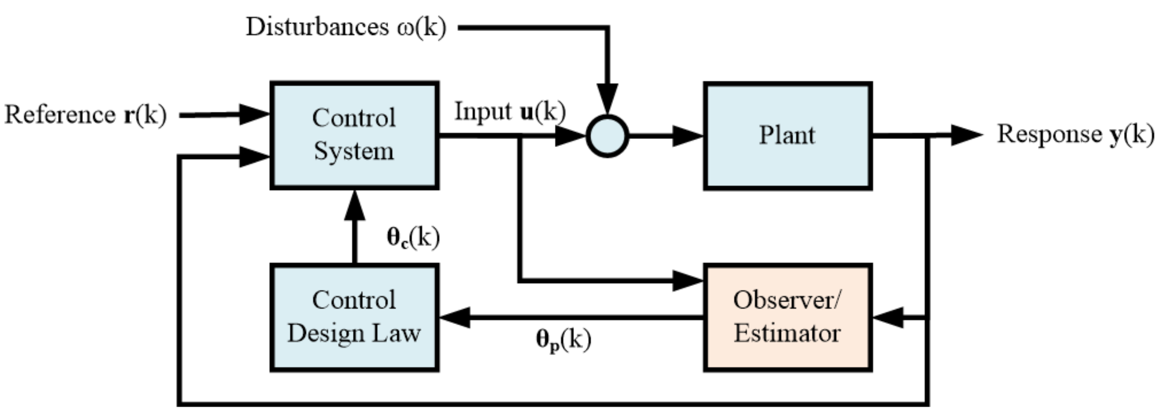

Figure 3.2 Role of an Observer/State Estimator in a discrete time control system

To estimate all the states of the system, one could in theory use a system with the same state equation as the plant to be observed . In other words, one could use the open-loop state space system defined by Eq. 3.1 and Eq. 3.2

$$\hat{\mathbf{x}}(\mathrm{k}+1) = \hat{\mathbf{A}}\cdot\hat{\mathbf{x}}(\mathrm{k}) + \hat{\mathbf{B}}\cdot\mathbf{u}(\mathrm{k}) \qquad \text{Eq. 3.1}$$

$$\hat{\mathbf{y}}(\mathrm{k}) = \hat{\mathbf{C}}\cdot\hat{\mathbf{x}}(\mathrm{k}) + \hat{\mathbf{D}}\cdot\mathbf{u}(\mathrm{k}) \qquad \text{Eq. 3.2}$$

where is $\hat{\mathbf{x}}(\mathrm{k}+1) = \hat{\mathbf{A}}\cdot\hat{\mathbf{x}}(\mathrm{k}) + \hat{\mathbf{B}}\cdot\mathbf{u}(\mathrm{k})$ is the estimated state space system equation of $\mathbf{x}(\mathrm{k}+1) = \mathbf{A}\cdot\mathbf{x}(\mathrm{k}) + \mathbf{B}\cdot\mathbf{u}(\mathrm{k})$ and $\hat{\mathbf{y}}(\mathrm{k}) = \hat{\mathbf{C}}\cdot\hat{\mathbf{x}}(\mathrm{k}) + \hat{\mathbf{D}}\cdot\mathbf{u}(\mathrm{k})$ is the estimated state space output equation of $\mathbf{y}(\mathrm{k}) = \mathbf{C}\cdot\mathrm{x}(\mathrm{k}) + \mathbf{D}\cdot\mathbf{u}(\mathrm{k})$ this is described in figure 3.3.

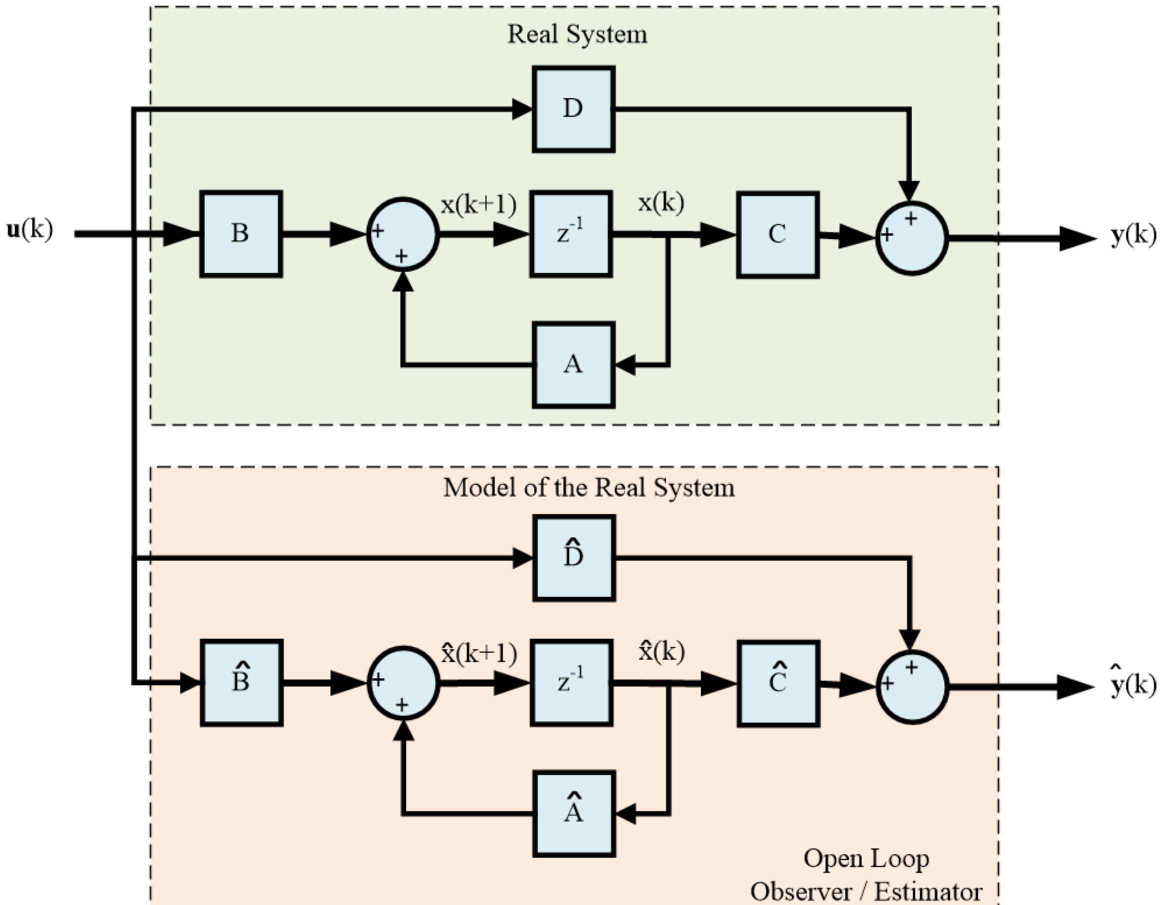

Figure 3.3 Open Loop Observer/Estimator

However, this open-loop estimator assumes perfect knowledge of the system dynamics and lacks the feedback needed to correct the errors that are inevitable in any implementation. This open loop observer has some limitations. First of all, the open loop observer will not work if **A** is unstable as the output will grow unbounded.

Secondly, if $\mathbf{A}$ is stable and there is an error between $\mathbf{A}$ and $\hat{\mathbf{A}}$, this error will grow over time uncorrected. However, as long as $\mathbf{A}$ and $\hat{\mathbf{A}}$ are relatively close to each other and stable, the initial errors $\mathbf{x}(0) \neq \hat{\mathbf{x}}(0)$ will die away leaving only the fore response. In a real application we have access to the output $\mathbf{y}(k)$ of the system and $\hat{\mathbf{y}}(k)$ is calculated, therefore if we observe that $\mathbf{y}(k)$ differs from $\hat{\mathbf{y}}$ (k) it would be unwise not to use this information to correct the state estimates in the right direction, so $\hat{\mathbf{y}}(k)$ will tend to $\mathbf{y}(k)$ over time. The output error $\mathbf{e}_{output}(k) = \mathbf{y}(k) - \hat{\mathbf{y}}(k)$ as depicted in figure 3.4 can be influenced as in any feedback control system, closing the loop, and making the proper adjustments to make the error $\mathbf{e}_{output}$ tend to zero in a pre-determined time. In order illustrate this let's multiply the error $\mathbf{e}_{output}$ by a gain matrix L called Observer Gain and feedback it as an additional input to the system . For simplicity let's assume there is no feedforward matrix $\mathbf{D}$.

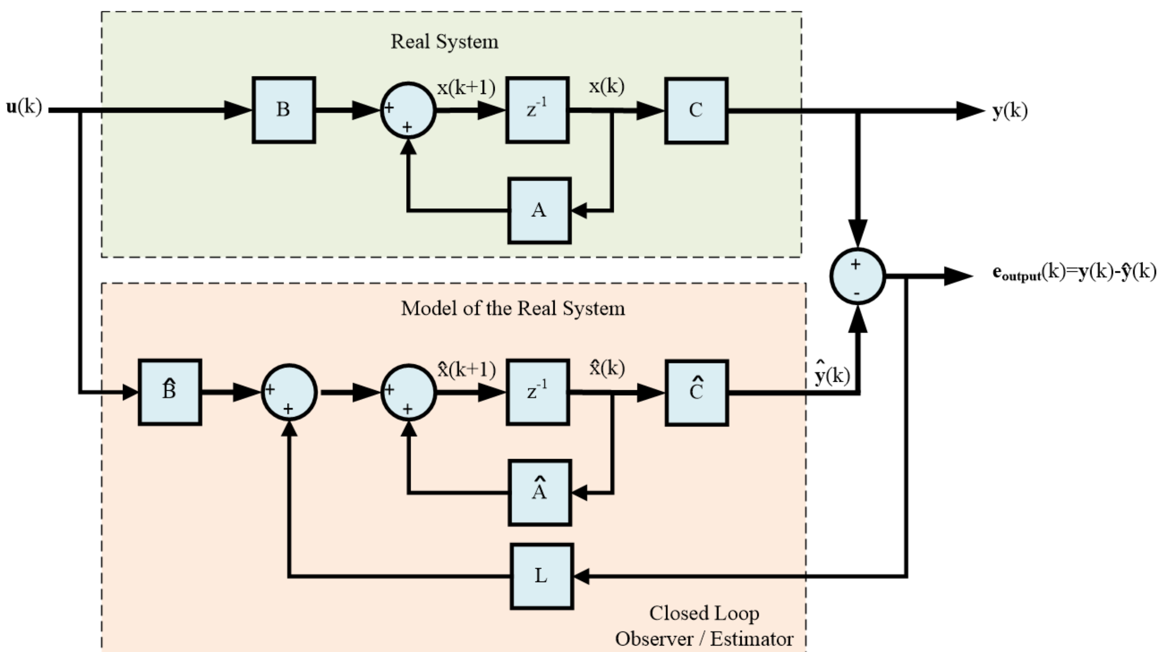

Figure 3.4 Closed Loop Observer/Estimator

The new state space equation for the close loop observer becomes Eq 3.3 and 3.4. We can define the error of the state estimator /observer as to $\mathbf{e}_{obs}(k)= \mathbf{x}(k) - \hat{\mathbf{x}}(k)$, as this is a linear time-invariant system its difference would also hold therefore $e_{obs}(k+1)= \mathbf{x}(k+1) - \hat{\mathbf{x}}(k+1)$.

$$\hat{\mathbf{x}}(k+1) = \hat{\mathbf{A}}\cdot\hat{\mathbf{x}}(k) + \hat{\mathbf{B}}\cdot\mathbf{u}(k) + \mathbf{L}(\mathbf{y}(k)-\hat{\mathbf{y}}(k)) \qquad \text{Eq. 3.3}$$

$$\hat{\mathbf{y}}(k) = \hat{\mathbf{C}}\cdot\hat{\mathbf{x}}(k) \qquad \text{Eq. 3.4}$$

The $\mathbf{e}_{obs}(k+1)$ becomes equation 3.5 and 3.6.

$$\mathbf{e}_{obs}(k+1)= \mathbf{A}\cdot\mathbf{x}(k) + \mathbf{B}\cdot\mathbf{u}(k) - \hat{\mathbf{A}}\cdot\hat{\mathbf{x}}(k)- \hat{\mathbf{B}}\cdot\mathbf{u}(k)-\mathbf{L}(\mathbf{y}(k)-\hat{\mathbf{y}}(k)) \qquad \text{Eq. 3.5}$$

$$\mathbf{e}_{obs}(k+1)= \mathbf{A}\cdot\mathbf{x}(k) - \hat{\mathbf{A}}\cdot\hat{\mathbf{x}}(k) + \mathbf{B}\cdot\mathbf{u}(k) - \hat{\mathbf{B}}\cdot\mathbf{u}(k) - \mathbf{L}(\mathbf{y}(k)-\hat{\mathbf{y}}(k)) \qquad \text{Eq. 3.6}$$

But as we model the system. There is a very good idea of $\hat{\mathbf{A}}$, $\hat{\mathbf{B}}$, and $\hat{\mathbf{C}}$ matrices such as $\mathbf{A}\approx\hat{\mathbf{A}}$, $\mathbf{B}\approx\hat{\mathbf{B}}$ and $\mathbf{C}\approx\hat{\mathbf{C}}$ therefore:

$$\mathbf{e}_{obs}(k+1)= \mathbf{A}\cdot(\mathbf{x}(k) -\cdot\hat{\mathbf{x}}(k)) - \mathbf{L}(\mathbf{y}(k)-\hat{\mathbf{y}}(k)) \qquad \text{Eq. 3.7}$$

$$\mathbf{y}(k)-\hat{\mathbf{y}}(k)=\mathbf{C}\cdot\mathbf{x}(k) - \hat{\mathbf{C}}\cdot\hat{\mathbf{x}}(k) \qquad \text{Eq. 3.8}$$

$$\mathbf{e}_{obs}(k+1)= \mathbf{A}\cdot(\mathbf{x}(k) -\cdot\hat{\mathbf{x}}(k)) - \mathbf{L}\cdot\mathbf{C}(\mathbf{x}(k)-\hat{\mathbf{x}}(k)) \qquad \text{Eq. 3.9}$$

$$\mathbf{e}_{obs}(k+1)= (\mathbf{A} - \mathbf{L}\cdot\mathbf{C})\cdot\mathbf{e}_{obs}(k) \qquad \text{Eq. 3.10}$$

The unforce general solution to the difference equation Eq. 3.10 is Eq 3.11. It can be seen that the observer error will decay to zero (Fig 3.5) in a desired time if **L** is chosen such that Eq. 3.10 is asymptotically stable, meaning that all eigen values of the matrix (**A-LC)** lie within the unit circle. Therefore, if $\mathbf{x}(k+1) = \mathbf{A}\cdot\mathbf{x}(k) + \mathbf{B}\cdot\mathbf{u}(k)$ and $\mathbf{y}(k) = \mathbf{C}\cdot x(k)$ is an observable system, the observer gain **L** may be chosen so as to place the eigenvalues in any desired configuration in order to achieve the desired observer dynamics[48].

$$\mathbf{e}_{\mathbf{obs}}(k) = (\mathbf{A} - \mathbf{L}\cdot\mathbf{C})^{k} \cdot \mathbf{e}_{\mathbf{obs}}(0) \qquad \text{Eq. 3.11}$$

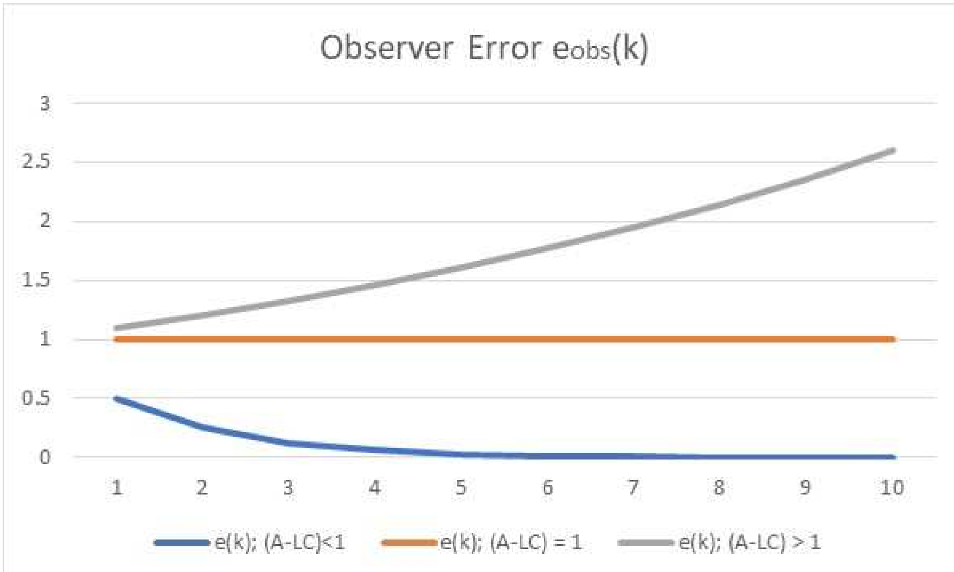

Figure 3.5 Observer Error e_{obs}(**A-LC**)

3.2 State Feedback and Separation Principle

The State matrix **A** of a state Space System is used to effectively understand if the system is stable or not by looking into the system Eigenvalues (λ) of the Matrix **A**. The eigenvalues of the matrix **A** are solutions of the equation determinant| z**I** – **A | =** 0, where z is the complex variable in the z discrete-time domain, which yield to the poles of the transfer function[49]. If the Eigenvalues/Poles of the system (λ) are within the unit cycle (zone A of figure 3.6) the system is Stable, if the Eigen Values are outside the unit cycle the system is unstable (zone C of figure 3.6), if equal to one the system is marginally unstable (zone B of figure 3.6).

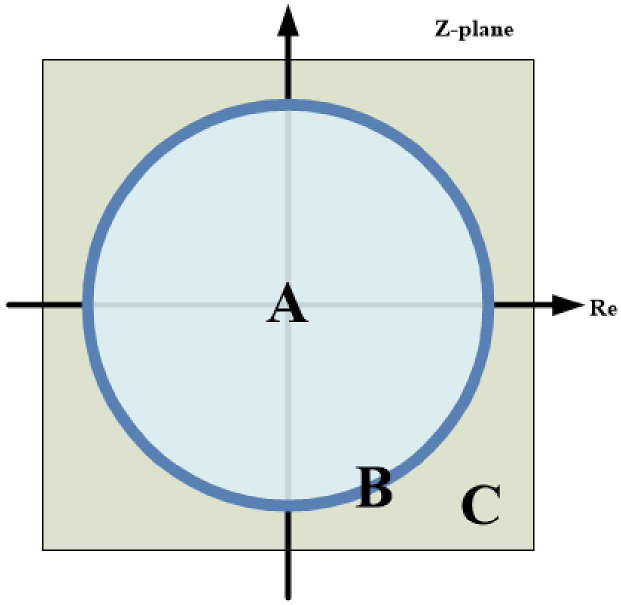

Figure 3.6 z-Plane

If all the state variables can be measured, and if the plant is completely known, then an optimal controller can frequently be realized as an instantaneous function generator whose inputs are the state variables. The effect of linear state variable feedback on systems of the form of equations 3.12 and 3.13. is to replace **u(k)** by **r**(k)= **u**(k) - **K**· **x**(k) where **K** is a *nxm* matrix of constants[50].

$$\mathbf{x}(k+1) = \mathbf{A}\cdot\mathbf{x}(k) + \mathbf{B}\cdot\mathbf{u}(k) \qquad \text{Eq. 3.12}$$

$$\mathbf{y}(k) = \mathbf{C}\cdot\mathbf{x}(k) \qquad \text{Eq. 3.13}$$

The closed-loop equation of motion **x**(k+1) is depicted figure 3.7 and described by Eq. 3.14, while the output state equation **y**(k) remains the same as Eq. 3.13.

$$\mathbf{x}(k+1) = (\mathbf{A}-\mathbf{B}\cdot K)\cdot\mathbf{x}(k) + \mathbf{B}\cdot\mathbf{r}(k) \qquad \text{Eq. 3.14}$$

It is well known that feedback can alter the pole locations of the system by manipulating the K gain matrix only if the system is controllable, then state variable feedback can be used to achieve any desired pole configuration.

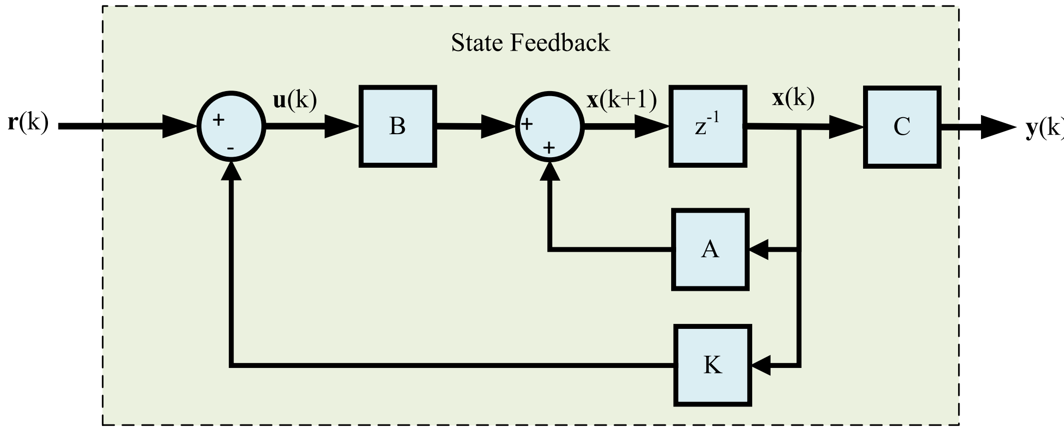

Figure 3.7 State Feedback Block Diagram.

However, key to the state feedback controller law $\mathbf{r}(k)= \mathbf{u}(k) - \mathbf{K}\cdot\mathbf{x}(k)$is that the state variables are known and accessible which is not always the case as described in the beginning of this chapter. In section 3.1 a solution was found by implementing a state estimator/observer. This brings us to the following problem statement, is it possible to combine the state feedback control law and the estimator state law into one as depicted in figure 3.8.

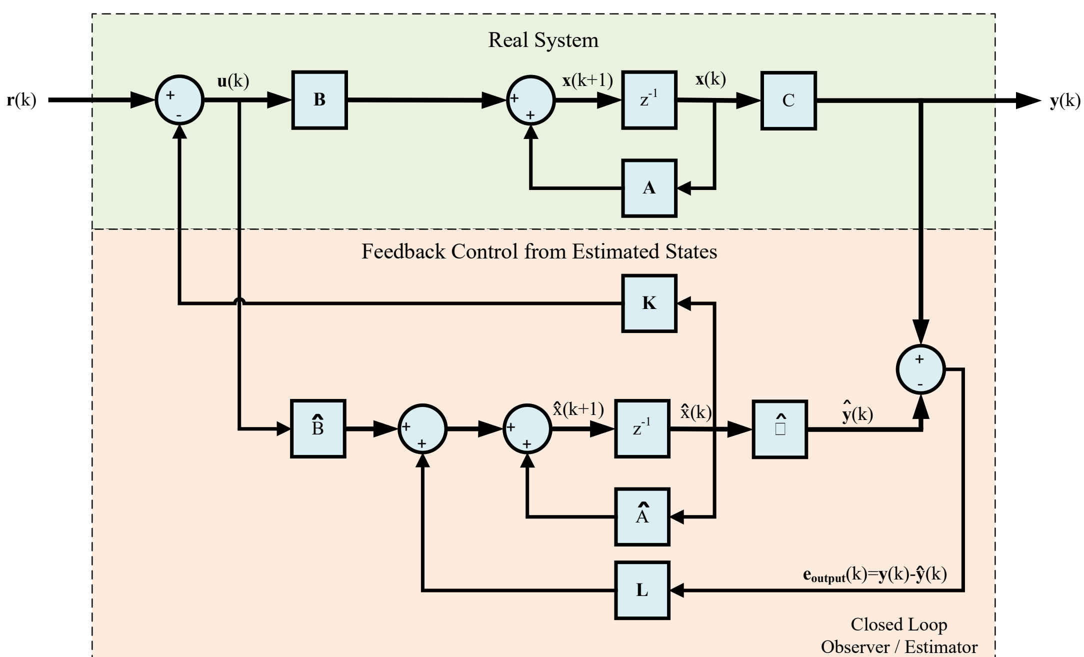

Figure 3.8 Estimated State Feedback Control

The answer is Yes, it is possible but what would be the effects on the system dynamics due to the fact that the control law was designed assuming the true state feedback instead of the estimated states, this is called the Separation Principle which would allow to independently determine the matrices **K** and **L**.

If the system pair of matrices (**A** , **B**) is controllable then the state feedback $\mathbf{u}(k) = \mathbf{r}(k) - \mathbf{K}\cdot\mathbf{x}(k)$ can place the system poles / eigen values ($\mathbf{A}-\mathbf{B}\cdot\mathbf{K}$) in any desired position in the z-plane, if the system pair of matrices (**A** , **C**) is observable the observer poles ($\mathbf{A}-\mathbf{L}\cdot\mathbf{C}$) can be place in any desired position in the z-plane by selecting the proper gain **L**. if $\mathbf{x}(k)$ is not available it is natural to apply the state feedback to the estimated state as following: $\mathbf{u}(k) = \mathbf{r}(k) - \mathbf{K}\cdot\hat{\mathbf{x}}(k)$. Assuming as $\mathbf{A}\approx\widehat{\mathbf{A}}$, $\mathbf{B}\approx\widehat{\mathbf{B}}$ and $\mathbf{C}\approx\widehat{\mathbf{C}}$, this will lead to the new state space equations Eq. 3.15 and Eq. 3.16:

$$\mathbf{x}(k+1)=\mathbf{A}\cdot\mathbf{x}(k) - \mathbf{B}\cdot\mathbf{K}\cdot\hat{\mathbf{x}}(k) + \mathbf{B}\cdot\mathbf{r}(k) \qquad \text{Eq. 3.15}$$

$$\hat{\mathbf{x}}(k+1)=(\mathbf{A} - \mathbf{L}\cdot\mathbf{C})\hat{\mathbf{x}}(k) + \mathbf{B}\big(\mathbf{r}(k) - \mathbf{K}\cdot\hat{\mathbf{x}}(k)\big) + \mathbf{L}\cdot\mathbf{C}\cdot\mathbf{x}(k) \qquad \text{Eq. 3.16}$$

That combine leads to new state space system:

$$\begin{bmatrix}\mathbf{x}(k+1)\\ \hat{\mathbf{x}}(k+1)\end{bmatrix} = \begin{bmatrix}\mathbf{A} & -\mathbf{B}\cdot\mathbf{K}\\ \mathbf{L}\cdot\mathbf{C} & \mathbf{A}-\mathbf{L}\cdot\mathbf{C}-\mathbf{B}\cdot\mathbf{K}\end{bmatrix}\cdot\begin{bmatrix}\mathbf{x}(k)\\ \hat{\mathbf{x}}(k)\end{bmatrix} + \begin{bmatrix}\mathbf{B}\\ \mathbf{B}\end{bmatrix}\mathbf{r}(k) \qquad \text{Eq. 3.17}$$

$$\mathbf{y}(k)= [\mathbf{C} \quad \mathbf{0}]\cdot\begin{bmatrix}\mathbf{x}(k)\\ \hat{\mathbf{x}}(k)\end{bmatrix} \qquad \text{Eq. 3.18}$$

Equations 3.17 and 3.18 described the feedback system in figure 3.8, from the new augmented matrix A it is not obvious how we can affect the dynamics of the system by setting separately the values of the gain matrices **L** and **K**. This will require to approach the problem from the observer perspective and the state using a transformation matrix **P** as following:

$$\begin{bmatrix}\mathbf{x}(k)\\ \mathbf{e_{obs}}(k)\end{bmatrix} = \begin{bmatrix}\mathbf{x}(k)\\ (\mathbf{x}(k)-\hat{\mathbf{x}}(k))\end{bmatrix} = \begin{bmatrix}\mathbf{I} & \mathbf{I}\\ \mathbf{I} & -\mathbf{I}\end{bmatrix}\cdot\begin{bmatrix}\mathbf{x}(k)\\ \hat{\mathbf{x}}(k)\end{bmatrix} = \mathbf{P}\cdot\begin{bmatrix}\mathbf{x}(k)\\ \hat{\mathbf{x}}(k)\end{bmatrix} \qquad \text{Eq. 3.19}$$

Where $\mathbf{P}^{-1} = \mathbf{P}$, therefore we can obtain the following equivalent state equation:

$$\begin{bmatrix}\mathbf{x}(k+1)\\ \mathbf{e_{obs}}(k+1)\end{bmatrix} = \begin{bmatrix}\mathbf{A}-\mathbf{B}\cdot\mathbf{K} & \mathbf{B}\cdot\mathbf{K}\\ 0 & \mathbf{A}-\mathbf{L}\cdot\mathbf{C}\end{bmatrix}\cdot\begin{bmatrix}\mathbf{x}(k)\\ \mathbf{e_{obs}}(k)\end{bmatrix} + \begin{bmatrix}\mathbf{B}\\ 0\end{bmatrix}\mathbf{r}(k) \qquad \text{Eq. 3.20}$$

$$\mathbf{y}(k) = [\mathbf{C} \quad \mathbf{0}]\cdot\begin{bmatrix}\mathbf{x}(k)\\ \mathbf{e_{obs}}(k)\end{bmatrix} \qquad \text{Eq. 3.21}$$

The **A** matrix in Eq. 3.20 is block triangular; therefore, its eigenvalues are the union of those of ($\mathbf{A} - \mathbf{B}\cdot\mathbf{K}$) and ($\mathbf{A} - \mathbf{L}\cdot\mathbf{C}$). Thus, inserting the state estimator does not affect the eigenvalues of the original state feedback; nor are the eigenvalues of the state estimator affected by the connection. Thus, the design of state feedback and the design of state estimator can be carried out independently.

3.3 Effect of Stability of Digital Systems due to the sampling time

The main difference between analog feedback control systems and digital feedback control systems is the effect that the sampling rate has on the transient response. Changes in sampling rate not only change the nature of the response from overdamped to underdamped, but also can turn a stable system into an unstable one. In the s-plane, the region of stability is the left half-plane. If a transfer function, G(s), is transformed into a sampled-data transfer function, G(z), the region of stability on the z-plane can be evaluated from the definition, $z = e^{T\cdot s}$ [1], where T is the sampling time and $s = \alpha + j\omega$, we obtain:

$$z = e^{T\cdot s} = e^{T\cdot(\alpha+j\omega)} = e^{T\cdot\alpha}\cdot e^{T\cdot j\omega}$$

$$= e^{T\cdot\alpha}\cdot(\cos\omega T + j\cdot\sin\omega T) \qquad \text{Eq. 3.22}$$

$$= e^{T\cdot\alpha}\cdot\angle\omega T$$

Each region of the s-plane can be mapped into a corresponding region on the z-plane (Figure 3.6). Points that have positive values of α are in the right half of the s-plane, from Eq. (3.22), the magnitudes of these mapped points are $e^{\alpha \cdot T} > 1$. Thus, points in the right half of the s-plane map into points outside the unit circle on the z-plane (Region C) . Points on the jω-axis, region B, have zero values of α and yield points on the z-plane with magnitude = 1, the unit circle. Hence, points on the jω-axis in the s-plane map into points on the unit circle on the z-plane. Finally, points on the s-plane that yield negative values of α (left–half-plane roots)map into the inside of the unit circle on the z-plane. Therefore, the selection of the sampling rate has a direct influence in the stability of the observer and the system.

CHAPTER FOUR

HANDLING UNCERTINTY IN STATE OBSERVER/ESTIMATOR MODEL

The main purpose of every feedback loop is to decrease the effect of uncertainties of the overall performance of the system. This also is applicable to the close loop observer system. In reality, feedback as a design tool for dynamic systems has the potential to offset uncertainty. Feedback can be used for stabilization but inappropriately designed may reduce rather than enlarge the regions of stability of the system [51] .

The term robustness refers to the preservation of desirable system properties, mainly stability and performance under structured and unstructured uncertainties. The design of state feedback through optimal control was found to have desirable robustness properties. To be more specific, seeking control law for **u**(k) in a state space system $\mathbf{x}(k+1) = \mathbf{A}\cdot\mathbf{x}(k) + \mathbf{B}\cdot\mathbf{u}(k)$ such that the closed-loop system is stable and minimizes the quadratic performance criterion given by the cost equation 4.1[49]

$$J=\frac{1}{2}\mathbf{x}^{T}(N)\cdot\mathbf{S}(N)\cdot\mathbf{x}(N)+\frac{1}{2}\sum_{k=0}^{N-1}\left[x^{T}(k)\cdot\mathbf{Q}\cdot x(k)+u^{T}(k)\cdot\mathbf{R}\cdot u(k)\right] \qquad \text{Eq. 4.1}$$

Where $\mathbf{u}(k) = -\mathbf{K}(k)\cdot\mathbf{x}(k)$ and $\mathbf{K}(k)$ is equal to equation 4.2[49]

$$\mathbf{K}(k)=\left[\mathbf{R}+\mathbf{B}^{T}\cdot\mathbf{S}(k+1)\cdot\mathbf{B}\right]^{-1}\cdot\mathbf{B}^{T}\cdot\mathbf{S}(k+1)\cdot\mathbf{A} \qquad \text{Eq. 4.2}$$

The equation state feedback control law provides impressive robustness in terms of gain and phase margins and copes with parametric and other types of uncertainties, it has been recognized that these robustness properties are lost when an observer is included in the feedback loop. Simply stated, the loss of robustness in observer-based controller design is due to the signal transfer from the control **u**(k) to the observer through the control distribution matrix [52], [53]. Therefore, in order to address the robustness of the observer under structured and unstructured plant uncertainties a different approach will be developed in the feedback loop by aiming to reduce the output error $\mathbf{y}(k) - \hat{\mathbf{y}}(k)$ as illustrated in figure 4.1.

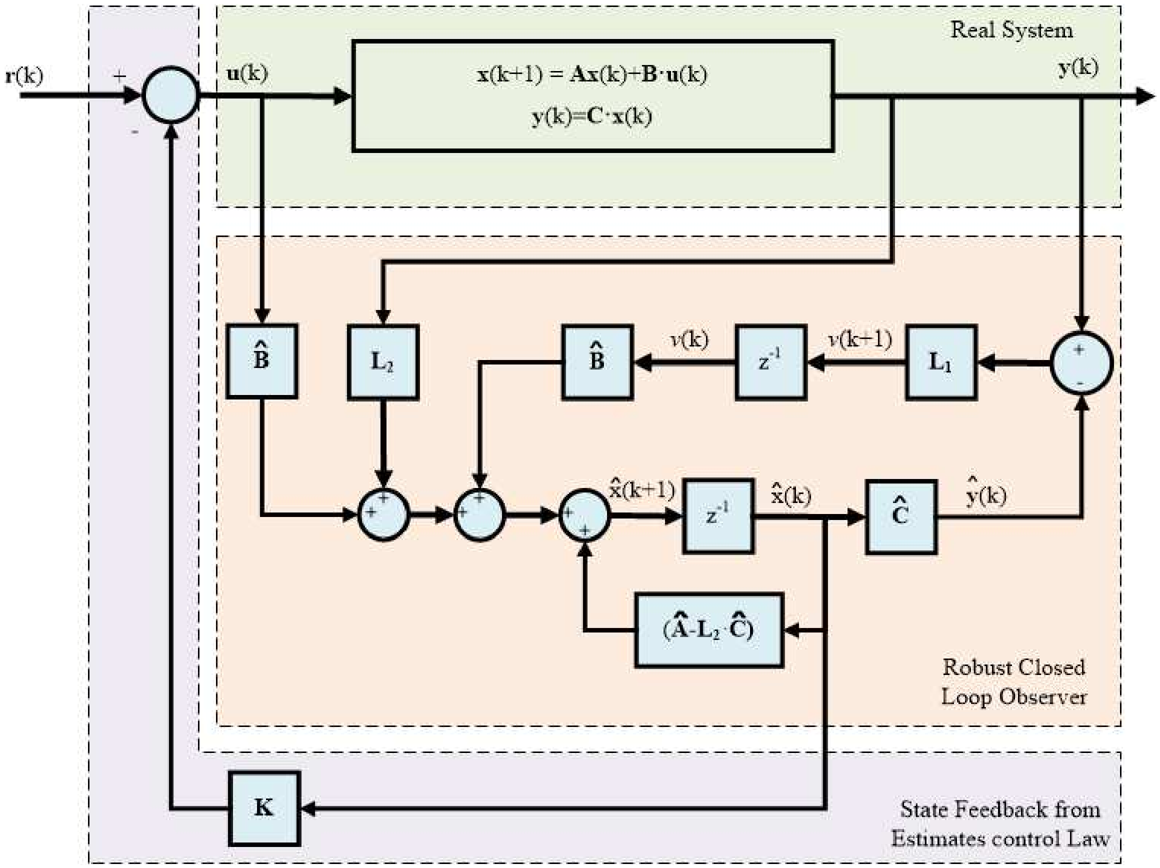

Figure 4.1 Robust Closed Loop Observer

The development of such robust closed loop observer will be discussed in section 4.1.

4.1 Robust Closed Loop Observer

The implementation of the robust observer starts by augmenting the original state equations Eq. 3.1 and 3.2 by a new state $\boldsymbol{v}(k+1)$ equal to the output error $\mathbf{e}(k)=\mathbf{y}(k) - \hat{\mathbf{y}}(k)$ times a new gain $\mathbf{L}_1$, as described figure 4.2. If the $\mathbf{e}(k)$ error is zero, then the closed lop observer will follow its original configuration however If the error $\mathbf{e}(k) \neq 0$, the error will be multiplied by a gain $\mathbf{L}_1$ added from its previous values to correct for steady state error.

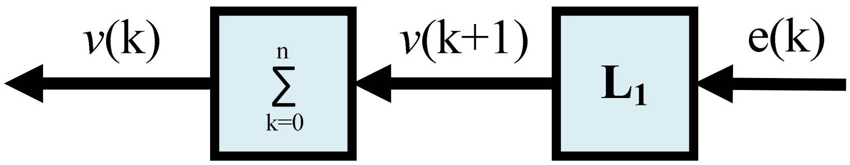

Figure 4.2 New state for Robust Closed Loop Observer

The Augmented state space equations are 4.3 and 4.4 and the control law follows equation 4.5.

$$\hat{\mathbf{x}}(k+1)=\left(\hat{\mathbf{A}} - \mathbf{L_2}\cdot\hat{\mathbf{C}}\right)\cdot\hat{\mathbf{x}}(k)+\mathbf{L_2}\cdot\mathbf{y}(k)+\hat{\mathbf{B}}\cdot\mathbf{u}(k)+\hat{\mathbf{B}}\cdot\boldsymbol{v}(k) \qquad \text{Eq. 4.3}$$

$$\boldsymbol{v}(k+1)=\mathbf{L_1}\cdot(\ \mathbf{y}(k)+\hat{\mathbf{C}}\cdot\hat{\mathbf{x}}(k)\ ) \qquad \text{Eq. 4.4}$$

$$\mathbf{u}(k) = r(k) - \mathbf{K}\cdot\hat{\mathbf{x}}(k) \qquad \text{Eq. 4.5}$$

The robust observer state equations can be augmented by defining a $\mathbf{z}(k)$ as in equation 4.6 and 4.7.

$$\mathbf{z}(k)=\begin{bmatrix}\hat{\mathbf{x}}(k)\\ \boldsymbol{v}(k)\end{bmatrix} \qquad \text{Eq. 4.6}$$

$$\mathbf{z}(k+1)=\begin{bmatrix}\hat{\mathbf{x}}(k+1)\\ \mathbf{v}(k+1)\end{bmatrix} \qquad \text{Eq. 4.7}$$

The new augmented robust observer state space equations can be written as equation 4.8.

$$\mathrm{z}(k+1)= \left(\ \hat{\mathrm{A}}_x\text{-}\mathrm{L}_x\cdot\hat{\mathrm{C}}\ \right)\cdot \mathrm{z}(k) + \mathrm{L}_x\cdot\mathrm{y}(k) + \hat{\mathrm{B}}\cdot\mathrm{u}(k) + \hat{\mathrm{B}}\cdot\boldsymbol{v}(k) \qquad \text{Eq. 4.8}$$

Where:

$$\mathbf{A_x}=\begin{bmatrix}\hat{\mathbf{A}} & \hat{\mathbf{B}}\\ \mathbf{0} & \mathbf{0}\end{bmatrix},\qquad \mathrm{B_x}=\begin{bmatrix}\hat{\mathrm{B}}\\ 0\end{bmatrix},\qquad \mathbf{C_x}=[\hat{\mathbf{C}}\quad \mathbf{0}]\qquad \mathbf{L_x}=\begin{bmatrix}\mathbf{L}_2\\ \mathbf{L}_1\end{bmatrix}$$

The adjusted control law $\mathbf{u}(k) = r(k) - \mathbf{K}_x \cdot \hat{\mathbf{x}}(k)$ with $\mathbf{K}_x$ equal to equation 4.8

$$\mathbf{K_x}=[\mathbf{K} \quad \mathbf{0}] \qquad \text{Eq. 4.9}$$

Since pair $\{\mathbf{A},\mathbf{C}\}$ is observable (assumption for closed loop observer), the pair $\{\mathbf{A_x}, \mathbf{C_x}\}$ is also observable any eigenvalue/pole placement assignment technique can be employed to find $\mathbf{L}_x$ such that $(\hat{\mathbf{A}}_x - \mathbf{L}_x \cdot \hat{\mathbf{C}})$ is stable.

$$\begin{bmatrix} \mathbf{x}(k+1) \\ \hat{\mathbf{x}}(k+1) \\ \mathbf{v}(k+1) \end{bmatrix} = \begin{bmatrix} \hat{\mathbf{A}} & -\hat{\mathbf{B}}\cdot\mathbf{K} & \mathbf{0} \\ \mathbf{L_2}\cdot\hat{\mathbf{C}} & \hat{\mathbf{A}}-\mathbf{L_2}\cdot\hat{\mathbf{C}}-\hat{\mathbf{B}}\cdot\mathbf{K} & \mathbf{0} \\ \mathbf{L_1}\cdot\hat{\mathbf{C}} & -\mathbf{L_1}\cdot\hat{\mathbf{C}} & \mathbf{0} \end{bmatrix} \cdot \begin{bmatrix} \mathbf{x}(k) \\ \hat{\mathbf{x}}(k) \\ \mathbf{v}(k) \end{bmatrix} + \begin{bmatrix} \hat{\boldsymbol{B}} \\ \hat{\boldsymbol{B}} \\ \mathbf{0} \end{bmatrix} \mathbf{r}(k) \qquad \text{Eq. 4.10}$$

Defining the state estimation error by $\mathbf{e}_{obs}(k)= \mathbf{x}(k) - \hat{\mathbf{x}}(k)$, one can define the transformation matrix $\mathbf{P}$ and $\mathbf{P}^{-1}$ as following:

$$\mathrm{P}=\begin{bmatrix} I & 0 & 0 \\ -I & I & 0 \\ 0 & 0 & I \end{bmatrix} \qquad \mathbf{P}^{-1}=\begin{bmatrix} \mathbf{I} & \mathbf{0} & \mathbf{0} \\ \mathbf{I} & \mathbf{I} & \mathbf{0} \\ \mathbf{0} & \mathbf{0} & \mathbf{I} \end{bmatrix}$$

Using an equivalent transformation in the form of $\bar{\mathbf{x}}=\mathbf{P}\cdot\mathbf{x}$, $\bar{\mathbf{A}}=\mathbf{P}\cdot\mathbf{A}\cdot\mathbf{P}^{-1}$, $\bar{\mathbf{B}}=\mathbf{P}\cdot\mathbf{B}$, $\bar{\mathbf{C}}=\mathbf{C}\cdot\mathbf{P}^{-1}$ and $\bar{\mathbf{D}}=\mathbf{D}$ the equivalent system described by Eq 4.10 is illustrated in equation 4.11 which establishes the separation property of robust-observer-based state feedback control system.

$$\begin{bmatrix} \mathbf{x}(k+1) \\ \mathbf{e}_{obs}(k+1) \\ \mathbf{v}(k+1) \end{bmatrix} = \begin{bmatrix} \hat{\mathbf{A}}-\hat{\mathbf{B}}\cdot\mathbf{K} & -\hat{\mathbf{B}}\cdot\mathbf{K} & \mathbf{0} \\ \mathbf{0} & \hat{\mathbf{A}}-\mathbf{L}_2\cdot\hat{\mathbf{C}} & \mathbf{0} \\ \mathbf{0} & -\mathbf{L}_1\cdot\hat{\mathbf{C}} & \mathbf{0} \end{bmatrix} \cdot \begin{bmatrix} \mathbf{x}(k) \\ \mathbf{e}_{obs}(k) \\ \mathbf{v}(k) \end{bmatrix} + \begin{bmatrix} \hat{\mathbf{B}} \\ \mathbf{0} \\ \mathbf{0} \end{bmatrix} \boldsymbol{r}(k) \qquad \text{Eq. 4.11}$$

Therefore, we can place the poles of the augmented system and robust closed observer by adjusting the gain matrices $\mathbf{K_x}$ and $\mathbf{L}_x$ separately. This additional Gain $\mathbf{L}_1$ has an integral part as an additional degree of freedom in comparison to the well-known Luenberger observer. This additional degree of freedom can be used to improve the accuracy of steady-state estimation and the robustness of estimation against unknown inputs.

CHAPTER FIVE

ADAPTIVE ESTIMATION AND CONTROL

In everyday language, “to adapt” means to change a behavior to conform to new circumstances. Intuitively, an adaptive controller is thus a controller that can modify its behavior in response to changes in the dynamics of the process and the character of the disturbances. Therefore, an adaptive control can be viewed as a system that can automatically adjust its parameters to compensate for variations in the characteristics of the process it controls. Since ordinary feedback also attempts to reduce the effects of disturbances and plant uncertainty, the question of the difference between feedback control and adaptive control immediately arises, however all literature seems to agree, and a well adopted definition of a non-adaptive control system is a constant-gain feedback system is not an adaptive system [54]. In this dissertation we will adopt the pragmatic definition that an adaptive controller is a controller with <u>adjustable parameters</u> and <u>a mechanism for adjusting those parameters</u>.

A very important question we should ask ourselves is why adaptive control should be implemented as the controller becomes nonlinear because of the parameter adjustment mechanism. The reason lies in the tradeoff between model accuracy, performance error and complexity of the implementation. This is depicted in figure 5.1, while having a controller with a fixed gain in order to achieve low performance error, the accuracy of the model must be high. In the other hand, the higher the model accuracy the higher the complexity of implementation due to very high order systems.

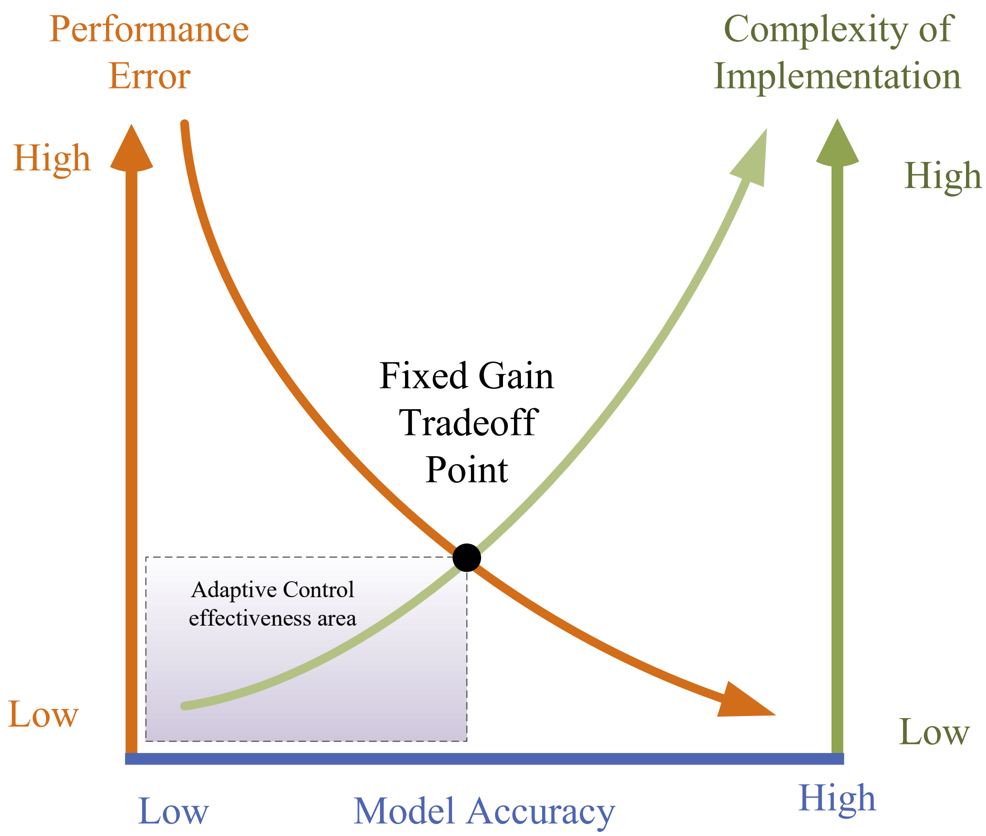

Figure 5.1 Adaptive Control Effectiveness Area

Therefore, the optimal point for a fixed gain controller is the lowest order of the system modeling in order to have a performance of the error that is acceptable, and stability is guarantee, leaving the task to decrease improve performance error to the adaptive gain controller (dotted box in figure 5.1).

In a simplistic way, the adaptive controller can be assumed as a two-loop controller, one with a fixed gain and a second one with a variable gain and a means to adjust the fixed gain controller (figure 5.2).

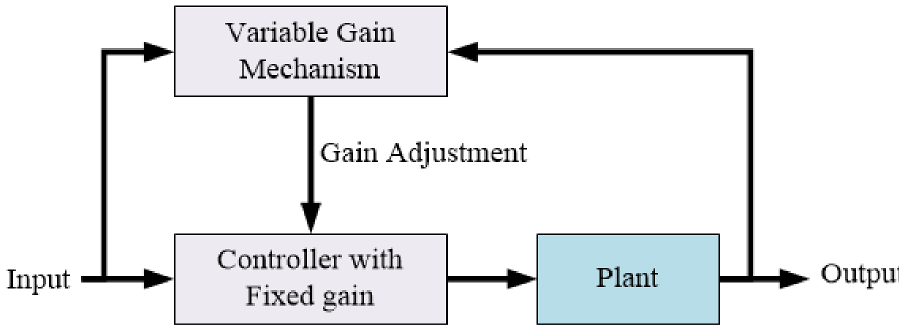

Figure 5.2 Adaptive Controller

The concept of control adaptability can be extended to state observers as the goal of the observer is to track the states **x**(k) of the plant in such way that $\hat{\mathbf{x}}(k) \approx \mathbf{x}(k)$, this can be portrayed in figure 5.3.

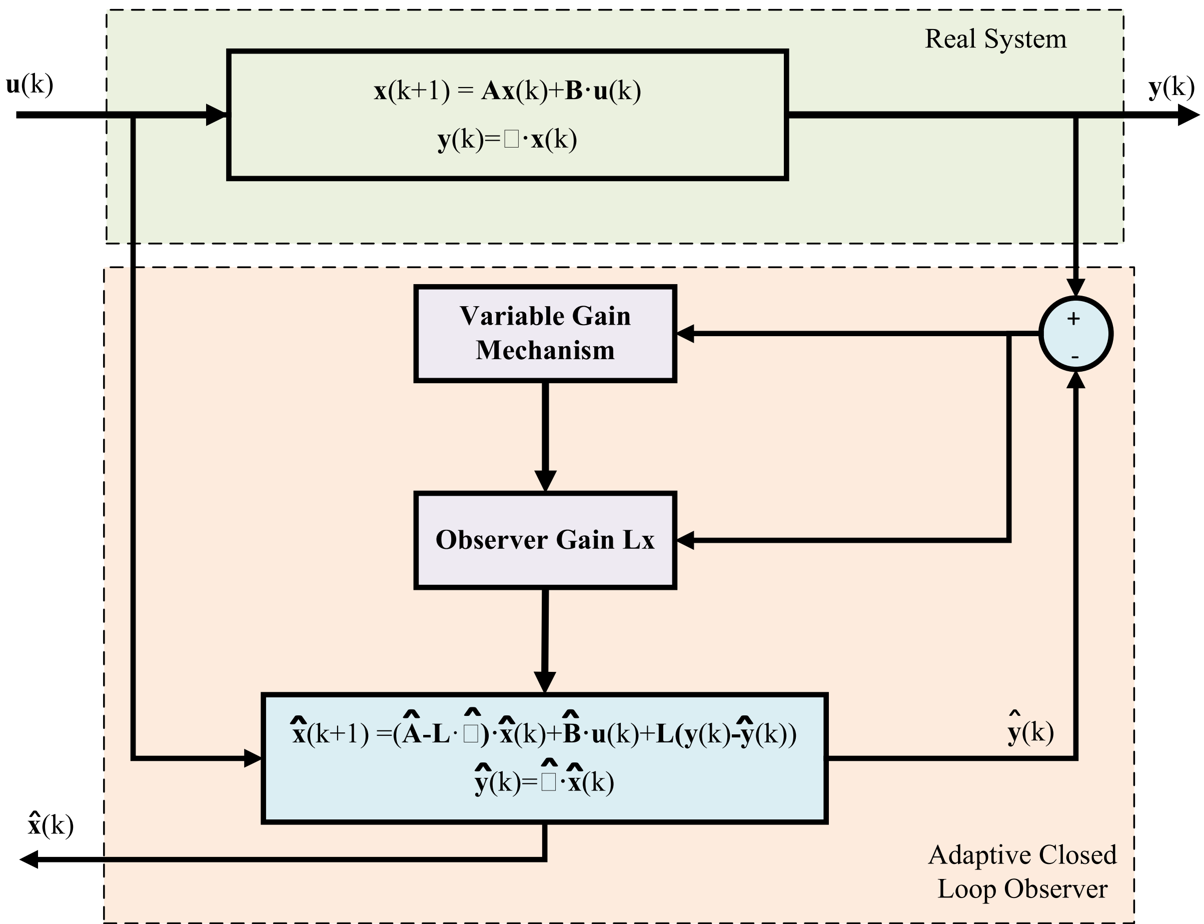

Figure 5.3 Adaptive Observer

The typical tasks that are achieved through adaptive controls are: automatic tuning of controllers, building up a gain schedule for various operations points, and maintaining a system's performance. Adaptive systems can be categorized into four types: Model Reference Adaptive Control (MRAC), Self-Tuning Controllers (STC), Dual Control and Gain Scheduling,

MRAC systems intend to solve a problem in which the system performance specification is given in terms of a reference model, this model describes the ideal behavior of the system therefore the parameters of the controller are adjusted so the plant performance matches the model specification, becoming an optimization. STC are a type of adaptive control systems that can adjust their parameters automatically to achieve optimal performance under changing conditions.

STC systems can optimize their own internal running parameters to maximize or minimize the fulfillment of an objective function, typically maximizing efficiency or error minimization. STC control systems confront some challenges that limit their applicability and effectiveness. One of the challenges is the tradeoff between the speed and accuracy of the adaptation process. If the adaptation is too fast, it may cause instability or oscillations. If the adaptation is too slow, it may not catch up with the changes or disturbances. Another challenge is selecting and estimating the parameters that need to be tuned. This requires a good understanding of the system behavior and the objectives of the control. Moreover, some parameters may be hard to measure or depend on other factors that are not easily accessible or observable.

Dual Control deals with the control of systems whose characteristics are initially unknown. It is called dual because in controlling such a system the controller's objectives have two parts, an action part: to control the system as well as possible based on current system knowledge and an investigation part: to experiment with the system so as to learn about its behavior and control it better in the future. The approach is so complicated, that so far it has not been possible to use it for practical problems [54].

Gain scheduling is an adaptive method and technique that deals with nonlinear systems processes, processes with time variations or situations where the requirements on the control change with the operating conditions[4]. To properly use this technique, it is necessary to find the measurable variables, called scheduling variables, that correlate well with changes in the process dynamics. The scheduling variable can be for instance the output or input signal of a system, the control signal, the error between a desired output and real output or any other external variable. The key, however, is to find a correlation so a Gain Scheduling law can be formulated. Gain scheduling is a very effective way of controlling systems whose dynamics change with the operating conditions such as the case of a Zeta Converter. One of the disadvantages of Gain scheduling is the effort required for its implementation. To implement gain scheduling with analog techniques, it is rather difficult as special hardware is required such as function generators and multipliers. Such components have been quite expensive to design and operate. Gain scheduling has thus been used only in special cases, such as in autopilots for high-performance aircraft. However , Gain scheduling is very easy to implement in computer-controlled systems requiring some extra lines of code.

The characteristic of Gain Scheduling combined with its effortless implementation in digital control-based systems makes it ideal method for the Adaptive method to be implemented in the Robust Observer for this dissertation.

5.1 Gain-Scheduled Adaptive Closed Loop Observer

Gain scheduling is a practical and powerful method for the control of nonlinear systems. As described before a gain-scheduled controller is formed by interpolating between a set of linear controllers derived for a corresponding set of plant linearizations associated with several operating points. The resulting controller is a linear system whose parameters (gains) are adjusted (scheduled) as a function of the external scheduling variables. Gain scheduling is attractive because it exploits linear control design methods that are theoretically mature, are well understood, and involve computationally efficient synthesis procedures. Because the control design is based on linear approximations to the plant, one can guarantee that at each operating point, the feedback system has the desired stability and performance properties. In addition, because the controller gains are adjusted to reflect the plant operating conditions, the gain-scheduled control system has the potential of responding rapidly to changing operating conditions. Although the gain-scheduling approach is a simple extension of linear design methods, the technique can guarantee closed-loop stability and performance only in a local sense. Stability and performance properties of the gain-scheduled designs must be inferred from extensive simulation studies. The operating region where stability and performance are ensured is difficult to quantify. Furthermore, one must typically resort to heuristic methods to derive the scheduling law [55].

For the Zeta Converter Robust state observer, linearizations has been developed in chapter two and three, however in order to compensate for any remaining uncertainties in the plant due an adaptive observer gain scheduling will be developed for the Robust Observer L_1 as depicted in figure 5.4 .

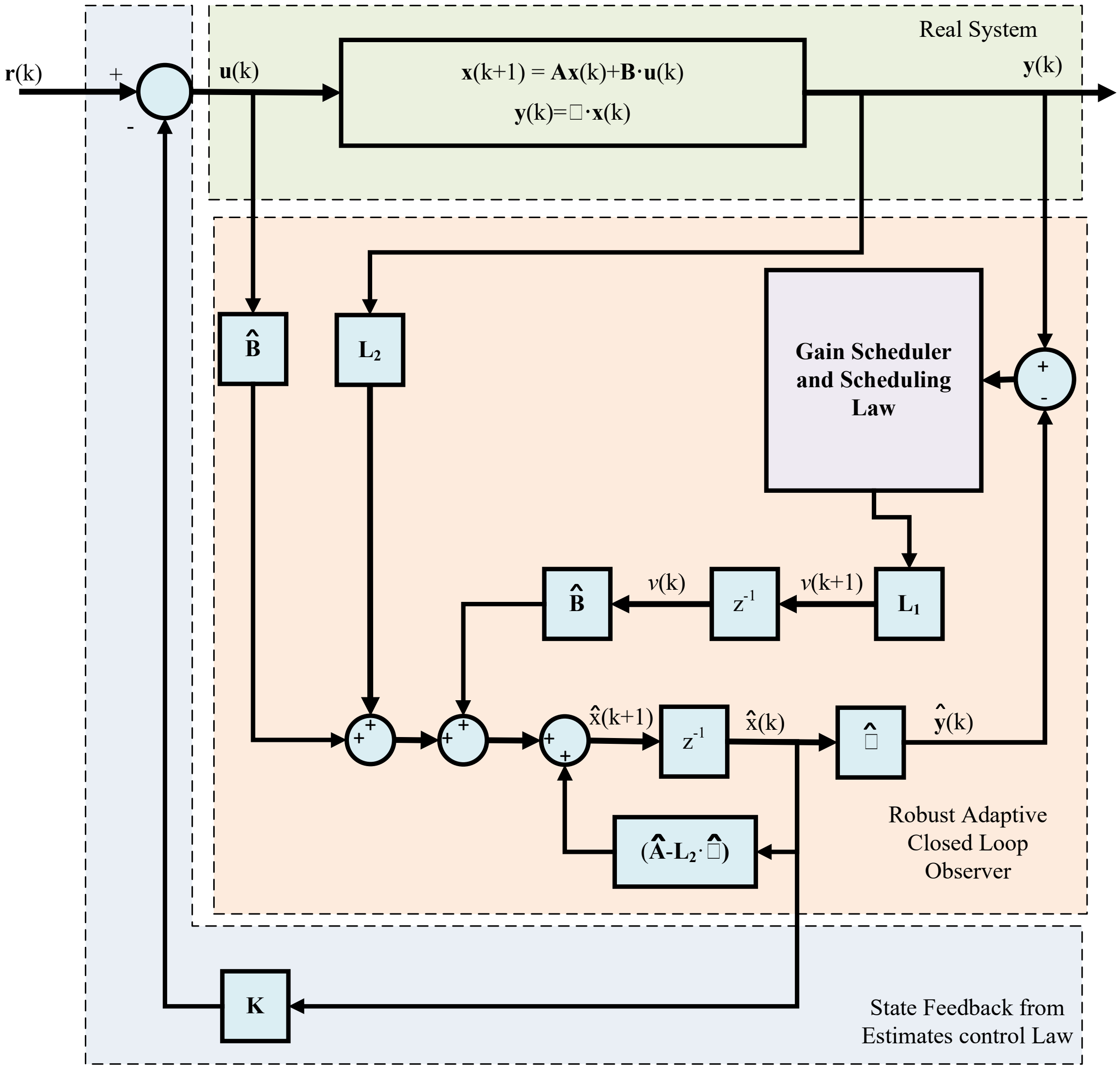

Figure 5.4 Robust Adaptive Closed Loop Observer

The scheduling variable will be based on the observer output error $\mathbf{e}_{\mathbf{output}} = \mathbf{y}(k) - \hat{\mathbf{y}}(k)$, while the scheduling law will be based on the percentage of the error, if the error percentage is big the gain L1 will be set properly to modify the poles of the observer for a faster response. If the error percentage is small the gain L1 will be set properly to modify the poles of the observer for a slower response thus smaller or no overshoot. A gain interpolation between these two set points will be developed into an if-like look-up table (Table 5.1) based on extensive simulations which will be the address in chapter 6.

If e% $\geq$ value v_1 then L_1 = $Gain_{L1.1}$
If value v_1 < e% $\leq$ value v_2 then L_1 = $Gain_{L1.2}$
If value v_{n-1} < e% $\leq$ value v_n then L_1 = $Gain_{L.n-1}$
Otherwise L_1 = $Gain_{L.n}$

Table 5.1 Gain Scheduler and Scheduling Law Look-Up Table

CHAPTER SIX

ROBUST ADAPTIVE OBSERVER APPLICATION TO MODERN POWER CONVERTERS

As delineated in chapter one , this dissertation has five objectives, four of them will be address here:

1. Identify a Discrete-Time **Full-State Observer** that can properly estimate the plant states in the presence of plant uncertainties in a Zeta Power Converter.
2. Identify, evaluate, and compare a **Robust Full-State Observer** that could improve the performance of the full-state Observer.
3. Identify, evaluate, and compare an **Adaptive and Robust Full-State observer** that could improve the performance of the full-state Observer.
4. Prove that the estimated states can be used in combination with the state feedback gain by placing the closed loop poles to achieve a maximum 30% OS of output voltage with load current changes +/- 70%: input voltage changes +/- 50% and other plan uncertainties +/- 20%.
5. Build a MATLAB&SIMULINK® Model that will simulate the dynamics of the Zeta Converter, State Observer, and State Feedback control law to verify objective one through four.

Therefore, this chapter will be an application chapter of the theory developed in chapters two through five.

Section 6.1 will define the dynamic characteristics of the Full-State Observer, positions of its poles in the z-plane, it will calculate the observer L Gain required to achieve them. It will evaluate its performance against plant uncertainties.

Sections 6.2 will focus on developing the robust Observer Lx gain and compare its performance to the Full-State Observer under plant uncertainties.

Section 6.3 will define heuristically the thresholds for the Adaptive Gain Scheduling Law L_1 and compare its performance to the Robust-Observer under plant uncertainties.

Section 6.4 will use the estimated states to develop a state-feedback controller in such a way that the output of the power converter achieves the performance indicated in objective four.

MATLAB&SIMULINK® will be used for modeling and to perform all calculations, the MATLAB script can be found in Appendix A.

6.1 Zeta Power Converter Full-State Observer

In order to develop the model for the Zeta Power converter, the following component values will be used as depicted in figure 6.1 and described in table 6.1.

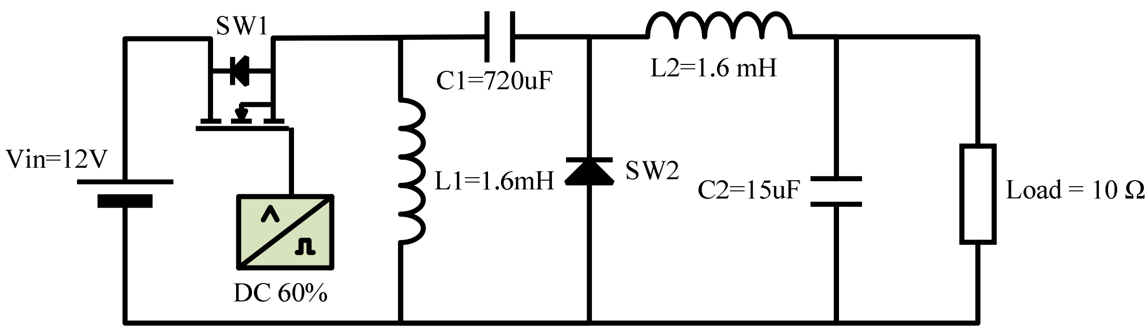

Figure 6.1 Zeta Power Converter

Input Voltage Vin	12V
Duty Cycle DC	60 %
Bypass Capacitor C1	720 uF
Inductor L1	1.6 mH
Inductor L2	1.6 mH
Output Capacitor	15 uF
Output Load	10 Ohms
Output Voltage	18 V

Table 6.1 Zeta Power Converter Values

In order to achieve a good performance, the poles of the Closed Loop State observer should be five to ten times faster than the poles of the Open Loop observer so the closed loop observer can compensate any deviations of the state faster than the states of the open loop. However, care must be taken to do not make the closed loop poles of the observer very fast because it will cause instabilities as the State-Observer would try to compensate for any small error in the Closed Loop Observer before letting it settle, therefore we need to create a sort of natural hysteresis. For this Full-State Observer the poles will be set to ten times faster than the poles of the open loop one. The damping factor ζ will determine the amount of overshoot of the state in the estimator. As illustrated in figure 6.2 a $\zeta = 0$ would yield to an oscillating state, while a $\zeta \geq 1$ will create an over damped or critically damped response. The greater the damping factor is the smaller the overshoot. For this full-state observer we will set the damping factor equal to $\zeta = 1.1$, no overshot.

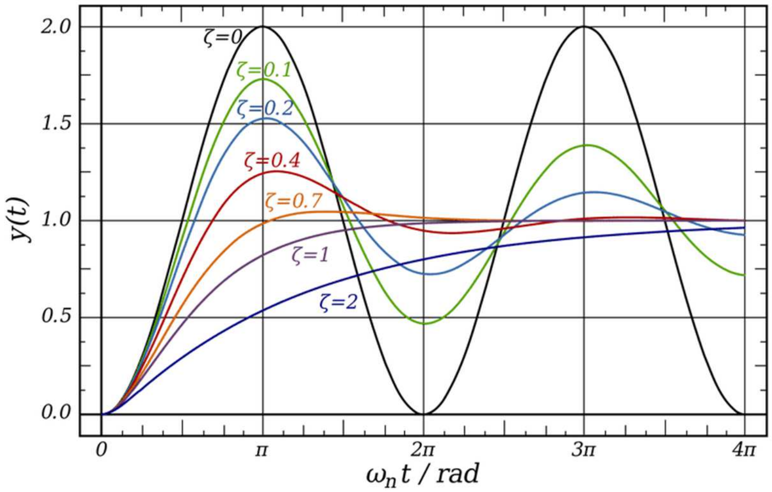

Figure 6.2 Second order step response damping ratio

In the presence of no plant uncertainties the discrete open loop full-state estimator (figure 6.4) follows exactly the discretized plant states (figure 6.3) as well as the discrete closed loop full-state observer (figure 6.5), as expected, all high abstraction model is illustrated in Figure 6.6. Figure 6.7 shows step response to a voltage input step from 0V to 12V.

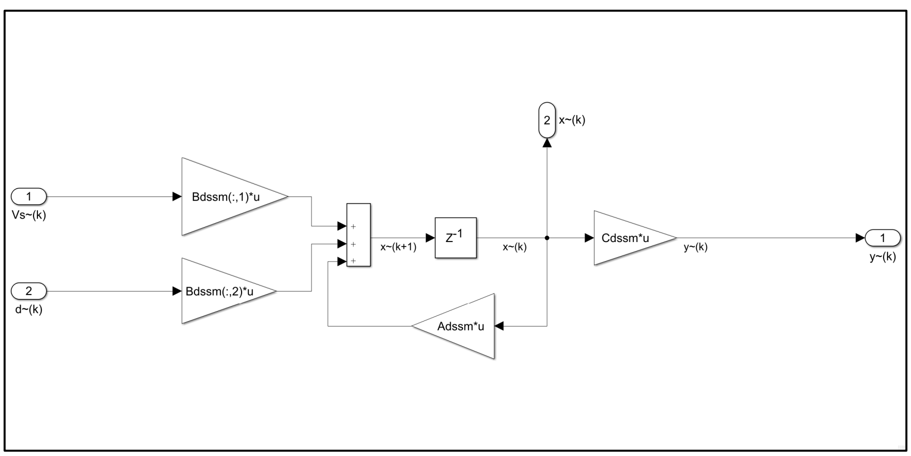

Figure 6.3 Discretized Plant

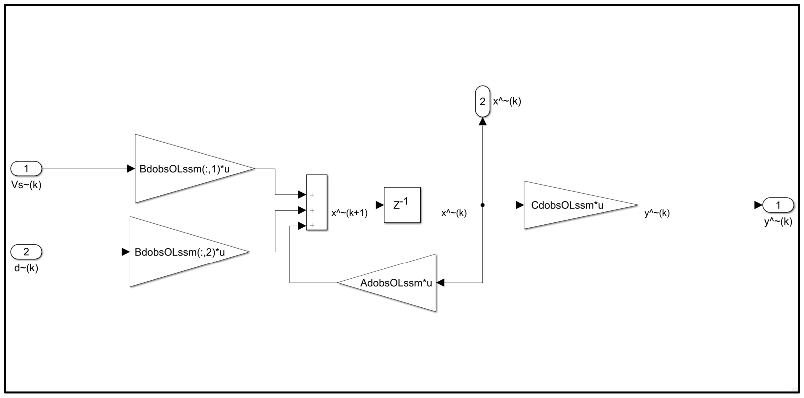

Figure 6.4 Discrete Open loop full-state estimator

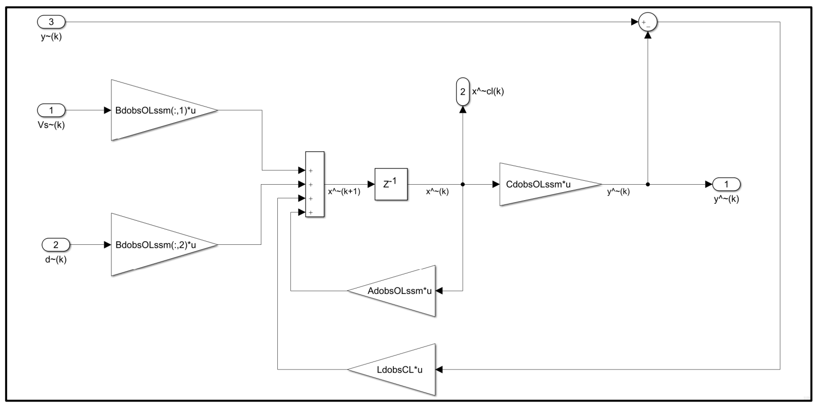

Figure 6.5 Closed loop full-state estimator

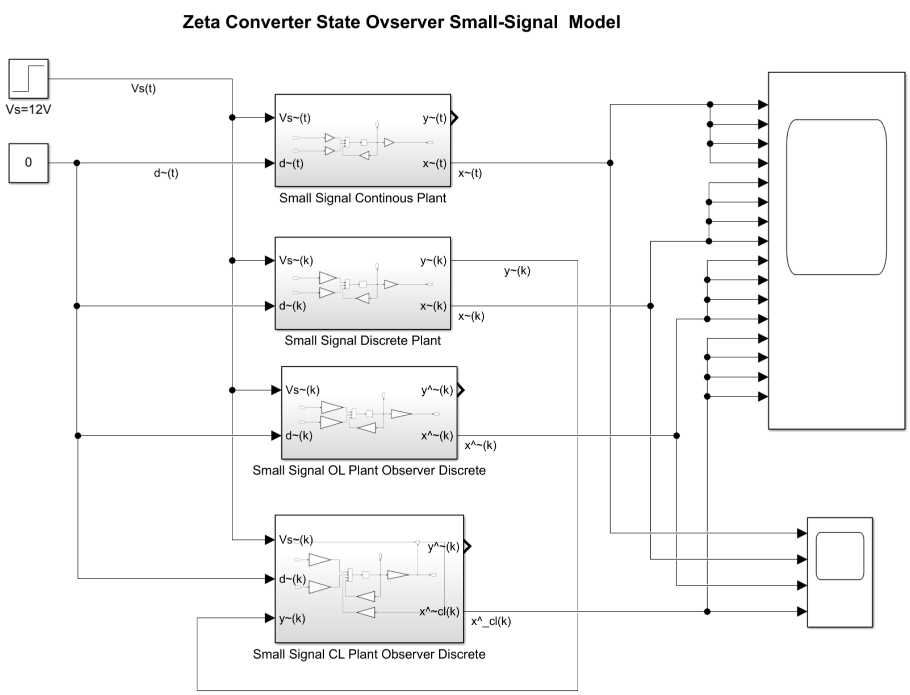

Figure 6.6 High Level Abstraction Model Zeta Power Converter

In the presence of plant uncertainties, the performance of the open loop observer starts to deteriorate in comparison to the plant states, however the closed loop observer tracks the plant states very accurately. Figure 6.8 shows the comparison side to side with a forced plant uncertainty of 10%, meaning that our modeling of the Zeta Power Converter contains a 10% error in the A system and B input matrices as depicted in the bellow MATLAB code abstract.

```
%%%%%%%%%%%%%%%%%%%%%%%%%%%%%%%%%%%%%%%%%%%%%%%%%%%%%%%%%%%%%%%%%%%%%%%%%%%%%%%%%%%%%%%%%
%                               Plant uncertainty                                       %
%%%%%%%%%%%%%%%%%%%%%%%%%%%%%%%%%%%%%%%%%%%%%%%%%%%%%%%%%%%%%%%%%%%%%%%%%%%%%%%%%%%%%%%%%
Unc      = 0.10;
%%%%%%%%%%%%%%%%%%%%%%%%%%%%%%%%%%%%%%%%%%%%%%%%%%%%%%%%%%%%%%%%%%%%%%%%%%%%%%%%%%%%%%%%%
%             Open Loop Observer  Zeta Converter Continous Plant Modeling               %
%%%%%%%%%%%%%%%%%%%%%%%%%%%%%%%%%%%%%%%%%%%%%%%%%%%%%%%%%%%%%%%%%%%%%%%%%%%%%%%%%%%%%%%%%
AobsOL      = (1-Unc)*A ;
BobsOL      = (1-Unc)*B ;
```

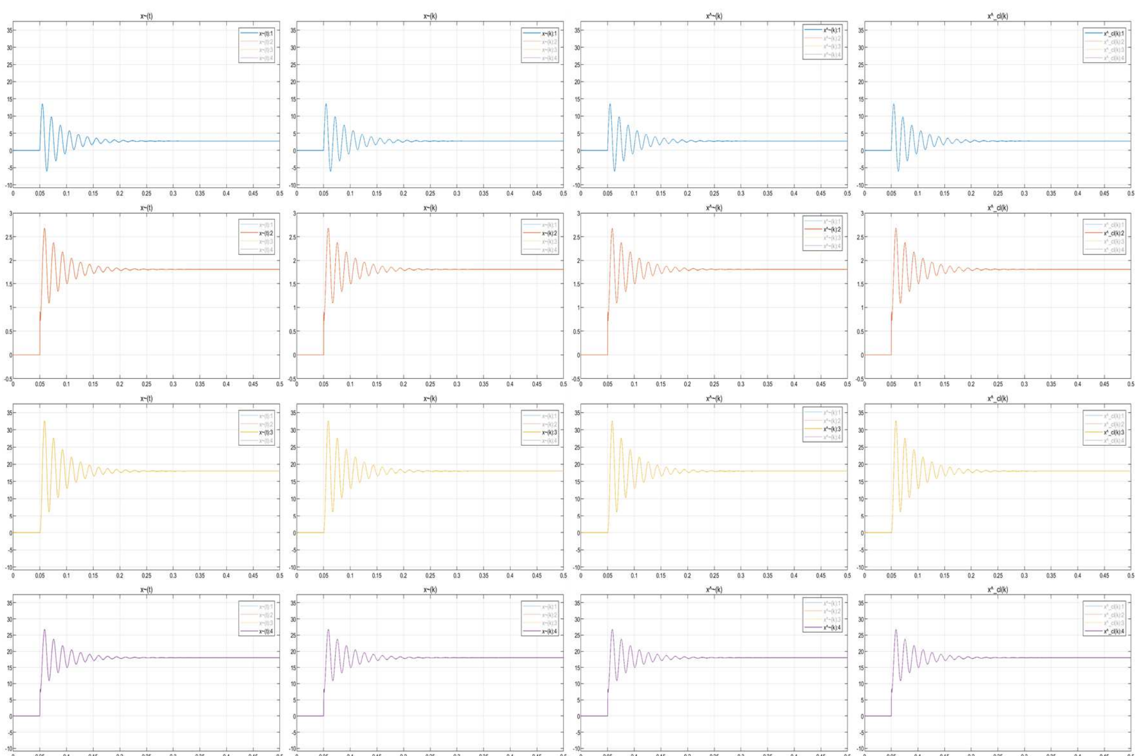

Continuous Plant states | Discrete Plant states | Open Loop Estimated States | Closed Loop Estimated States

Figure 6.7 Plant and Full State Transient Response

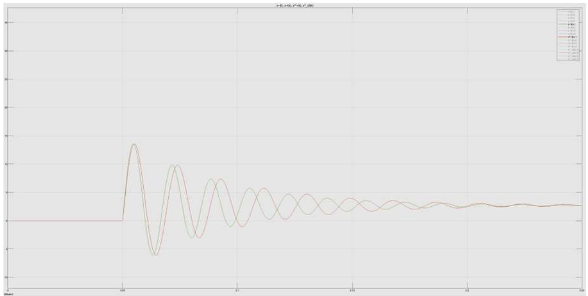

Plant State vs Open Loop Observer (x_1)

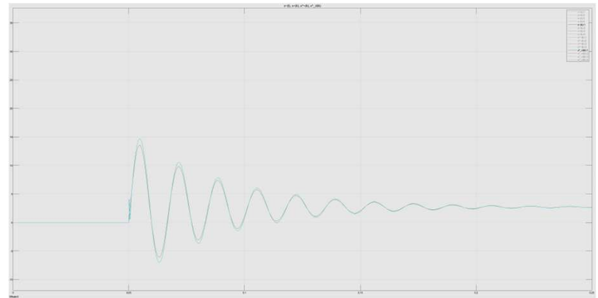

Plant State vs Closed Loop Observer (x_1)

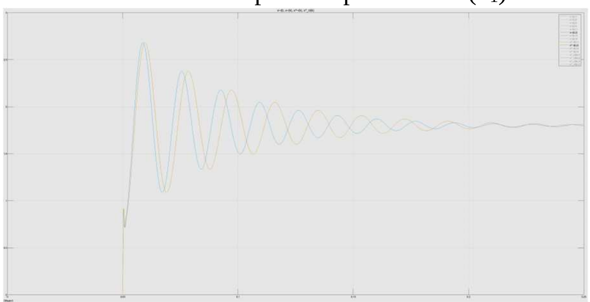

Plant State vs Open Loop Observer (x_2)

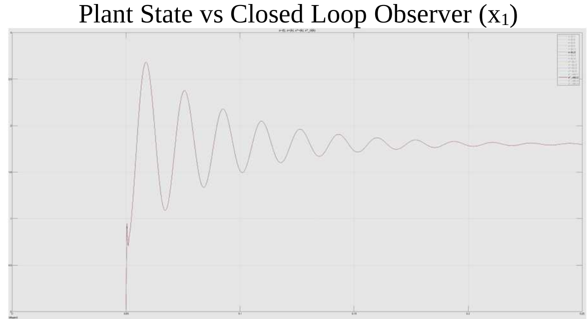

Plant State vs Closed Loop Observer (x_2)

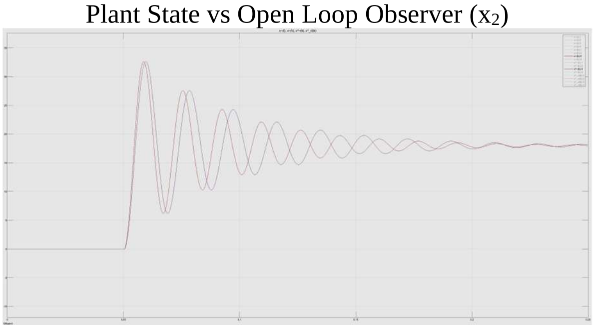

Plant State vs Open Loop Observer (x_3)

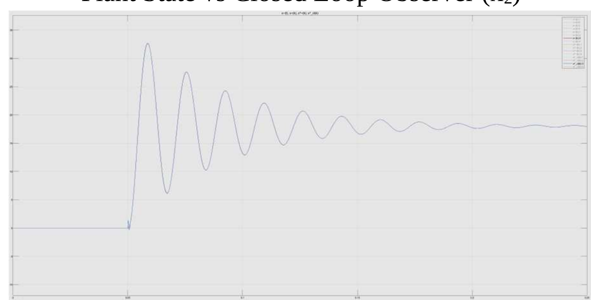

Plant State vs Closed Loop Observer (x_3)

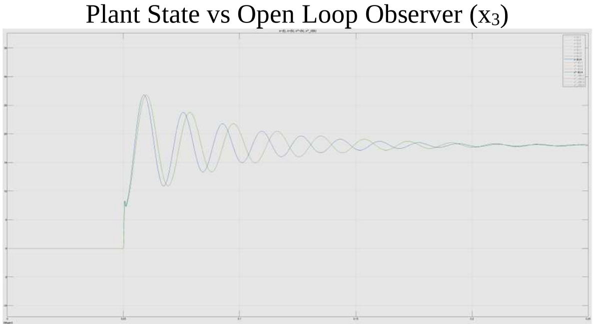

Plant State vs Open Loop Observer (x_4)

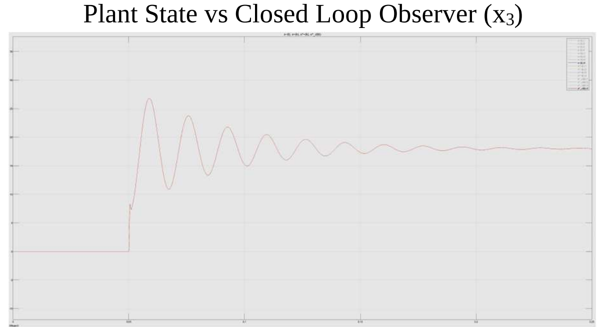

Plant State vs Closed Loop Observer (x_4)

Figure 6.8 Step response Closed and Open Loop Observer with 10% Plant Uncertainties.

The open and closed loop observer is run with an extreme of 99% Plant Uncertainties illustrated in the bellow MATLAB script.

```
%%%%%%%%%%%%%%%%%%%%%%%%%%%%%%%%%%%%%%%%%%%%%%%%%%%%%%%%%%%%%%%%%%%%%%%%%%%%%%%%%%%%%%%%%
%                               Plant uncertainty                                       %
%%%%%%%%%%%%%%%%%%%%%%%%%%%%%%%%%%%%%%%%%%%%%%%%%%%%%%%%%%%%%%%%%%%%%%%%%%%%%%%%%%%%%%%%%
Unc     = 0.99;
```

The step response transient response can be seen in figures 6.9, 6.10, 6.11 and 6.12.

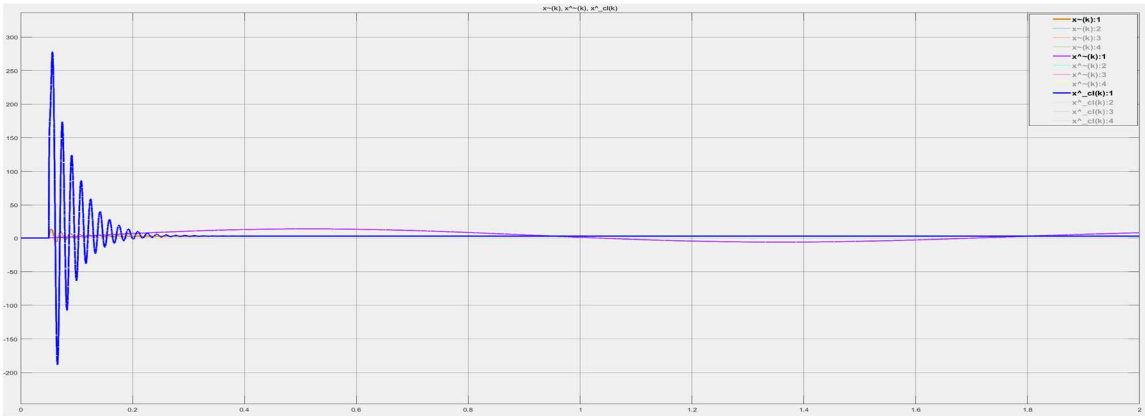

Figure 6.9 Plant State, Open and Closed Loop Observer (x_1)

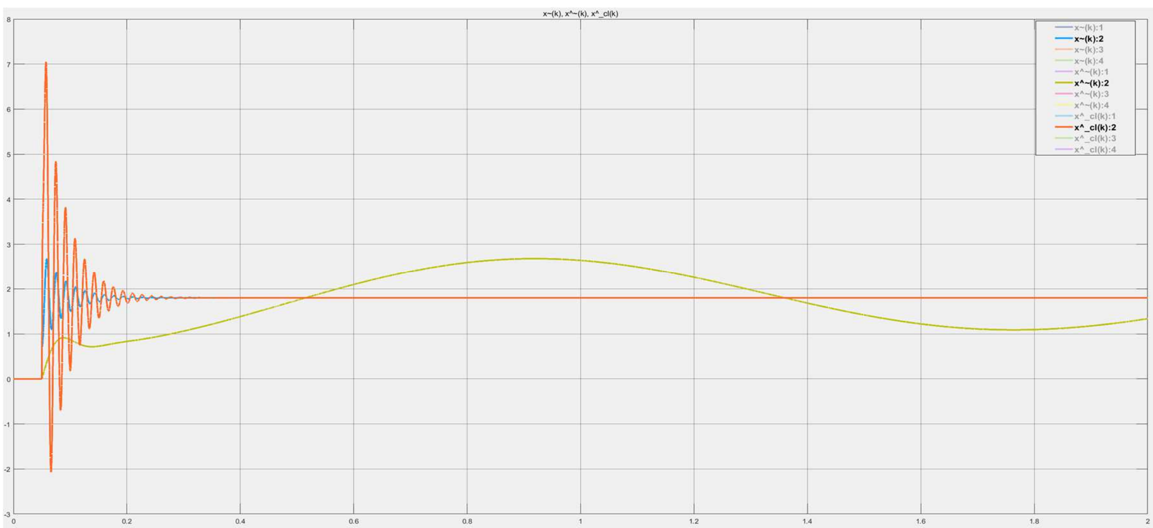

Figure 6.10 Plant State, Open and Closed Loop Observer (x_2)

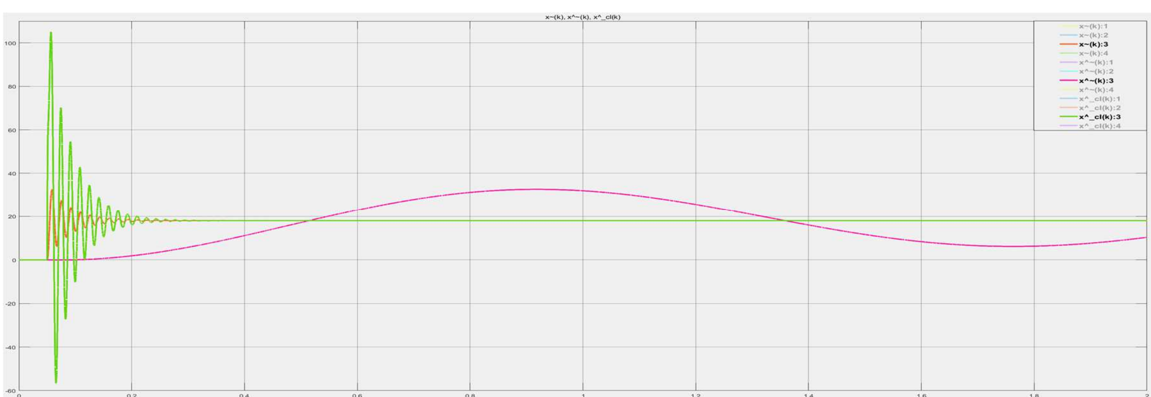

Figure 6.11 Plant State, Open and Closed Loop Observer (x_3)

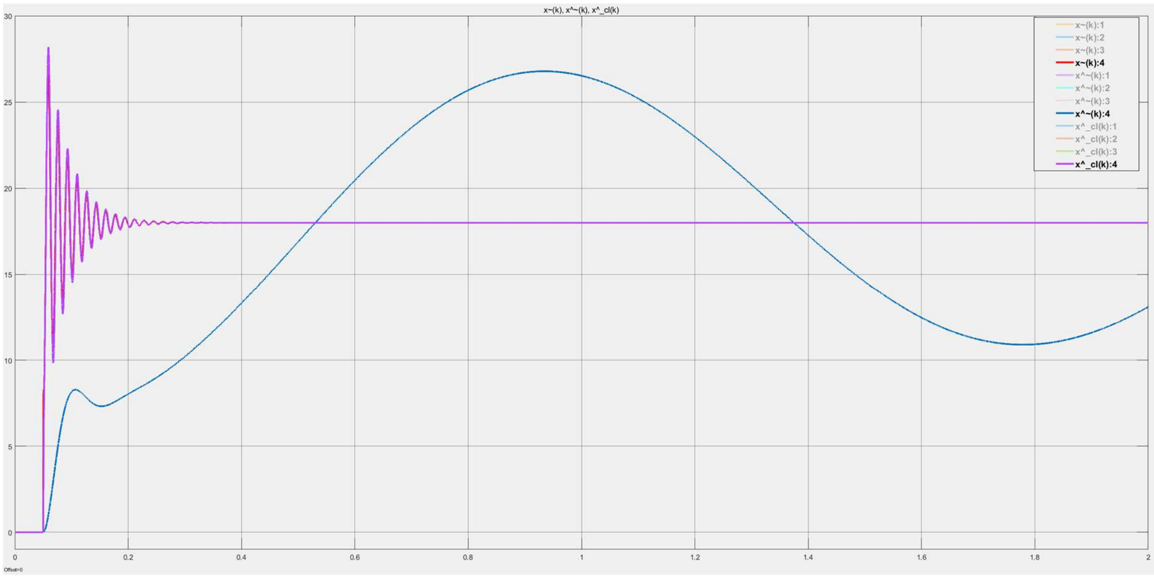

Figure 6.12 Plant State, Open and Closed Loop Observer (x_4)

It is extremely important to know that even in the presence of having very bad initial models estimates (Plant Uncertainties) the closed loop observer estimated states converge to the Plant states. For $i_{L1}(k)=x_1(k)$; $i_{L2}(k)=x_2(k)$ and $v_{C1}(k)=x_3(k)$ there is some initial oscillations, but the oscillations died after about 0.3 seconds and $v_{C2}(k)=x_4(k)$ which is the output of the converter as well, the closed loop observer corrects the error very quickly (due to the output feedback).

<u>6.2 Zeta Power Converter Robust Full-State Observer</u>

In this section we will design the Robust observer by adding an additional pole to error of the full state observer and its respective gain will be calculated. The Robust observer implementation is illustrated in figure 6.13 with a dotted box in red.

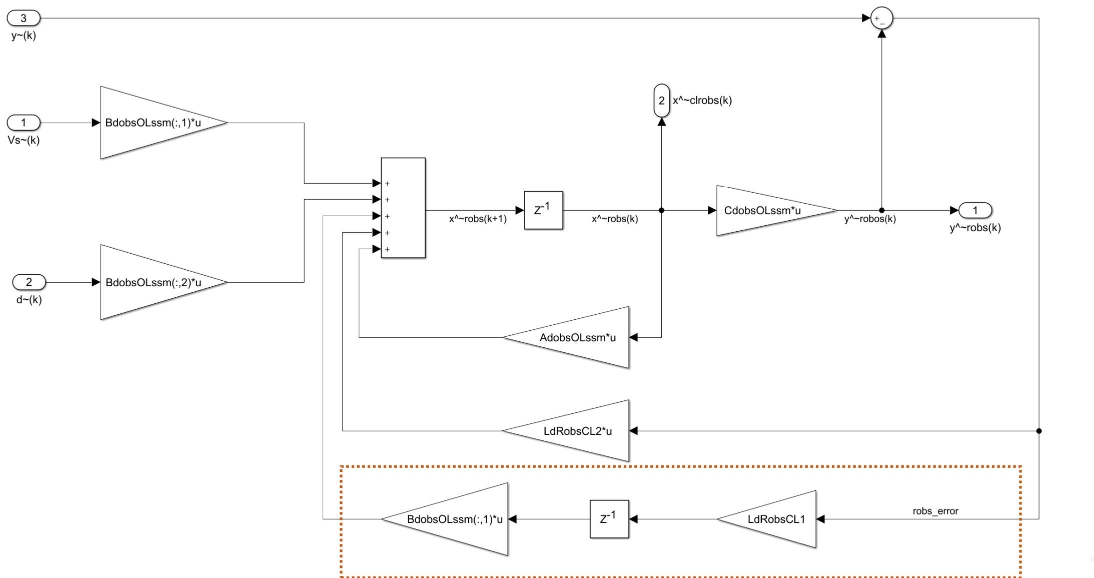

Figure 6.13 Robust Full-State Observer

As can be seen observer error which happens to be the Output of the Zeta Converter is adjusted via a gain LdRobsCL1 and integrated. The output of the Zeta Converter will be the key parameter that will be control therefore it is of interest that its performance under Plant uncertainties is robust.

The closed loop observer will be compared to the robust one however due to the high tolerance to plant uncertainties its performance will be evaluated by calculating the absolute error and integrating the error over time in order to assess the cumulative error. The additional pole for the gain LdRobsCL1 is set at P_4= - 0.9 in the z-plane within the unit circle which is a stable pole. Figure 6.14 shows the high-level abstraction of the robust closed loop observer compared to the closed loop observer.

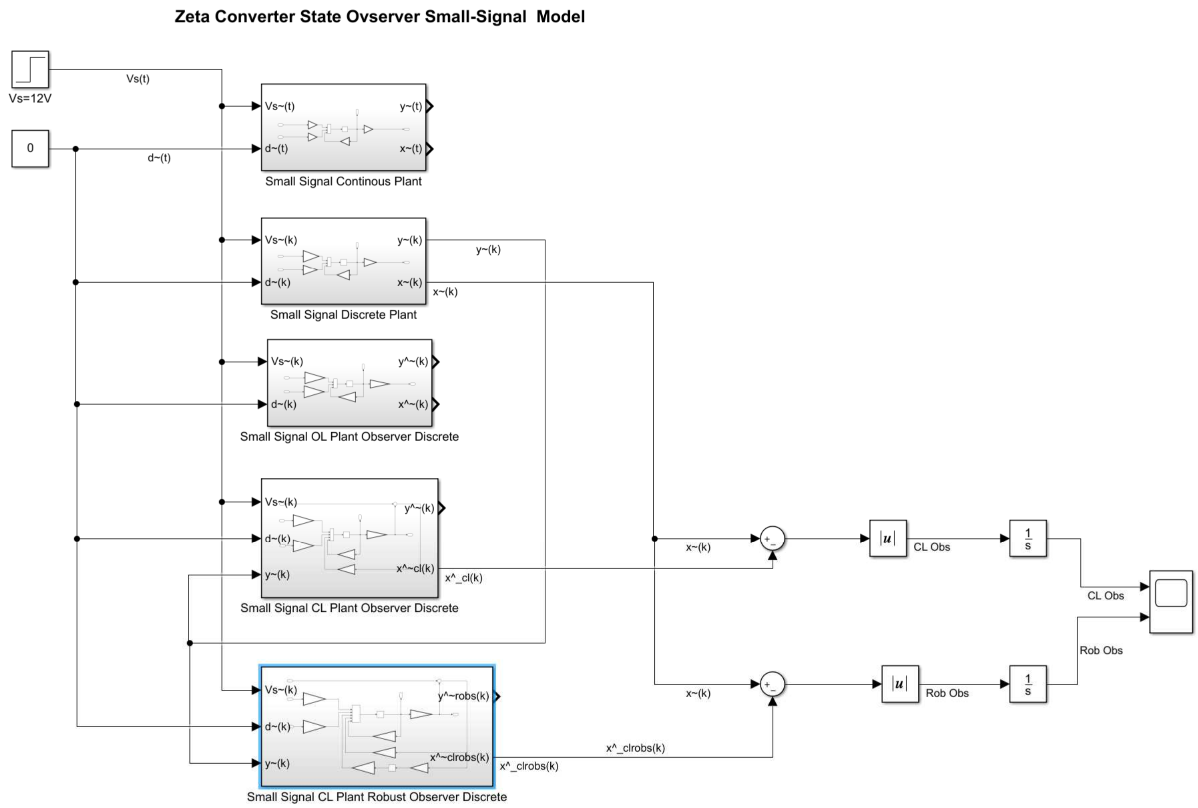

Figure 6.14 High Level Abstraction of Robust and Closed Loop Full State Estimator

The additional gain helps the performance of the observer as it can be seen in figures 6.15 and 6.16 where the error of the closed loop and robust observer are plotted over time.

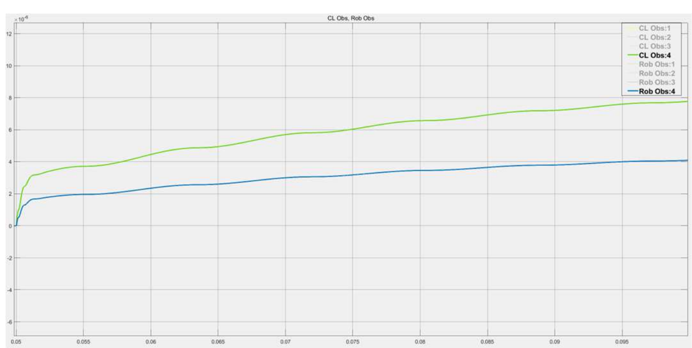

Figure 6.15 Closed loop and Robust Observer error with 10% Plan Uncertainty $x_4(k)$

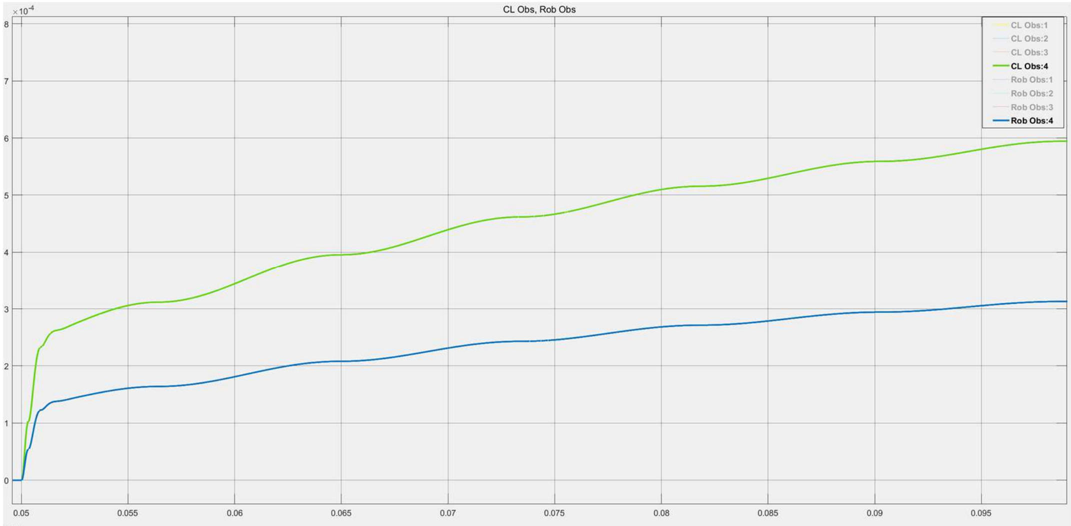

Figure 6.16 Closed loop and Robust Observer error with 40% Plan Uncertainty $x_4(k)$

It is obvious and expected that as the plant uncertainties decrease so it's the error till it becomes zero when the uncertainties of the plant are zero. In the next section we will demonstrate the final step by using the robust observer estimated states and using state feedback placed the poles of the Zeta Power Converter to the desired location to demonstrate the control goals are met.

6.3 Zeta Power Converter State-Feedback controller using a Robust Full-State Observer

As described in chapter three the separation principle allows to detach the calculation of the location of the poles for the state observer and state feedback control. The state feedback control method is applied to the Zeta Power Converter using the robust state observer as illustrated in figure 6.17. The comparison will be made between a compensated continuous real plant system and an uncompensated one to assess the performance of the design. Note that the Analog to Digital Converter block known as ADC are Sample and Hold (S/H) blocks which converter the analog input to a digital value for the digital controller to perform the calculations and DAC is a Zero-order hold (ZOH) reconstructs the digital signal back to an analog one.

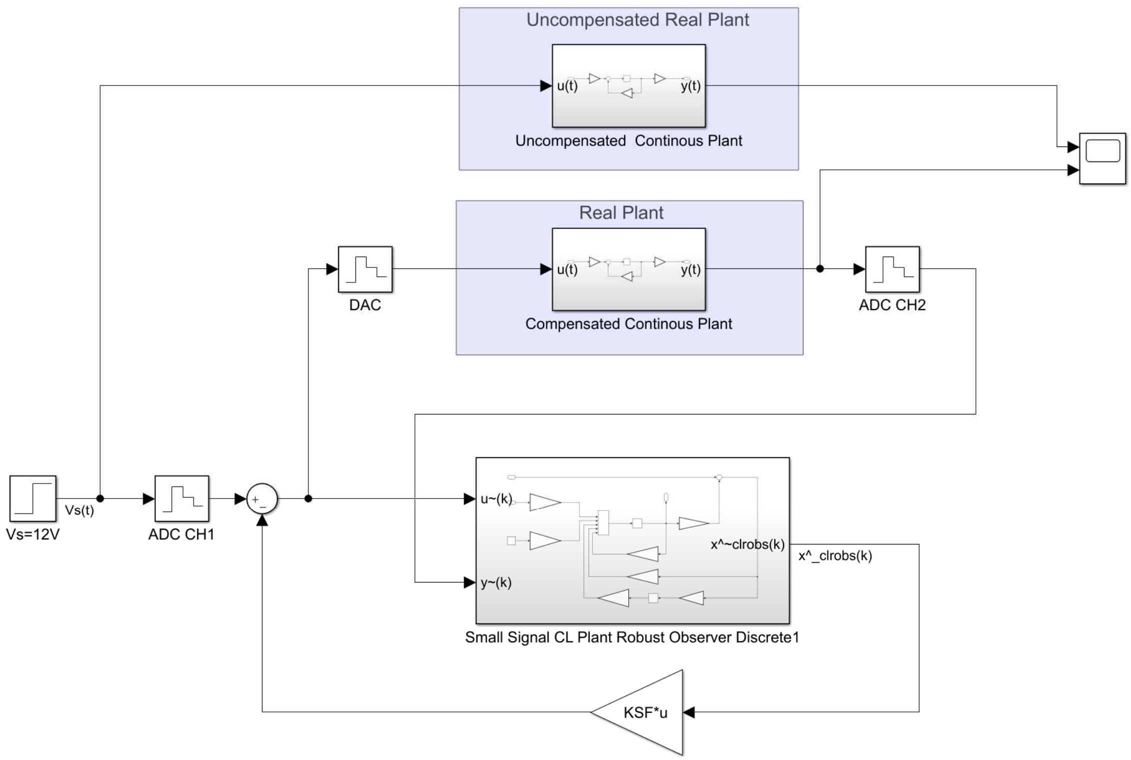

Figure 6.17 Power Zeta Converter State Feedback with Robust State Observer

The poles of the Zeta Converter are calculated to achieve an Overshoot (OS) of less than 30% (target design objective) based on equation 6.1 the damping ration must be $\zeta \geq 0.3579$, for this design we select a $\zeta = 0.5912$.

$$\xi = \frac{-\ln\left(\frac{\%0S}{100}\right)}{\sqrt{\pi^2 + \left(\ln\left(\frac{\%0S}{100}\right)\right)^2}} \qquad \text{Eq. 6.1}$$

The natural frequency ω_n is left to be the estimated modeling plant natural frequency as we are only concerned about %OS. With 0% plant uncertainties the uncompensated plant has a peak value of ~26.78 V with a steady state final value of 18

V, therefore the %OS approximately 48.61%, however the compensated plant %OS is approximately 7.83% which meets the design objective as illustrated in figure 6.18.

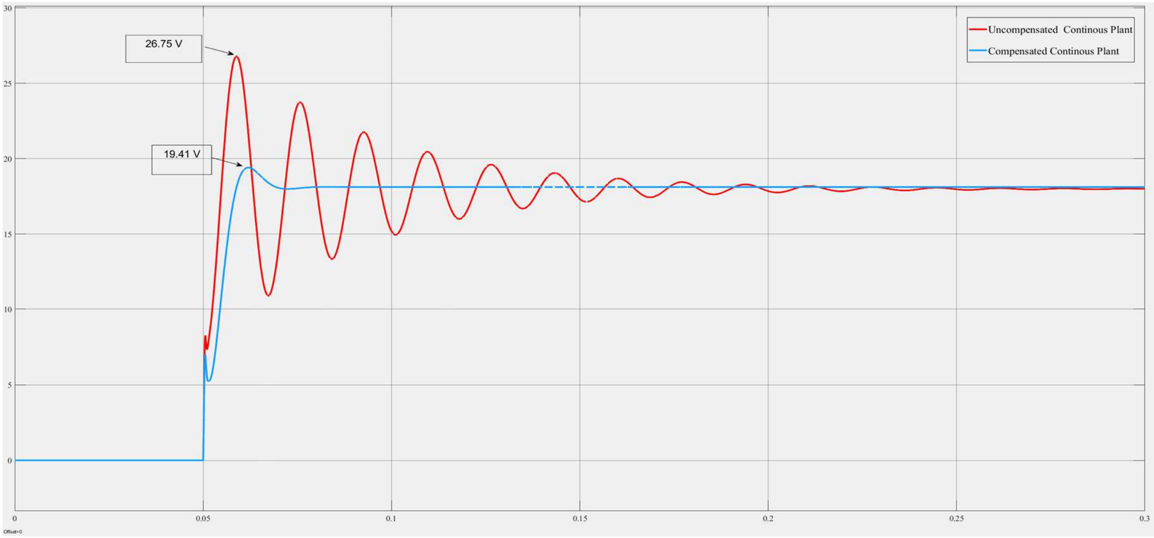

Figure 6.18 Power Zeta Converter Transient Response with State Feedback from robust Observer with no plant uncertainties

With plant uncertainties of 20% the percentage of overshoot is of the uncompensated plant is approximately 48.61% while the compensated overshoot one is approximately 2.33% as illustrated in figure 6.19.

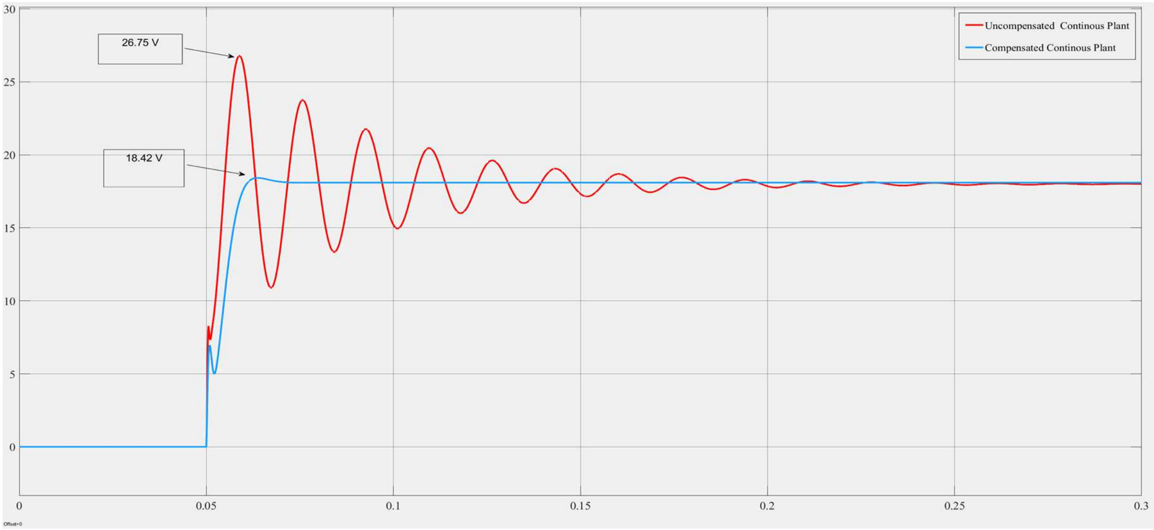

Figure 6.19 Power Zeta Converter Transient Response with State Feedback from robust Observer with 20% plant uncertainties

One very important remark is that as the uncertainties increase the estimated states of slow down as previously described in section 6.1 to a point that the controller no longer can compensate and the system becomes unstable, this is observed in figure 6.20 and 6.21 when the plant uncertainties 61% and 62% respectively. With 61% plant uncertainties the state feedback controller can still converge however with uncertainties ≥ 62% the output growths unbounded.

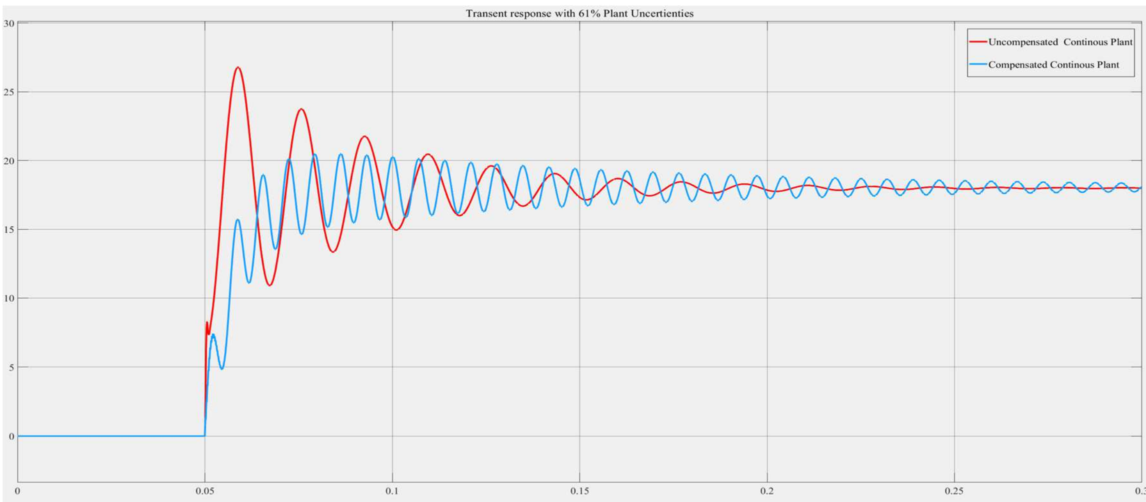

Figure 6.20 Power Zeta Converter Transient Response with State Feedback from robust Observer with 61% plant uncertainties

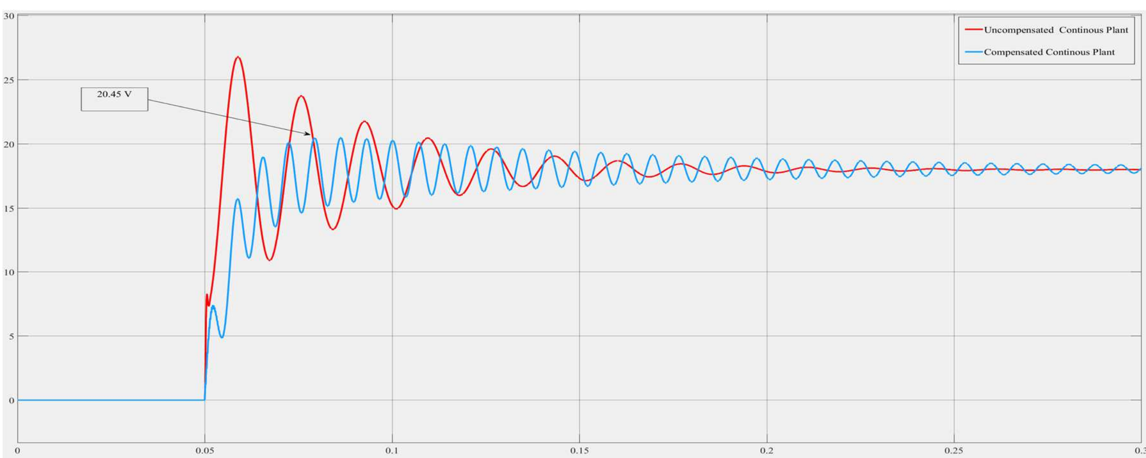

Figure 6.21 Power Zeta Converter Transient Response with State Feedback from robust Observer with 62% plant uncertainties

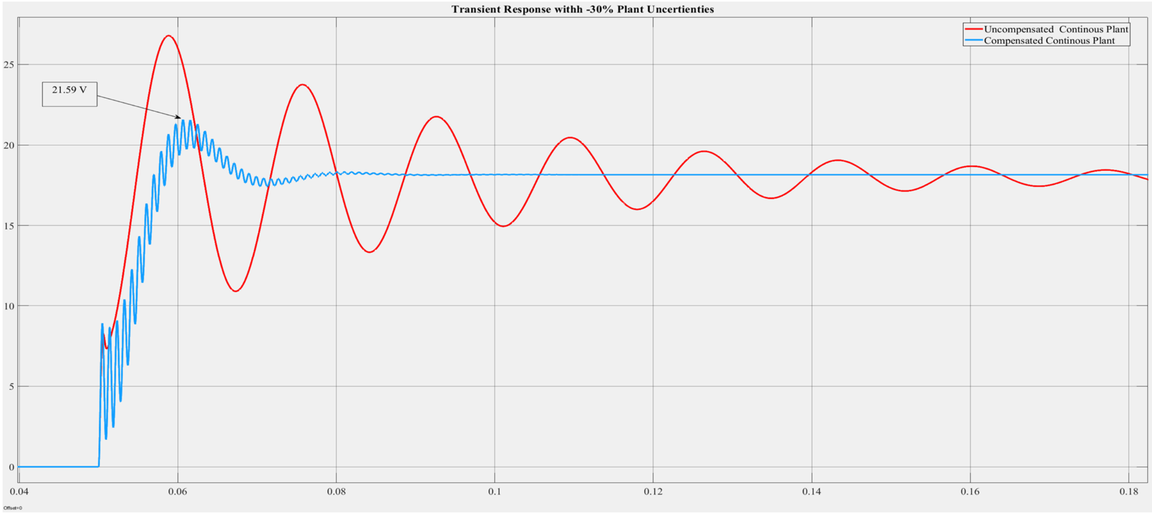

Figure 6.22 Power Zeta Converter Transient Response with State Feedback from robust Observer with -30% plant uncertainties

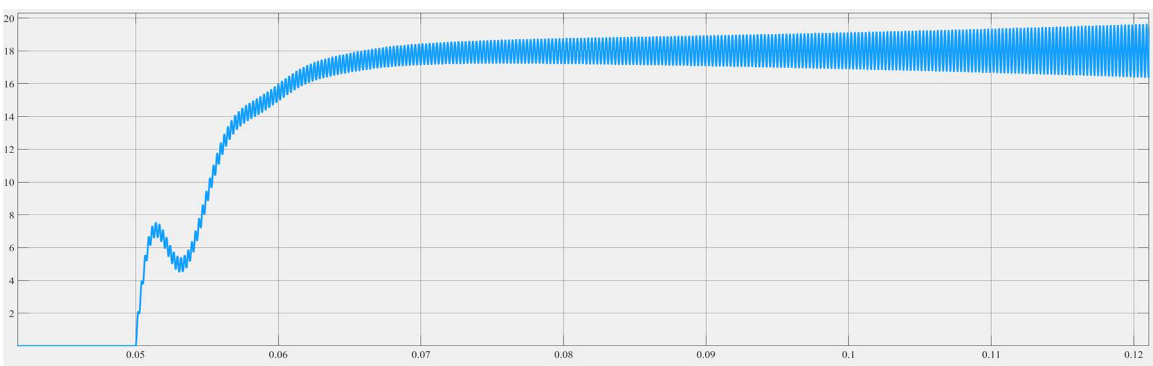

Figure 6.23 Power Zeta Converter Transient Response with State Feedback from robust Observer with 42.23% plant uncertainties and Ts =1us

In this chapter, we were successfully able to implement a discrete state- feedback from states from the robust full-state observer/estimator and apply it to a nonlinear Zeta Power converter. The State-Feedback controller has been proved to be very robust against plant uncertainties up to +61% having a performance of 11.11% of overshot and 20% for plant uncertainties -30% therefore meeting the design objectives.

CHAPTER SEVEN

CONCLUSION AND FUTURE WORK CONVERTERS

7.1 Conclusion and future work

The aim of this research was to identify a novel way of controlling Zeta Converters using robust adaptive state observers and state feedback in the discrete-time domain that yields robustness in the presence of plant uncertainties. Based on the quantitative analysis performed mathematically and proved with simulation (MATLAB&SIMULINK) it can be concluded that it was possible to find a discrete controller to achieve the design objectives stated at the beginning of the research. The state feedback controller was able to compensate for plant uncertainties up to +61% and -30% when the design objective was 20% by adapting the robust observer pole P4 from negative 0.9 to positive 0.9 respectively. As described in section 3.3 the sampling time has an effect on the stability of the system under same plant uncertainties. A changed from 10 us to 1 us sampling time makes the poles of the robust observer closer to the unit circle stability boundary.

While this this research has met the objectives also raises the question if this control technique can be applied to other converters and observer or if a different adaptive scheme could be implemented using the input as an additional scheduling variable to extend the robustness to plan uncertainties which could be later explore in a future work . Additional extension for research could also include the adaptability method posting the question could Model Reference Adaptive Observer (MRAO), Artificial Intelligence / Machine Learning or a Self-Tuning Observer Controllers (STO) could yield a better performance.

Appendix A

MATLAB® Code for the Discrete State Feedback Power Converter controller with

Robust Full State Estimator/Observer.

```
%%%%%%%%%%%%%%%%%%%%%%%%%%%%%%%%%%%%%%%%%%%%%%%%%%%%%%%%%%%%%%%%%%%%%%%%%%%%%%%%%%%
%                           Zeta Converter State-Space Modeling                   %
%%%%%%%%%%%%%%%%%%%%%%%%%%%%%%%%%%%%%%%%%%%%%%%%%%%%%%%%%%%%%%%%%%%%%%%%%%%%%%%%%%%
clc;
close all ;
clear all ;

%%%%%%%%%%%%%%%%%%%%%%%%%%%%%%%%%%%%%%%%%%%%%%%%%%%%%%%%%%%%%%%%%%%%%%%%%%%%%%%%%%%
%                           Zeta Converter Continous Plant Modeling               %
%%%%%%%%%%%%%%%%%%%%%%%%%%%%%%%%%%%%%%%%%%%%%%%%%%%%%%%%%%%%%%%%%%%%%%%%%%%%%%%%%%%
d=  0.6     ;           % Steady State dutty Cycle
L1= 1.6e-3  ;           % Inductor L1 Value  =   1.6 mH
L2= 1.6e-3  ;           % Inductor L1 Value  =   1.6 mH
C1= 7.2e-4  ;           % Bypass capacitor   =   720 uF
C2= 1.5e-5  ;           % Output Capacitance =   15  uF
R=10        ;           % Load Resistance    =   10 Ohms
A   = [
        0               0      (-(1-d)/L1)       0        ;
        0               0      ( d/L2)       (-1/L2)      ;
        ((1 -d)/C1)    (-d/C1)     0             0        ;
        0              (1/C2)      0         (-1/(R*C2)) ;
        ];
B   = [
        d/L1 ;
        d/L2 ;
         0   ;
         0
         ];
C   = [ 0 0 0 1];
D   = [0]       ;
Vs  = 12        ;       % Input  Voltage
Vo  = (d/(1-d))*Vs ;    % Output Volatge
disp( ['Output Voltage Vo = ', num2str(Vo),' Volts' ] )
sys = ss(A,B,C,D) ;
%%%%%%%%%%%%%%%%%%%%%%%%%%%%%%%%%%%%%%%%%%%%%%%%%%%%%%%%%%%%%%%%%%%%%%%%%%%%%%%%%%%
%              Zeta Converter State-Space Modeling Discretization                 %
%%%%%%%%%%%%%%%%%%%%%%%%%%%%%%%%%%%%%%%%%%%%%%%%%%%%%%%%%%%%%%%%%%%%%%%%%%%%%%%%%%%
%Ts      = 0.000010;          % 10 us sampling time
Ts      = 0.000001;          % 1 us sampling time at 42.5Plan Uncertienty Unstable
sysd    = c2d(sys,Ts);
Adisc   = get(sysd,'A');
Bdisc   = get(sysd,'B');
Cdisc   = get(sysd,'C');
Ddisc   = get(sysd,'D');
%%%%%%%%%%%%%%%%%%%%%%%%%%%%%%%%%%%%%%%%%%%%%%%%%%%%%%%%%%%%%%%%%%%%%%%%%%%%%%%%%%%
%                                Plant uncertainty                                %
%%%%%%%%%%%%%%%%%%%%%%%%%%%%%%%%%%%%%%%%%%%%%%%%%%%%%%%%%%%%%%%%%%%%%%%%%%%%%%%%%%%
Unc     = 0.4223         ; %Unstable Ts 1us
%Unc      = -0.30       ; %adaptive robust observer pole location of +0.9
%Unc      =  0.60       ; %adaptive robust observer pole location of -0.9

%%%%%%%%%%%%%%%%%%%%%%%%%%%%%%%%%%%%%%%%%%%%%%%%%%%%%%%%%%%%%%%%%%%%%%%%%%%%%%%%%%%
%             Open Loop Observer  Zeta Converter Continous Plant Modeling         %
%%%%%%%%%%%%%%%%%%%%%%%%%%%%%%%%%%%%%%%%%%%%%%%%%%%%%%%%%%%%%%%%%%%%%%%%%%%%%%%%%%%
AobsOL     = (1-Unc)*A ;
BobsOL     = (1-Unc)*B ;
CobsOL     = C     ;
DobsOL     = D     ;
sysobsOL    = ss(AobsOL,BobsOL,CobsOL,DobsOL);
```

```
%%%%%%%%%%%%%%%%%%%%%%%%%%%%%%%%%%%%%%%%%%%%%%%%%%%%%%%%%%%%%%%%%%%%%%%%%%%%%%%%%%%%%%%%
%                 Open Loop Observer Zeta Converter Discretization                    %
%%%%%%%%%%%%%%%%%%%%%%%%%%%%%%%%%%%%%%%%%%%%%%%%%%%%%%%%%%%%%%%%%%%%%%%%%%%%%%%%%%%%%%%%
sysdobsOL = c2d(sysobsOL,Ts);
AdobsOL   = get(sysdobsOL,'A');
BdobsOL   = get(sysdobsOL,'B');
CdobsOL   = get(sysdobsOL,'C');
DdobsOL   = get(sysdobsOL,'D');

%%%%%%%%%%%%%%%%%%%%%%%%%%%%%%%%%%%%%%%%%%%%%%%%%%%%%%%%%%%%%%%%%%%%%%%%%%%%%%%%%%%%%%%%
%%%%%%%%%%%%%%%%%%%%%%%%%%%%%%%%%%%%%%%%%%%%%%%%%%%%%%%%%%%%%%%%%%%%%%%%%%%%%%%%%%%%%%%%
%                Zeta Converter Linearized Small-Signal Modeling                      %
%%%%%%%%%%%%%%%%%%%%%%%%%%%%%%%%%%%%%%%%%%%%%%%%%%%%%%%%%%%%%%%%%%%%%%%%%%%%%%%%%%%%%%%%
%%%%%%%%%%%%%%%%%%%%%%%%%%%%%%%%%%%%%%%%%%%%%%%%%%%%%%%%%%%%%%%%%%%%%%%%%%%%%%%%%%%%%%%%

%%%%%%%%%%%%%%%%%%%%%%%%%%%%%%%%%%%%%%%%%%%%%%%%%%%%%%%%%%%%%%%%%%%%%%%%%%%%%%%%%%%%%%%%
%                Zeta Converter State-Space Small-Signal Modeling                     %
%%%%%%%%%%%%%%%%%%%%%%%%%%%%%%%%%%%%%%%%%%%%%%%%%%%%%%%%%%%%%%%%%%%%%%%%%%%%%%%%%%%%%%%%

Aon  = [ 0        0           0           0           ;
         0        0           (1/L2)      (-1/L2)     ;
         0        (-1/C1)     0           0           ;
         0        (1/C2)      0           -1/(R*C2)   ;
       ];

Aoff = [ 0        0           -(1/L1)     0           ;
         0        0           0           (-1/L2)     ;
         (1/C1)   0           0           0           ;
         0        (1/C2)      0           -1/(R*C2)   ;
       ];
Assm = Aon*d + Aoff*(1-d);                %% Note Assm is equal to A large Model %%
Bon  = [ d/L1 ;
         d/L2 ;
         0    ;
         0
       ];
Boff = [ 0    ;
         0    ;
         0    ;
         0    ;
        ];
Bd = ((-(Aon - Aoff)*( inv(A)* B * Vs) ) + (Bon-Bon)*Vs );
Bssm = [ B  Bd];
Cssm = C;
Dssm = D;
sys_ssm = ss(Assm,Bssm,Cssm,Dssm) ;
%%%%%%%%%%%%%%%%%%%%%%%%%%%%%%%%%%%%%%%%%%%%%%%%%%%%%%%%%%%%%%%%%%%%%%%%%%%%%%%%%%%%%%%%
%      Zeta Converter State-Space Small-Signal Modeling Discretization                %
%%%%%%%%%%%%%%%%%%%%%%%%%%%%%%%%%%%%%%%%%%%%%%%%%%%%%%%%%%%%%%%%%%%%%%%%%%%%%%%%%%%%%%%%
sysdssm = c2d(sys_ssm,Ts);
Adssm   = get(sysdssm,'A');
Bdssm   = get(sysdssm,'B');
Cdssm   = get(sysdssm,'C');
Ddssm   = get(sysdssm,'D');
%%%%%%%%%%%%%%%%%%%%%%%%%%%%%%%%%%%%%%%%%%%%%%%%%%%%%%%%%%%%%%%%%%%%%%%%%%%%%%%%%%%%%%%%
%     Zeta Converter Open Loop Observer Small-Signal Continous Plant Modeling         %
%%%%%%%%%%%%%%%%%%%%%%%%%%%%%%%%%%%%%%%%%%%%%%%%%%%%%%%%%%%%%%%%%%%%%%%%%%%%%%%%%%%%%%%%
AobsOLssm     = (1-Unc)*Assm ;
BobsOLssm     = (1-Unc)*Bssm ;
CobsOLssm     = Cssm         ;
DobsOLssm     = Dssm         ;
sysobsOLssm   = ss(AobsOLssm,BobsOLssm,CobsOLssm,DobsOLssm);
```

```
%%%%%%%%%%%%%%%%%%%%%%%%%%%%%%%%%%%%%%%%%%%%%%%%%%%%%%%%%%%%%%%%%%%%%%%%%%%%%%%%%%%%
%     Zeta Converter Open Loop Observer Small-Signal Discrete Plant Modeling       %
%%%%%%%%%%%%%%%%%%%%%%%%%%%%%%%%%%%%%%%%%%%%%%%%%%%%%%%%%%%%%%%%%%%%%%%%%%%%%%%%%%%%
sysdobsOLssm = c2d(sysobsOLssm,Ts);
AdobsOLssm   = get(sysdobsOLssm,'A');
BdobsOLssm   = get(sysdobsOLssm,'B');
CdobsOLssm   = get(sysdobsOLssm,'C');
DdobsOLssm   = get(sysdobsOLssm,'D');
%%%%%%%%%%%%%%%%%%%%%%%%%%%%%%%%%%%%%%%%%%%%%%%%%%%%%%%%%%%%%%%%%%%%%%%%%%%%%%%%%%%%
% Zeta Converter OL Observer S-S Discrete Plant Natural Frequecy,Damp Ratio, Poles  %
%%%%%%%%%%%%%%%%%%%%%%%%%%%%%%%%%%%%%%%%%%%%%%%%%%%%%%%%%%%%%%%%%%%%%%%%%%%%%%%%%%%%
[WndobsOLssm,ZdobsOLssm,PdobsOLssm] = damp(sysdobsOLssm);
%%%%%%%%%%%%%%%%%%%%%%%%%%%%%%%%%%%%%%%%%%%%%%%%%%%%%%%%%%%%%%%%%%%%%%%%%%%%%%%%%%%%
%      Zeta Converter Closed Loop Observer S-S Discrete Plant Poles                 %
%%%%%%%%%%%%%%%%%%%%%%%%%%%%%%%%%%%%%%%%%%%%%%%%%%%%%%%%%%%%%%%%%%%%%%%%%%%%%%%%%%%%
WndobsCLssm = 10*WndobsOLssm         ; % Set Poles 10x Faster than System Poles
ZdobsCLssm  = 1.1*[1 ; 1 ; 1 ; 1]    ; % Set damping Ratio to 0.7
PdobsCLssm  = [
exp( Ts*( -(ZdobsCLssm(1)*WndobsCLssm(1)) + j*(WndobsCLssm(1)*sqrt(1-ZdobsCLssm(1)^2))));
exp( Ts*( -(ZdobsCLssm(2)*WndobsCLssm(2)) - j*(WndobsCLssm(2)*sqrt(1-ZdobsCLssm(2)^2))));
exp( Ts*( -(ZdobsCLssm(3)*WndobsCLssm(3)) + j*(WndobsCLssm(3)*sqrt(1-ZdobsCLssm(3)^2))));
exp( Ts*( -(ZdobsCLssm(4)*WndobsCLssm(4)) - j*(WndobsCLssm(4)*sqrt(1-ZdobsCLssm(4)^2))));
];
LdobsCL = place(AdobsOLssm',CdobsOLssm',PdobsCLssm')';
%%%%%%%%%%%%%%%%%%%%%%%%%%%%%%%%%%%%%%%%%%%%%%%%%%%%%%%%%%%%%%%%%%%%%%%%%%%%%%%%%%%%
%    Zeta Converter Closed Loop Robust Observer S-S Discrete Poles and Gain         %
%%%%%%%%%%%%%%%%%%%%%%%%%%%%%%%%%%%%%%%%%%%%%%%%%%%%%%%%%%%%%%%%%%%%%%%%%%%%%%%%%%%%
Azeros = [0 0 0 0];
Bzeros = [0];
AdRobsOLssm = [AdobsOLssm       BdobsOLssm(:,1);
               Azeros           Bzeros     ];
BdRobsOLssm1 = [ BdobsOLssm(:,1) ;
                 Bzeros          ];
BdRobsOLssm2 = [ BdobsOLssm(:,2) ;
                 Bzeros          ];
CdRobsOLssm = [ CdobsOLssm 0    ];
PdRobsCLssm = [ PdobsCLssm;
                -0.9  ];
RobsOLssm   = obsv(AdRobsOLssm,CdRobsOLssm);
if rank(RobsOLssm)== size(AdRobsOLssm,1)
    disp('Discrete Time System is Observable')
else
    disp('Discrete System is NOT Observable')
end
LdRobsCL = place(AdRobsOLssm',CdRobsOLssm',PdRobsCLssm')';
LdRobsCL1=LdRobsCL(5:5);
LdRobsCL2=LdRobsCL(1:4);
%%%%%%%%%%%%%%%%%%%%%%%%%%%%%%%%%%%%%%%%%%%%%%%%%%%%%%%%%%%%%%%%%%%%%%%%%%%%%%%%%%%%
%      Zeta Converter State Feedback Controller Desoign S-S Discrete CL Obs         %
%%%%%%%%%%%%%%%%%%%%%%%%%%%%%%%%%%%%%%%%%%%%%%%%%%%%%%%%%%%%%%%%%%%%%%%%%%%%%%%%%%%%
[WnST,zeta,p] = damp(sysdobsOLssm);
OS      = 0.10;                                                  % set target Overshoot to 10%
zetaSF  = (-log(OS) / (sqrt( pi^2 + log(OS)^2)))*[1 ; 1 ; 1 ; 1];       % Damping Ratio State Feedback
PSF     = [
exp( Ts*( -(zetaSF(1)*WnST(1)) + j*(WnST(1)*sqrt(1-zetaSF(1)^2))));
exp( Ts*( -(zetaSF(2)*WnST(2)) - j*(WnST(2)*sqrt(1-zetaSF(2)^2))));
exp( Ts*( -(zetaSF(3)*WnST(3)) + j*(WnST(3)*sqrt(1-zetaSF(3)^2))));
exp( Ts*( -(zetaSF(4)*WnST(4)) - j*(WnST(4)*sqrt(1-zetaSF(4)^2))));
];
KSF     = place(AdobsOLssm,BdobsOLssm(:,1),PSF);
```

REFERENCES

[1] Nise Norman S., *Control systems engineering*. 2004.

[2] A. S. Vasilyev and A. V. Ushakov, “Modeling of dynamic systems with modulation by means of Kronecker vector-matrix representation,” *Scientific and Technical Journal of Information Technologies, Mechanics and Optics*, pp. 839–848, Aug. 2015, doi: 10.17586/2226-1494-2015-15-5-839-848.

[3] D. G. Luenberger, “Observing the State of a Linear System,” *IEEE Transactions on Military Electronics*, vol. 8, no. 2, pp. 74–80, 1964, doi: 10.1109/TME.1964.4323124.

[4] Aström Karl J. and Hägglund Tore, *Advanced PID Control*, 1st ed. International Society of Automation, 2005.

[5] Aström Karl J. and Hägglund Tore, “The future of PID control,” 2001.

[6] Åström Karl. J. and Hägglund Tore, “Revisiting the Ziegler-Nichols step response method for PID control,” *J Process Control*, vol. 14, no. 6, pp. 635–650, Sep. 2004, doi: 10.1016/j.jprocont.2004.01.002.

[7] M. Sami. Fadali and Antonio. Visioli, *Digital control engineering : analysis and design*. Academic Press, 2013.

[8] Daniel M. Mitchell, *DC-DC Switching Regulator Analysis* , 1st ed. Mitchell, Daniel M.: McGraw-Hill, 1988.

[9] R. W. Erickson and D. Maksimović, *Fundamentals of Power Electronics*. Cham: Springer International Publishing, 2020. doi: 10.1007/978-3-030-43881-4.

[10] V. Choudhary, T. Hegarty, and D. Pace, “Under the hood of a noninverting buck-boost converter,” 2016. Accessed: Dec. 20, 2022. [Online]. Available: https://training.ti.com/under-hood-noninverting-buck-boost-converter

[11] P. R. Babu, S. R. Prasath, and R. Kiruthika, “Simulation and performance analysis of CCM Zeta converter with PID controller,” in *IEEE International Conference on Circuit, Power and Computing Technologies, ICCPCT 2015*.

[12] N. Siddharthan and B. Balasubramanian, “Performance evaluation of SEPIC, Luo and ZETA converter,” *International Journal of Power Electronics and Drive Systems (IJPEDS)*, vol. 10, no. 1, p. 374, Mar. 2019.

[13] A. J. Mahmud, M. H. Mithun, M. A. Khan, F. Faisal, M. M. Nishat, and M. A. Hoque, “Optimal Control and Performance Enhancement of DC-DC Bidirectional SEPIC Converter,” in *2022 IEEE 13th Annual Ubiquitous Computing, Electronics and Mobile Communication Conference, UEMCON 2022*, Institute of Electrical and Electronics Engineers Inc., 2022, pp. 437–443. doi: 10.1109/UEMCON54665.2022.9965670.

[14] A. Applications Journal, “High-Performance Analog Products,” 2010. [Online]. Available: www.ti.com/lprf

[15] Raymond A. Mack, *Demystifying Switching Power Supplies*, 1st ed. Newnes, 2011.

[16] P. Karamanakos, T. Geyer, and S. Manias, “Direct voltage control of DC-DC boost converters using enumeration-based model predictive control,” *IEEE Trans Power Electron*, vol. 29, no. 2, pp. 968–978, 2014, doi: 10.1109/TPEL.2013.2256370.

[17] E. Vuthchhay, C. Bunlaksananusorn, and H. Hirata, “Dynamic Modeling and Control of a Zeta Converter,” in *2008 International Symposium on Communications and Information Technologies*, IEEE, Oct. 2008, pp. 498–503. doi: 10.1109/ISCIT.2008.4700242.

[18] E. Vuthchhay and C. Bunlaksananusorn, “Modeling and control of a zeta converter,” in *2010 International Power Electronics Conference - ECCE Asia -, IPEC 2010*, 2010, pp. 612–619. doi: 10.1109/IPEC.2010.5543332.

[19] R. C. Viero and F. S. dos Reis, “Designing closed-loop controllers using a MatlabP® dynamic model of the Zeta converter in DCM,” in *2012 10th IEEE/IAS International Conference on Industry Applications, INDUSCON 2012*, 2012. doi: 10.1109/INDUSCON.2012.6452525.

[20] P. R. Babu, S. R. Prasath, and R. Kiruthika, “Simulation and performance analysis of CCM Zeta converter with PID controller,” in *IEEE International Conference on Circuit, Power and Computing Technologies, ICCPCT 2015*, Institute of Electrical and Electronics Engineers Inc., Jul. 2015. doi: 10.1109/ICCPCT.2015.7159506.

[21] Z. U. Haq and A. Ali, “Comparative study of Zeta converter and Boost converter Using PI controller,” in *7th International Conference on Electrical, Electronics and Information Engineering: Technological Breakthrough for Greater New Life, ICEEIE 2021*, Institute of Electrical and Electronics Engineers Inc., 2021. doi: 10.1109/ICEEIE52663.2021.9616826.

[22] K. J. Åström and T. Hägglund, “Revisiting the Ziegler-Nichols step response method for PID control,” *J Process Control*, vol. 14, no. 6, pp. 635–650, Sep. 2004, doi: 10.1016/j.jprocont.2004.01.002.

[23] M. M. Garg, Y. v. Hote, and M. K. Pathak, “PI controller design of a DC-DC Zeta converter for specific phase margin and cross-over frequency,” in *2015 10th Asian Control Conference: Emerging Control Techniques for a Sustainable World, ASCC 2015*, Institute of Electrical and Electronics Engineers Inc., Sep. 2015..

[24] Y. T. Yau, K. I. Hwu, C. W. Wang, and J.-J. Shieh, “ZETA Dual-Loop Control Based on Voltage Across Transferring Capacitor Sensed,” in *2019 IEEE 4th International Future Energy Electronics Conference (IFEEC)*, IEEE, Nov. 2019, pp. 1–3. doi: 10.1109/IFEEC47410.2019.9014971.

[25] M. M. Nishat, M. R. K. Shagor, H. Akter, S. A. Mim, and F. Faisal, “An Optimal Design of PID controller for DC-DC Zeta converter using Particle Swarm Optimization,” in *ICCIT 2020 - 23rd International Conference on Computer and Information Technology, Proceedings*, Institute of Electrical and Electronics Engineers Inc., Dec. 2020. doi: 10.1109/ICCIT51783.2020.9392676.

[26] K. Durgadevi and R. Karthik, “Performance Analysis of Zeta Converter Using Classical PID and Fractional Order PID Controller,” in *2018 International Conference on Power, Energy, Control and Transmission Systems (ICPECTS)*, IEEE, Feb. 2018, pp. 312–317.

[27] S. Suwannaprom, “PI controller design for ZETA converter,” in *ECTI-CON 2021 - 2021 18th International Conference on Electrical Engineering/Electronics, Computer, Telecommunications and Information Technology: Smart Electrical System and Technology, Proceedings*, Institute of Electrical and Electronics Engineers Inc., May 2021, pp. 866–869. doi: 10.1109/ECTI-CON51831.2021.9454717.

[28] A. Mehta and B. Naik, “Sliding mode controller with PI-type sliding function for zeta converter,” in *Lecture Notes in Electrical Engineering*, Springer Verlag, 2019, pp. 55–68. doi: 10.1007/978-981-13-3152-7_5.

[29] S. K. Pandey, S. L. Patil, S. B. Phadke, and A. S. Deshpande, “Investigation of sliding mode control of higher order DC-DC converters,” in *India International Conference on Power Electronics, IICPE*, IEEE Computer Society, Jun. 2016.

[30] Jumiyatun, M. Ashari, Soedibyo, O. Penangsang, and I. Mahmudi, “Fuzzy Based Wide Range Voltage Control of DC Step-Up Zeta Converter for Energy Management System,” in *2021 4th International Seminar on Research of Information Technology and Intelligent Systems, ISRITI 2021*, Institute of Electrical and Electronics Engineers Inc., 2021, pp. 423–428.

[31] D. A. M. Cirino, R. D. Zamora, and E. I. O. Rivera, “Passivity Based Controller for Photovoltaic Modules Using Zeta Converter,” in *2017 IEEE 44th Photovoltaic Specialist Conference (PVSC)*, IEEE, Jun. 2017, pp. 3044–3049. doi: 10.1109/PVSC.2017.8366613.

[32] H. Sarkawi, M. Hafiz Jali, T. A. Izzuddin, and M. Dahari, “DYNAMIC MODEL OF ZETA CONVERTER WITH FULL-STATE FEEDBACK CONTROLLER IMPLEMENTATION,” 2013. [Online]. Available: http://www.ijret.org

[33] Katsuhiko. Ogata, *Modern control engineering*. Prentice-Hall, 2010.

[34] H. Sarkawi and Y. Ohta, “Uncertain DC-DC Zeta Converter Control in Convex Polytope Model Based on LMI Approach,” *International Journal of Power Electronics and Drive Systems (IJPEDS)*, vol. 9, no. 2, p. 829, Jun. 2018, doi: 10.11591/ijpeds.v9.i2.pp829-838.

[35] Vladimír Bobál, Josef Böhm, Jaromír Fessl, and Jiří Macháček, *Digital Self-tuning Controllers*. London: Springer-Verlag, 2005. doi: 10.1007/b137409.

[36] "Process Control," *Mineral Processing Design and Operations*, pp. 763–816, 2016, doi: 10.1016/B978-0-444-63589-1.00020-4.

[37] J. Hahn and T. F. Edgar, "Process Control Systems," *Encyclopedia of Physical Science and Technology*, pp. 111–126, 2003, doi: 10.1016/B0-12-227410-5/00612-8.

[38] A. Gupta and D. S. Yan, "Process Control," *Mineral Processing Design and Operation*, pp. 622–671, 2006, doi: 10.1016/B978-044451636-7/50019-X.

[39] Youping Zhang and P. A. Ioannou, "A robust modification of a new class of adaptive controllers," in *Proceedings of 1995 American Control Conference - ACC'95*, American Autom Control Council, pp. 2510–2514. doi: 10.1109/ACC.1995.532297.

[40] Y. D. Landau, "Adaptive control: The model reference approach," *IEEE Trans Syst Man Cybern*, vol. SMC-14, no. 1, pp. 169–170, Jan. 1984, doi: 10.1109/TSMC.1984.6313284.

[41] A. Izadian, P. Khayyer, and H. Yang, "Adaptive voltage tracking control of zeta buck-boost converters," in *2012 IEEE Energy Conversion Congress and Exposition, ECCE 2012*, 2012, pp. 414–417. doi: 10.1109/ECCE.2012.6342792.

[42] A. Izadian and P. Khayyer, "Complementary adaptive control of Zeta converters," in *Proceedings of the 2013 IEEE International Electric Machines and Drives Conference, IEMDC 2013*, 2013, pp. 1338–1342. doi: 10.1109/IEMDC.2013.6556309.

[43] B. Moaveni, H. Abdollahzadeh, and M. Mazoochi, “Adjustable output voltage Zeta converter using neural network adaptive model reference control,” in *Proceedings - 2011 2nd International Conference on Control, Instrumentation and Automation, ICCIA 2011*, IEEE Computer Society, 2011, pp. 552–557. doi: 10.1109/ICCIAutom.2011.6356718.

[44] C. Y. Chan, “Adaptive Sliding-Mode Control of a Novel Buck-Boost Converter Based on Zeta Converter,” *IEEE Transactions on Circuits and Systems II: Express Briefs*, vol. 69, no. 3, pp. 1307–1311, Mar. 2022, doi: 10.1109/TCSII.2021.3107315.

[45] E. Vuthchhay and C. Bunlaksananusorn, “Dynamic modeling of a Zeta converter with state-space averaging technique,” in *5th International Conference on Electrical Engineering/Electronics, Computer, Telecommunications and Information Technology, ECTI-CON 2008*, 2008, pp. 969–972. doi: 10.1109/ECTICON.2008.4600593.

[46] R. D. Middlebrook and S. Cuk, “A general unified approach to modelling switching-converter power stages,” Institute of Electrical and Electronics Engineers (IEEE), Apr. 2015, pp. 18–34. doi: 10.1109/pesc.1976.7072895.

[47] G. (George H.) Ellis, *Observers in control systems : a practical guide*. Academic Press, 2002.

[48] M. Gopal, *Digital Engineering Control*, Second Edition. NEW AGE INTERNATIONAL (P) LIMITED, PUBLISHERS, 1998.

[49] K. Ogata, *Discrete-Time Control Systems*, 2nd Edition., vol. 2nd Edition. Prentice-Hall, 1994.

[50] R. W. Brocke, “Poles, Zeros, and Feedback: State Space Interpretation,” 1964.

[51] R. A. Freeman and P. Kokotović, *Robust Nonlinear Control: State-Space and Lyapunov Techniques* . Boston, MA: Birkhäuser Boston, 1996. doi: 10.1007/978-0-8176-4759-9.

[52] D. G. Luenberger, “Observers for Multivariable Systems,” *IEEE Trans Automat Contr*, vol. 11, no. 2, pp. 190–197, 1966, doi: 10.1109/TAC.1966.1098323.

[53] J. Doyle and G. Stein, “Robustness with observers,” *IEEE Trans Automat Contr*, vol. 24, no. 4, pp. 607–611, Aug. 1979, doi: 10.1109/TAC.1979.1102095.

[54] K. J. Åström and B. Wittenmark, *Adaptive Control: Second Edition*. Dover edition, 2008.

[55] C. J. Bett and W. K. Chen, *Gain-Scheduled Controllers; The Electrical Engineering Handbook.* Academic Press., 2004.